Group Invariant Methods of Some Multidimensional Fluid Flows with Heat Transfer Analysis

By

Muhammad NazimTufail

DEPARTMENT OF MATHEMATICS

QUAID-I-AZAM UNIVERSITY

ISLAMABAD, PAKISTAN

2016

Group Invariant Methods of Some Multidimensional Fluid Flows with Heat Transfer Analysis

By

Muhammad NazimTufail

Supervised By

Prof. Dr. Asif Ali

DEPARTMENT OF MATHEMATICS

QUAID-I-AZAM UNIVERSITY

ISLAMABAD, PAKISTAN

2016

Group Invariant Methods of Some Multidimensional Fluid Flows with Heat Transfer Analysis

By

Muhammad NazimTufail

A THESIS SUBMITTED IN THE PARTIAL FULFILLMENT OF THE

REQUIREMENTS FOR THE DEGREE OF

DOCTOR OF PHILOSOPHY

IN

MATHEMATICS

Supervised by

Prof. Dr. Asif Ali

DEPARTMENT OF MATHEMATICS
QUAID-I-AZAM UNIVERSITY
ISLAMABAD, PAKISTAN

2016

DECLARATION

I Muhammad NazimTufail S/O Muhammad TufailKhokhar, with Registration No. 03140913010, a student of Doctor of Philosophy at Quaid-i-Azam University, Islamabad Pakistan, do hereby solemnly declare that the thesis entitled “Group Invariant Methods of Some Multidimensional Fluid Flows with Heat Transfer Analysis” submitted by me in partial fulfillment of the requirement for Doctor of Philosophy degree in Mathematics is my original work and has not been submitted and shall not, in future, be submitted by me for obtaining any degree from this or any other university or institution.

Date: 20-10-2016 Signature_____

(Muhammad NazimTufail)

Dedication

To my father Muhammad TufailKhokhar

and mother ShaghuftaNasreen

for their enthusiasm,

compassion,

and patience

Acknowledgement

PraiseistoAllahAlmighty,CreatorandSustainerofthe heavensandtheearth,andeverythingbetweenthem,Lordoflords,whogavemethepotentialandabilitytocompletethisdissertation.Allofmyrespectandvenerationgoestothe HolyProphetMuhammad(Peacebeuponhim)whoshowedhumanitytherightpath,broughtthemessageofpeace, loveandemphasizedthenecessityandimportanceofknowledge.Respectisdueforhisfamily,friends,companionsandallfollowers(peacebeuponallofthem).

I owe my deepest gratitude to Prof. Dr. Asif Ali who not only supervised this dissertation but always been a source of stimulation for me. He always encouraged me to set prodigious goals and to find own ways to achieve them. His stimulating suggestions, conscious guidance and superb planning abetted me in the completion of this thesis. This dissertation could not have been completed without generous support and guidance of DrAhmerMehmood. His fabulous provision, valuable suggestions and careful readings are extremely accredited in the completion of this work.I am also grateful to Prof. Dr. Tasawar Hayat, chair department of Mathematics, for providing research oriented environment and excellent facilities at the department. I would always be indebted to all my teachers of Quaid-i-Azam University by whom I gained marvelous skills and knowledge. I would like to express my heartfelt thanks to HEC (Higher Education Commission, Pakistan) for the financial support throughout this study and the IRSIP (International Research Support Initiative Program) of HEC in award of fellowship and travel grants for my research at the Brock University, Canada.

I gratefully acknowledge the marvelous company of my closest friends Adnan S. Butt, Attaullah, Dr. AwaisYousaf, Dr. AbdurRazaqand Ifzan Arshad; we spend delightful moments together at QAU. I am thankful to my colleagues, my seniors and juniors (Dr. Amanullah Dar, Dr. Sufian, Dr. Majid, Dr. Azeem, Dr. Saira, and M. Nasir) for their moral support and good wishes. Moreover, I am thankful to all those numerous well-wishers who prayed for my success, I am not being able to mention here all of them.

Finally, my sincere gratitude goes to my parents who supported me indirectly with great concern, generous support, love and prayers for my achievements. Words are countless to say thank to those benevolent hands that sincerely raised me with gentle love, care and patience. Without their prayers and sacrifices I could not be able to successfully complete whole of my educational career. Many thanks go to my brothers AsimTufail, Ghulam Mohiudin, Ghulam Jilani and ZaighamMohiudin and my sisters for their great concern and encouragement.May almighty Allah reward all of them with great honor in this world and the world hereafter Ameen.

Muhammad NazimTufail
Oct. 20, 2016

Preface

In this thesis,a multidimensional fluid flows with heat transfer by using the Lie group approach is investigated. In the first chapter, a brief introduction and background of symmetries,Navier-Stokes equations for the fluid flow, energy equations, boundary layer equations, and some basic definitions of flow and heat characteristics are given. Chapter one also has three pages of historical notes.

In chapter two,two different cases are studied. In case (i), the invariants for MHD non-Newtonian fluid flow with heat transfer in the presence of source/sink effects is investigated. In case (ii), the system of ordinary differential equations by using the group theoretic method to analyze the MHD non-Newtonian fluid flow with thermal radiation effects is studied. In particular, for both cases an invariant and find the analytic solutions after considering the stretching sheet phenomenon has been opted.

In chapter three, thenon-Newtonian unsteady flow with viscous dissipation effects are studied. After finding the invariants, an analytic solution for the governing system of differential equations is calculated. An unsteady stretching sheet case is considered to observe the flow characteristics.

In chapter four, two cases namely; (i) the stagnation point flow phenomenon in the presence of thermal radiation effects are taken into account. The governing equations are simplified through group a theoretic method. For a particular invariant we consider the flat plate case to observe the flow characteristics.In case (ii) the similarity analysis of MHD Hall current effects on free convective non-Newtonian flow with heat transfer phenomenon is presented.By considering flat plate case the governing system of ordinary differential equations are solved by numerical technique to observe the flow behavior.

In chapter five, the non-Newtonian flow with heat and mass transfer over the stretching walls in the presence of source/sink effects are analyzed by using Lie group method. The influence of different physical parameters on velocity, temperature and concentration profiles are presented through graphs and tables.

In chapter six, the Lie group analysis of MHD non-Newtonian flow with heat transfer over a stretching rotating surface is reported. Flow characteristics are also investigated through graphs and tables.

Chapters seven summarize the presented study and suggest some future work.

Contents

Chapter 1

Introduction

The history of differential equations started when Newton discovered Calculus as integrals in 1665 - 1666. After that, many mathematicians of that century, for example, Leibniz and Bernoulli contributed to the field of differential equations. They worked on the solution of various types of equations. In 1712, Ricatti introduced a method for the solution of a differential equation, now known as the Ricatti equation, while Clairaut studied and solved a special type of differential equation now known as the Clairaut differential equation. He also gave some remarkable results on the existence of an integrating factor for first order differential equations. Solution by series method and variation of parameters method are inventions of Euler. The Laplacian of a function and the Fourier transformation play a vital role in calculating the solution of differential equations. These were developed by P. S. Laplace and J. Fourier respectively. In this field, the contributions of Taylor, d'Alembert, Lagrange, Legendre and Bessel cannot be ignored.

Cauchy investigated the existence and uniqueness of the solution of differential equations in the 19th century, while Lipschitz developed the existence theorem for first order differential equations. Other notable contributions were made by Hermite, Liouville, Riemann, Kovalevski, Laguerre, Noether, Gauss and Lie. The history of partial differential equations started in the 18th century after Euler's work in this era. After that, d'Alembert, Lagrange, Laplace and Riemann made efforts for the development of this field. The vast use of partial differential equations in every branch of science makes this theory valuable for research.

The (1 + 1)-dimensional wave equation was studied by d'Alembert in 1752, and in 1759 it

was extended to the (1+2)-dimensions by Euler. Further work was done by Daniel Bernoulli in 1762 to extend it to the (1 + 3)-dimensions. The Euler equation for incompressible flows was modelled by Euler in 1755. The Monge-Ampere equation was studied by Monge in 1775. The Laplace equation was discussed in 1780 by Laplace. The heat equation was introduced by Fourier between 1810 and 1822. Similarly, the Laplace and Poisson equations, Navier-Stokes equations, Maxwell's equations, the Helmholtz equation, Kdv equation and many more are the discoveries of the 19th century. In 1747 d'Alembert and in 1748 Euler introduced the method of separation of variables and superposition solution of linear equations. In the 19th century, many powerful tools were introduced and mathematicians worked on the solution of partial differential equations. The method of Green's functions was introduced in 1835 for Laplace's equation. The power series methods have been used by Euler, d'Alembert, Laplace and others. Existence and uniqueness of the solutions for Laplace's equation for any continuous Dirichlet boundary data was proved in 1880 by Poincare. The successive approximation method to obtain solution of nonlinear partial differential equation was applied by Picard in early 1880 while in 1898, Poincare proved a remarkable result about the existence of the solution of a nonlinear equation.

At the end of 19th century, Lie discovered a systematic method for the solution of differential equations and applied the theory of groups for this purpose. He considered a differential equation as a surface in the space of independent and dependent variables together with its derivatives. In 1870, he presented a mechanism for finding a transformation which maps solutions of a differential equation to other solutions of the same differential equation. These transformations satisfy all the axioms of a group and hence are called symmetry or Lie group. One of the amazing properties of these symmetry groups is that when a symmetry is applied to the partial differential equation, it provides an extra constraint on that partial differential equation which reduces the dimension (number of independent variables) of the partial differential equation by one. Reduction, analysis and classification of a differential equation are the revolutionary aspects of Lie theory. Lie's contribution is considered as one of the important chapters of the modern theory of differential equations.

The first few chapters of Cohen's book [1] give a very lucid description of the concept of a Lie group and the idea of invariance under a group. In his 1906 treatise on The Theory of Dif-

ferential Equations, Andrew Forsyth [2] devoted several chapters to Lie groups and Backlund transformations. It is a fact, however, that shortly thereafter, Lie's ideas fell into obscurity and remained so until soon after World War II. As researchers began to turn more and more often to nonlinear problems and as the inherent importance of symmetries began to be recognized, Lie's ideas gained renewed interest. The Lie algorithm used to analyze the symmetry of mathematical expressions was developed to an advanced state through the pioneering efforts of Ovsiannikov [3] and his students in the Soviet Union. In the United States, Garrett Birkhoff [4] at Harvard, the son of George Birkhoff, played a key role in bringing attention to Lie's ideas by clarifying the relationship between group invariance and dimensional analysis as applied to problems in fluid mechanics. Fluid mechanics, governed by nonlinear equations from which a rich variety of simplified nonlinear and linear approximations can be derived, is an especially fertile source of examples and applications of group theory. During the same period, new ideas about the role of similarity solutions as approximations to realistic complex physical problems were being developed by Barenblatt and Zel'dovich [5] in the Soviet Union. By the late 1960s and early 1970s the whole field was active again, and new applications of group theory were being developed by a number of researchers, including Ibragimov in the Soviet Union [6], Bluman and Cole at Caltech [7], Anderson, Kumei, and Wulfman at the University of the Pacific [8], Chester at Bristol [9], Harrison and Estabrook at the Jet Propulsion Laboratory [10], and many others. Today, group analysis in one form or the other, is the central topic of a number of excellent textbooks, including Hansen [11], Ames [12], Olver [13], Bluman and Kumei [14], Rogers and Ames [15], Stephani [16], and later Ibragimov [17], Andreev et al. [18], Hydon [19] , Baumann [20] and Bluman and Anco [21]. The valuable collection of results by researchers around the world are contained in the CRC series edited by Ibragimov [22] which gives testimony to the achievements of the last half century or so. Today, symmetry analysis constitutes the most important (indeed one might say the only) widely applicable method for finding analytical solutions of nonlinear problems. The Lie algorithm can be applied virtually to any system of ODEs and PDEs. Moreover the procedure is highly systematic and amenable to programming with symbolic manipulation software. As a result sophisticated software tools are now available for analyzing the symmetries of differential equations [23-25]. Also the review of symbolic software for group analysis is given by Hydon [19] and Hereman [26].

Similarity analysis reduces the number of variables that govern partial differential equations (pde) and consequently changes it to an ordinary differential equations (ode). Methods available in the literature for similarity analysis can be classified as (i) Dimensionless Analysis, (ii) Free Parameter, (iii) Separation of variables, and (iv) Group Theory [11,12]. Among these, the group methods can be considered to be the most powerful, sophisticated, and systematic methods to generate similarity transform and is widely used. In case of group theory, the similarity solution is the invariant solution of initial and boundary value problems. Group invariant transformations do not change the structure form of the equations under investigation. When the similarity variables are substituted into the original system of PDEs the result is a new system in one fewer variables thus achieving a simplification of the problem. The substitution process can be quite difficult if the integrals happen to be complicated functions of the old variables. However, in practice, the groups that find the widest application tend to be elementary dilation and translation groups for which the characteristic equations can be separated. This makes it relatively easy to choose which integrals to use as new independent variables and which ones to use as dependent variables. Normally the new independent variables would be arranged to involve only the original independent variables although, in principle, that need not be the case and there are situations where one might want to exchange independent and dependent variables.

By using this method one can find symmetries of almost any differential equation (if they exist) and these symmetries can simplify the analysis of physical problems.

Sakiadis [27] initiated the study of boundary layer flow over a continuous solid surface moving with constant speed. Crane [28] analyzed the steady fluid flow past a stretching sheet and presented a closed form solution to it. The heat and mass transfer effects over a permeable sheet stretching in its own plane was examined by Gupta and Gupta [29]. Grubka and Bobba [30] assumed power law distribution of temperature and used Kummer's function to study the heat transfer phenomenon along a linearly stretching surface. Liu [31] investigated the flow and heat transfer of an electrically conducting fluid of second grade in a porous medium over a stretching sheet. Anjali et al. [32] studied the effects of viscous and Joules dissipation on hydromagnetic flow, heat and mass transfer past a stretching porous surface. Bhargava et al. [33] used finite element techniques to study the pulsating flow of non-Newtonian fluid known as Casson fluid in

a non-Darcian porous medium. Beg et al. [34] analyzed the free convection MHD flow, heat and mass transfer over a stretching surface through a saturated porous medium and also examined the Soret and Dufour effects during the flow phenomenon. Yurusoy and Pakdemirli [35] used group theoretical analysis to obtain the exact solution of second grade fluid over a stretching surface. Mehmood et al. [36] used symmetry reduction to examine unsteady MHD aligned second grade flow and found the general solution. Afify [37] made use of Lie symmetries to study MHD aligned creeping flow and heat transfer in second grade fluids. Later, Arasu et al. [38] investigated Lie theoretical analysis to study the thermal diffusion effects on free convection flow over a porous stretching sheet with variable stream conditions. However, it is required to analyze the non-Newtonian fluid with source/sink effects over permeable stretching sheet. This work has been investigated through group theoretic method in the chapter 2 section 1 of this thesis. In this chapter we calculate the exact solutions of the governing system. The work has also been published in Indian Journal of Physics [39].

The boundary layer flow of an electrically conducting fluid and radiative heat transfer situation arises in many practical applications such as in electrical power generation, solar power technology, space vehicle re-entry, nuclear reactors etc. Also, radiative heat transfer occurs in many geophysical and engineering applications such as nuclear reactors, migration of moisture through air contained in fibrous insulations, nuclear waste disposal, dispersion of chemical pollutants through water-saturated soil. Because of its important applications many researchers analyzed this flow and heat transfer phenomena in different geometries. Chamkha [40] considered coupled heat and mass transfer by natural convection in the presence of magnetic field and radiation effects. Mahmoud [41] also examined the thermal radiation effect on unsteady MHD free convection flow past a vertical plate. The effects of viscous dissipation and radiation on thermal boundary layer over a nonlinearly stretching sheet was discussed by Cortell [42]. The radiation effects on Blasius flow was investigated by Bataller [43]. Hsiao [44] determined the radiation effects with mixed convection over a nonlinearly stretching sheet. Thermal radiation effects are also important in non-Newtonian fluid flows due to their applications in industrial processes. We consider the Casson fluid flow with MHD, over permeable stretching sheet in the presence of thermal radiation effects. This problem has been discussed in Chapter 2 section 2 by using the Lie group method. This work also been published in Journal of Applied Fluid

Mechanics [45].

Unsteady non-Newtionian fluid flows are also important in engineering and science. For example, Eldabe et al. [46] examined the effects of couple stresses on MHD of a non-Newtonian unsteady flow between parallel porous plates. Ali et al. [47] analyzed unsteady boundary layer flow adjacent to permeable stretching surface in a porous medium. Unsteady flow near a stretching surface with viscous dissipation in presence of external magnetic field was discussed by Abel et al. [48]. The effects of couple stress and wall mass flux of pulsatile non-Newtonian flow through a channel were studied by Zueco et al. [49]. Mahmoud et al. [50] solved the case for MHD flow with heat transfer in a non-Newtonian liquid film over an unsteady stretching sheet. Mukhopadhyay et al. [51] examined the Maxwell fluid flow past an unsteady stretching permeable surface embedded in a porous medium with thermal radiation effects. Khader et al. [52] investigated the thin film flow and heat transfer of Powell-Eyring fluid over an unsteady stretching sheet with internal heat generation by using the numerical approach. We have extended the idea of MHD flow of non-Newtonian fluid over an unsteady stretching sheet with viscous dissipation effects by using the group invariant method. In detail we have presented this in chapter 3. The work is already accepted for publication in Journal of Applied Fluid Mechanics and Technical Physics.

Stagnation point flow phenomenon and heat transfer is important in the process of polymer extrusion, paper production, insulating materials, glass drawing, continuos casting, fine fibermate and many others. First time the two-dimensional stagnation-point flow of a viscous fluid toward a linear stretching surface was analyzed by Chiam [53]. The effects of heat transfer in the stagnation point flow toward a stretching surface is studied by Mahapatra and Gupta [54]. The steady stagnation point flow of an incompressible micropolar fluid over a stretching surface was investigated by Nazar et al. [55]. Mahapatra et al. [56] found the oblique stagnation point flow of an incompressible viscoelastic fluid towards a stretching surface. Numerous studies such as [57-62] have been devoted to this topic under varied assumptions. Hamad et al. [63] applied the Lie group method to investigate radiation effects on heat and mass transfer in MHD stagnation-point flow with temperature dependent viscosity. We extend the work of Hamad by considering non-Newtonion fluid by considering the Casson Fluid Model with thermal radiation effects through Lie group technique. This problem is presented in Section 1 of Chapter 4 of this

thesis.

In an ionized gas where the density is low and/or the magnetic field is very strong, the conductivity normal to the magnetic field is reduced due to the free spiralling of electrons and ions about the magnetic lines of force before suffering collisions, also a current is induced in a direction normal to both the electric and the magnetic fields. This phenomenon, well known in the literature, is called the Hall effect. The study of magnetohydrodynamic viscous flows with Hall currents has important engineering applications in problems of magnetohydrodynamic generators and of Hall accelerators as well as in flight magnetohydrodynamics. The magnetohydrodynamic free convection flow of an electrically conducting fluid along a hot semi-infinite vertical flat plate is of considerable interest in the technical field due to its frequent occurrence in industrial and technological applications. The effect of Hall currents on the magnetohydrodynamic boundary layer flow past a semi-infinite flat plate was first considered by Katagiri [64]. Pop [65] analyzed the Hall effects on hydromagnetic flow near an accelerated plate. Hossain [66-68] studied the effect of Hall current on unsteady hydromagnetic free convection flow near an infinite vertical porous plate and along a porous flat plate as well. Later on, many scientists [69-72] worked on Hall effects by considering different geometries. Dresner [73] found the similarity solution of nonlinear partial differential equations. Some study of group invariance with boundary value problems can be found in [74]. Pakdemirli [75] used the similarity method to analyze the boundary layer equations of a class of non-Newtonian fluids. Furthermore, Megahed et al. [76] calculated the similarity variables of Hall effects on free convection flow and mass transfer past a semi-infinite vertical flat plate by applying the Lie group technique. The extension of above mentioned work has been taken into account for non-Newtonian Casson fluid with thermal heat generation. Governing partial differential equations are transformed to ordinary differential equations by using scaling symmetries. This study constitutes the 4th Chapter, Section 2 of this dissertation.

Flows through channels have applications in the fields of binary gas diffusion, microfluidic devices, surface sublimation, ablation cooling, filtration, grain regression and modeling of air circulation in the respiratory system. Laminar air-flow systems have been used by the aerospace industry to control particulate contamination. The use of laminar flow equipment has eliminated the occurrence of false-positive tests due to extraneous laboratory contamination. The problem

of the laminar steady incompressible flow through a porous channel with suction/injection through the walls was studied by Berman [77]. Terrill [78] considered the laminar flow with large injection in a uniformly porous channel. Two dimensional flow of a viscous fluid in a channel with porous walls was analyzed by Cox [79]. The problem of flow through channel was further studied by Shrestha and Terril [80,81], Brady [82], Waston et al. [83], Robinson [84], and Taylor et al. [85] under various flow assumptions and boundary conditions. Sutton et al. [86] presented the exact solution to Navier Stokes equations for the motion of an incompressible viscous fluid in a channel with different pressure gradients. An exact solution was found by Fang [87] of slip MHD viscous flow over a stretching sheet. It is quite necessary to find the non-Newtonion fluid flow with heat transfer analysis by considering the source/sink effects through group theoretic approach. Moreover, we also consider parallel walls with mass transfer phenomena. This particular study has been done in Chapter 5.

The study of flow field due to a rotating disk has found many applications in different fields of engineering and industry. A number of real processes can be undertaken using disk rotation such as: fans, turbines, centrifugal pumps, rotors, viscometers, spinning disk reactors and other rotating bodies. The history of rotating disk flows goes back to the celebrated paper by Von Karman [88] who initiated the study of incompressible viscous fluid over an infinite plane disk rotating with a uniform angular velocity. This model is further investigated by many researchers to provide analytical and numerical results for better understanding of the flow behavior due to rotating disk. The use of similarity transformations to convert governing Navier Stokes equations for axi-symmetric flow into a system of coupled nonlinear ordinary differential equations was originated by Von Karman [88] and the numerical results for these equations were presented by Cochran [89]. Millsaps and Pohlhausen [90] considered the effects of heat transfer over a rotating disk at a constant temperature. Finding exact solutions for the Navier–Stokes equations is of fundamental importance in understanding and development of fluid mechanics. Von Karman and Lin [91] gave the mathematical proof for the existence of exact solutions. Initially Fang [92] proposed the steady flow over a rotating and stretching disk. Further, Fang and Zhang [93] studied the flow between two stretching disks. Awad [94] presented an asymptotic model to analyze the heat transfer phenomena over a rotating disk for large Prandtl numbers. The exact solutions for heat and mass transfer over a permeable rotating

disk of viscous fluid were presented by Turkyilmazoglu [95]. Shevchuk [96] published a book on convective heat and mass transfer in rotating disk systems, which also shines light on rotating disk systems. Recently, the combined effects of magnetohydrodynamic on radially stretching disk were analyzed by Turkyilmazoglu [97]. Flow due to a rotating rough and porous disk with heat and mass transfer phenomenon also studied by Turkyilmazoglu [98]. More recently, Asghar et al. [99] examined the viscous fluid with heat transfer over a stretching rotating disk by using the Lie group approach. We observe that all of above mentioned studies were undertaken for viscous fluid. It is also important to consider the rotating stretching disk for non-Newtonion case. In Chapter 6 we have worked on this particular flow phenomenon by employing the Lie group approach.

1.1 Preliminaries

In this section we present a number of definitions that will provide the necessary background for this thesis. We discuss various aspects of symmetries, Navier-Stokes equations for the flow and energy equations, boundary layer equations and some basic definitions of flow and heat characteristics most of which are well known.

1.1.1 Symmetries

The symmetry group of a system of differential equations is the largest local group of transformations acting on the independent and dependent variables of the system with the property that it transforms solutions of the system to other solutions. Let $\mathcal{S}$ be a system of differential equations. A symmetry-group of the system $\mathcal{S}$ is a local group of transformations $\mathcal{G}$ acting on an open subset $\mathcal{M}$ of the space of independent and dependent variables for the system with the property that whenever $u = f(x)$ is a solution of $\mathcal{S}$, and whenever $g \cdot f$ is defined for $g \in G$, then $\tilde{u} = g \cdot f(x)$ is also a solution of the system.

Definition 1 *A vector field* $\mathbf{v}$ *on* M *assigns a tangent vector* $\mathbf{v} \mid_x \in TM \mid_x$ *to each point* $x \in M$, *with* $\mathbf{v} \mid_x$ *varying smoothly from point to point. In local coordinates* $(x^1, ..., x^p)$ *a vector field has the form*

$$\mathbf{v} \mid_x = \xi^1(x)\frac{\partial}{\partial x^1} + \xi^2(x)\frac{\partial}{\partial x^2} + ... + \xi^p(x)\frac{\partial}{\partial x^p}, \tag{1.1}$$

where each $\xi^i(x)$ is a smooth function of x. (Technically, we should put the symbol $|_x$ on each $\partial/\partial x^i$ to indicate in which tangent space $TM\,|_x$it lies.)

For $(x,u) \in M \subset X \times U$ consisting of independent variables $(x^1,...,x^p)$ and all dependent variables $(u^1,u^2,...,u^q)$ a vector field on M takes the form

$$\overrightarrow{V} = \sum_{i=1}^{p} \xi^i \frac{\partial}{\partial x^i} + \sum_{\alpha=1}^{q} \sum_{J} \phi_\alpha^J \frac{\partial}{\partial u_J^\alpha}. \tag{1.2}$$

The general formula for prolongation

$$\overset{(n)}{\Pr}\, \overrightarrow{V} = \overrightarrow{V} + \sum_{\alpha=1}^{q} \sum_{J} \phi_\alpha^J(x, u^{(n)}) \frac{\partial}{\partial u_J^\alpha}, \tag{1.3}$$

defined on the corresponding jet space $M^{(n)} \subset X \times U^{(n)}$, in which the second summation being over all unordered, multi-indices $J = (j_1, j_2, ..., j_k)$, with $1 \leq j_k \leq p$, $1 \leq k \leq n$. The coefficient functions ϕ_α^J of $\Pr^{(n)} \overrightarrow{V}$ are given by the following formula:

$$\phi_\alpha^J(x, u^{(n)}) = D_J(\phi_\alpha - \sum_{i=1}^{p} \xi^i u_i^\alpha) + \sum_{i=1}^{p} \xi^i u_{J,i}^\alpha, \tag{1.4}$$

where $u_i^\alpha = \partial u^\alpha / \partial x^i$, and $u_{J,i}^\alpha = \partial u_J^\alpha / \partial x^i$, in which p is the number of the independent variables, ξ^i are the coefficients of the partial derivative of the independent variables, q is the number of dependent variables, and D_i is the total derivative given by

$$D_i f = \frac{\partial f}{\partial x^i} + \sum_{\alpha=1}^{q} \sum_{J} u_{J,i}^\alpha \frac{\partial f}{\partial u_J^\alpha}, \tag{1.5}$$

where

$$u_{J,i}^\alpha = \frac{\partial u_J^\alpha}{\partial x^i} = \frac{\partial^{k+1} u^\alpha}{\partial x^i \partial x^{j_1} ... \partial x^{j_k}}, \tag{1.6}$$

and $J = (j_1, j_2, ..., j_k), 0 \leq J \leq n$, n is the highest order derivative appearing in f.

1.1.2 Lie brackets

The most important operation on vector fields is their Lie bracket or commutator. This is most easily defined in terms of their actions as derivations on functions. Specifically, if v and w are

vector fields on M, then their Lie bracket $[v, w]$ is the unique vector field satisfying

$$[v, w](f) = v(w(f)) - w(v(f)), \tag{1.7}$$

for all smooth functions $f : M \to \mathbb{R}$. It is easy to verify that $[v, w]$ is indeed a vector field. In local coordinates, if

$$v = \sum_{i=1}^{m} \xi^i(x) \frac{\partial}{\partial x^i}, w = \sum_{i=1}^{m} \eta^i(x) \frac{\partial}{\partial x^i}, \tag{1.8}$$

$$[v, w] = \sum_{i=1}^{m} \{v(\eta^i) - w(\xi^i)\} \frac{\partial}{\partial x^i} = \sum_{i=1}^{m} \sum_{j=1}^{m} \left\{ \xi^j \frac{\partial \eta^i}{\partial x^j} - \eta^j \frac{\partial \xi^i}{\partial x^j} \right\} \frac{\partial}{\partial x^i}. \tag{1.9}$$

Proposition 2 *The Lie bracket has the following properties:*

(a) Bilinearity

$$[cv + c'v', w] = c[v, w] + c'[v', w], \tag{1.10}$$

where c, c' are constants.

(b) Skew-Symmetry

$$[v, w] = -[w, v]. \tag{1.11}$$

(c) Jacobi Identity

$$[u, [v, w]] + [w, [u, v]] + [v, [w, u]] = 0. \tag{1.12}$$

1.1.3 Structure constants

Suppose g is any finite-dimensional Lie algebra, so g is the Lie algebra of some Lie group G. If we introduce a basis $\{v_1, ..., v_r\}$ of g, then the Lie bracket of any two basis vectors must again lie in g. Thus there are certain constants c_{ij}^k, $i, j, k = 1, 2, ..., r$ called the structure constants of g such that

$$[v_i, v_j] = \sum_{k=1}^{r} c_{ij}^k v_k, \ \ i, j = 1, 2, ..., r. \tag{1.13}$$

Note that since v_i's form a basis, if we know the structure constants, then we can recover the Lie algebra g just by using (1.13) and the bilinearity of the Lie bracket.

1.1.4 Commutator tables

The most convenient way to display the structure of a Lie algebra is to write it in tabular form. If g is an r-dimensional Lie algebra and $v_1, ..., v_r$ form a basis for g, then the commutator table for g will be the $r \times r$ table whose $(i,j) - th$ entry expresses the Lie bracket $[v_i, v_j]$. Note that the table is always skew-symmetric since $[v_i, v_j] = -[v_j, v_i]$; in particular, the diagonal entries are all zero. The structure constants can be easily read off the commutator table; namely c_{ij}^k is the coefficient of v_k in the $(i,j) - th$ entry of the table.

1.1.5 Solvable Lie algebras

If we consider nth order ordinary differential equations admitting r-parameter Lie group of transformations. We can show that if $r = 1$ then the order can be reduced constructively by one; if $n \geq 2$ and $r = 2$ the order can be reduced constructively by two; if $n \geq 3$ and $r \geq 3$ it will not necessarily follow that the order can be reduced by more than two. However if the r-dimensional Lie algebra of infinitesimal generators of the admitted r-parameter group has a q-dimensional solvable subalgebra then the order of the differential equation can be reduced constructively by q.

Definition 3 *A subalgebra $\varphi \subset \pounds$ is called an ideal or normal subalgebra of $\pounds$ if for any $X \in \varphi, Y \in \pounds$, [X,Y]$\in \pounds$.*

Definition 4 *$\pounds^q$ is q-dimensional solvable Lie algebra if there exists a chain of sub algebras*

$$\pounds^{(1)} \subset \pounds^{(2)} \subset ...\pounds^{(q-1)} \subset \pounds^{(q)} = \pounds^q,$$

such that $\pounds^{(k)}$ is a k-dimensional Lie algebra and $\pounds^{(k-1)}$ is an ideal of $\pounds^{(k)}$, $k = 1, 2, ..., q$. [$\pounds^{(0)}$ is the null ideal which has no nonzero vectors].

Definition 5 *$\pounds$ is called an Abelian Lie algebra if for any $X_\alpha, X_\beta \in \pounds$, $[X_\alpha, X_\beta] = 0$.*

Proposition 6 *Every two-dimensional Lie algebra is solvable.*

1.1.6 The adjoint representation

The adjoint representation of a Lie group on its Lie algebra is often most easily reconstructed from its infinitesimal generators. If $\mathbf{v}$ generates the one- parameter subgroup $\{exp(\varepsilon \mathbf{v})\}$, then we let $ad\ \mathbf{v}$ be the vector field on g generating the corresponding one-parameter group of adjoint transformations

$$ad\ \mathbf{v}\mid_w = \frac{d}{d\varepsilon} \mid_{\varepsilon=0} Ad(\exp(\varepsilon \mathbf{v}))\mathbf{w}, \mathbf{w} \in \mathbf{g}.$$

A fundamental fact is that the infinitesimal adjoint action agrees (up to sign) with the Lie bracket on g.

Definition 7 *Let G be a Lie group with Lie algebra g. For each $\mathbf{v} \in g$, the adjoint vector ad $\mathbf{v}$ at $w \in g$ is*

$$ad\ \mathbf{v}\mid_w = [w, v] = -[v, w],$$

where we are using the identification of $Tg|_w$with g itself since g is a vector space.

In term of Lie series we represent as

$$\begin{aligned} Ad(\exp(\varepsilon \mathbf{v}))\mathbf{w} &= \sum_{n=0}^{\infty} \frac{\varepsilon^n}{n!}(ad\mathbf{v})^n\mathbf{w} \\ &= \mathbf{w} - \varepsilon[\mathbf{v}, \mathbf{w}] + \frac{\varepsilon^2}{2!}[\mathbf{v}, [\mathbf{v}, \mathbf{w}]] - .... \end{aligned} \tag{1.14}$$

Definition 8 *Two Lie subalgebras L_1 and L_2 of a Lie algebra L are similar if there exists an inner automorphism $\phi \in Int(L)$ such that $\phi(L_1) = L_2$. Since the similarity between Lie subalgebras is a relation of equivalence, all subalgebras of the given Lie algebra L are decomposed into classes of similar algebras. A set of the representatives of each class is called an optimal system of subalgebras.*

Therefore, the knowledge of an optimal system of subalgebras of the principal Lie algebra of a system of differential equations provides a method of classifying H–invariant solutions [13,100].

1.1.7 Governing laws

Mostly, three fundamental laws of conservation are used to discuss the characteristics of viscous incompressible fluids. These laws are given by

$$\operatorname{div}\mathbf{V} = 0, \text{ (Law of conservation of mass)}, \tag{1.15}$$

$$\rho\frac{D\mathbf{V}}{Dt} = \operatorname{div}\mathbf{T}+\rho\mathbf{b}, \text{ (Law of conservation of momentum)}, \tag{1.16}$$

$$\rho c_p\frac{DT}{Dt} = \mathbf{T}.\mathbf{L} + k\nabla^2 T, \text{ (Law of conservation of energy)}, \tag{1.17}$$

where ρ is the density, $\mathbf{V}$ is velocity vector, D/Dt denotes the substantive derivative which is a combination of the local derivative with respect to time (in unsteady flows) $\partial/\partial t$ and the convective derivative (due to translation), $\mathbf{b}$ is the body force, k is the thermal conductivity of the fluid, c_p is the specific heat, T is the temperature, $\mathbf{T}$ is the Cauchy stress tensor and for viscous fluid it is defined as

$$\mathbf{T} = -p\mathbf{I} + \mu\mathbf{A}_1, \tag{1.18}$$

where p is the pressure, $\mathbf{I}$ the identity tensor, μ the viscosity, $\mathbf{A}_1$ is the extra stress tenser and is given by

$$\mathbf{A}_1 = \mathbf{L} + \mathbf{L}^{tr}, \tag{1.19}$$

here $\mathbf{L}$ is the velocity gradient, $\mathbf{T}\cdot\mathbf{L}$ is the trace of the product of both matrices and is defined as

$$\mathbf{T}\cdot\mathbf{L} = Tr(\mathbf{TL}), \tag{1.20}$$

where 'Tr' denotes the trace of matrix. The divergence div of any vector function $V(x, y, z; t)$ in Cartesian coordinates is defined as

$$\operatorname{div}\mathbf{V} = \frac{\partial u}{\partial x} + \frac{\partial v}{\partial y} + \frac{\partial w}{\partial z}. \tag{1.21}$$

Hence the law of conservation of momentum is modified by considering the effects of magneto-hydrodynamic as

$$\rho\frac{D\mathbf{V}}{Dt} = \operatorname{div}\mathbf{T}+\rho\mathbf{b} + \mathbf{J}\times\mathbf{B}, \tag{1.22}$$

where $\mathbf{J}$ is the current density, $\mathbf{B} = \mathbf{B}_0 + \mathbf{b}_0$ is the magnetic flux, $\mathbf{B}_0$ is applied magnetic field and $\mathbf{b}_0$ the induced magnetic field. This includes the following four laws of conservation in addition to (1.15)-(1.17)

$$\operatorname{div}\mathbf{E} = \frac{1}{\epsilon_0}\rho, \text{(Gauss's law)}, \tag{1.23}$$

$$\operatorname{curl}\mathbf{E} = -\frac{\partial \mathbf{B}}{\partial t}, \text{(Faraday's law)}, \tag{1.24}$$

$$\operatorname{curl}\mathbf{B} = \mu_0\mathbf{J}, \text{(Ampere's law with Maxwell's correction)}, \tag{1.25}$$

$$\operatorname{curl}\mathbf{B} = \mathbf{0}, \text{(Gauss's law for magnetism)}, \tag{1.26}$$

where μ_0 is the magnetic permeability, ϵ_0 is the permittivity of free space, and $\mathbf{E}$ is the electric field. The boundary layer free convection flow, generalized Ohm's law and Maxwell's equations are given by [75,82,83]

$$\operatorname{div}\mathbf{V} = 0, \tag{1.27}$$

$$(\mathbf{V}.\operatorname{grad})\mathbf{V} = -\left(\frac{1}{\rho}\right)\operatorname{grad} p + \upsilon\left(1 + \frac{1}{\beta}\right)\nabla^2\mathbf{V} + \mathbf{g}\beta_1(T - T_\infty) + \left(\frac{1}{\rho}\right)\mathbf{j}\times\mathbf{B}, \tag{1.28}$$

$$(\mathbf{V}.\operatorname{grad})T = \frac{k}{\rho c_p}\nabla^2 T - \operatorname{div} q_r, \tag{1.29}$$

$$\mathbf{j} = \sigma\left(\mathbf{E} + \mathbf{V}\times\mathbf{B} - \frac{1}{en_e}\mathbf{j}\times\mathbf{B} - \frac{1}{en_e}\operatorname{grad} p_e\right), \tag{1.30}$$

$$\operatorname{div}\mathbf{B} = 0, \tag{1.31}$$

$$\vec{\nabla}\times\mathbf{B} = 0, \tag{1.32}$$

$$\vec{\nabla}\times\mathbf{E} = 0. \tag{1.33}$$

1.1.8 Basic definitions for flow characteristics

Here we write some basic definitions for flow characteristics.

Boundary-layer thickness

In the boundary-layer region where the velocity gradient is large, the velocity of the fluid u rises rapidly from 0 at the wall to the free stream velocity U_∞ asymptotically. Practically, we

define the boundary-layer thickness δ as the distance from the wall where u=0.99U_∞ or in other words, the boundary-layer thickness is the distance from the wall where the fluid velocity is equal to 99% of the unperturbed free stream velocity.

Skin friction

The boundary layer produces a drag on the plate due to the viscous stresses which are developed at the wall. The skin friction at the wall τ_w is defined as the viscous force per unit area acting at the surface and, in Cartesian coordinate system, is given by

$$\tau_w = \lim_{y \to 0} \mu \left(\frac{\partial u}{\partial y} \right). \tag{1.34}$$

The local skin friction coefficient C_f on the wall is defined by

$$C_f = \frac{\tau_w}{\rho U_\infty^2}. \tag{1.35}$$

Nusselt number

When a fluid at one temperature is in contact with a solid surface at different temperature, and its rate to unit area is given by

$$q_w = -k \frac{\partial T}{\partial y} \mid_{y=0}, \tag{1.36}$$

where k is the conductivity of the fluid. The Nusselt number Nu is the dimensionless quantity which represents the ratio of convective to conductive heat transfer across (normal to) the boundary and is defined by

$$Nu = \frac{q_w x}{k(T_w - T_\infty)}, \tag{1.37}$$

where q_w is the heat transfer rate at the surface, x the distance of the flow from the surface edge, T_w is the surface temperature and T_∞ is the ambient temperature.

Reynolds number

The Reynolds number R is a dimensionless number which frequently arises in the fluid flow problems when the dimensional analysis is performed. It gives a measure of the ratio of inertial

forces to viscous forces and consequently quantifies the relative importance of these two types of forces for given flow conditions. The Reynolds number provides the basis for the distinction of the flow system as either laminar or turbulent. This number is defined as

$$R = \frac{UL}{\nu}, \tag{1.38}$$

where ν is the kinematic viscosity, U is the mean velocity of the fluid and L is the characteristic length of the geometry.

Prandtl number

In heat transfer analysis of fluid flow, the most commonly occurred dimensionless quantity is the Prandtl number Pr defined as

$$\mathrm{Pr} = \frac{\mu C_p}{k}. \tag{1.39}$$

The Prandtl number is the ratio of viscous diffusion rate to the thermal diffusion rate. Clearly, this parameter involves fluid properties only, rather than length and velocity scales of the flow hence there are dramatic differences among the fluids in their relative Prandtl numbers.

Eckert number

Another quantity of fundamental importance usually arises in the dimensionless energy equation, if the viscous dissipation is taken into account, is the Eckert number Ec. The Eckert number is given by

$$Ec = \frac{U^2}{C_p \Delta T}. \tag{1.40}$$

The Eckert number is the ratio of kinetic energy to the Enthalpy driving force in heat transfer.

Casson fluid model

The rheological equation of state for an isotropic and incompressible flow of a Casson fluid [101] is

$$\tau_{ij} = \begin{cases} 2(\mu_B + \frac{p_y}{\sqrt{2\pi}})e_{ij}, \pi > \pi_c, \\ 2(\mu_B + \frac{p_y}{\sqrt{2\pi_c}})e_{ij}, \pi < \pi_c. \end{cases} . \tag{1.41}$$

Here $\pi = e_{ij}e_{ij}$ is the product of the component of deformation rate with itself, e_{ij} is the $(i,j)th$ component of the deformation rate, π_c is a critical value of this product based on the non-Newtonian model, μ_B is plastic dynamic viscosity of the non-Newtonian fluid and p_y is the yield stress of fluid.

Casson fluid is a shear thinning fluid which exhibits yield stress and behaves like a solid if a shear stress is less than the applied yield stress. On the other hand it starts to move if a shear stress is greater than the applied yield stress. Such fluids have many applications in engineering processes. Examples of Casson fluid include jelly, tomato sauce, honey, soup, concentrated fruit juices, and human blood etc.

1.1.9 Boundary-layer equations in Cartesian coordinates

In developing a mathematical theory of boundary layers, the first step is to show the existence, as the Reynolds number R tends to infinity or the kinematic viscosity ν tends to zero, of a limiting form of the equations of motion, different from that obtained by putting $\nu = 0$ in the first place. A solution of these limiting equations may then reasonably be expected to describe approximately the flow in a laminar boundary layer for which R is large but not infinite. This is the basis of the classical theory of laminar boundary layers. The full equation of motion for Casson fluid, two-dimensional flow are

$$\frac{\partial u}{\partial x} + \frac{\partial v}{\partial y} = 0, \tag{1.42}$$

$$\frac{\partial u}{\partial t} + u\frac{\partial u}{\partial x} + v\frac{\partial u}{\partial y} = -\frac{\partial p}{\partial x} + \nu(1 + \frac{1}{\beta})\left[\frac{\partial^2 u}{\partial x^2} + \frac{\partial^2 u}{\partial y^2}\right], \tag{1.43}$$

$$\frac{\partial v}{\partial t} + u\frac{\partial v}{\partial x} + v\frac{\partial v}{\partial y} = -\frac{\partial p}{\partial y} + \nu(1 + \frac{1}{\beta})\left[\frac{\partial^2 v}{\partial x^2} + \frac{\partial^2 v}{\partial y^2}\right], \tag{1.44}$$

where u, v are the velocity components in x-, y-directions, respectively. A wall is located in the plane $y = 0$. We consider non-dimensional variables

$$x' = \frac{x}{L}, y' = \frac{y}{\delta}, u' = \frac{u}{U}, v' = \frac{v}{U}\frac{L}{\delta}, p' = \frac{p}{\rho U^2}, t' = t\frac{U}{L}, \tag{1.45}$$

where δ is the boundary layer thickness at $x = L$, which is unknown. We will obtain an estimate for it in terms of the Reynolds number R, U is the flow velocity, which is aligned in the $x-$direction parallel to the solid boundary. The non-dimensional form of the governing equations is

$$\frac{\partial u'}{\partial x'} + \frac{\partial v'}{\partial y'} = 0, \tag{1.46}$$

$$\frac{\partial u'}{\partial t'} + u'\frac{\partial u'}{\partial x'} + v'\frac{\partial u'}{\partial y'} = -\frac{\partial p'}{\partial x'} + \frac{\nu}{UL}(1+\frac{1}{\beta})\frac{\partial^2 u'}{\partial (x')^2} + \frac{\nu}{UL}\frac{L^2}{\delta^2}(1+\frac{1}{\beta})\frac{\partial^2 u'}{\partial (y')^2}, \tag{1.47}$$

$$\frac{\partial v'}{\partial t'} + u'\frac{\partial v'}{\partial x'} + v'\frac{\partial v'}{\partial y'} = -\frac{L^2}{\delta^2}\frac{\partial p'}{\partial y'} + \frac{\nu}{UL}(1+\frac{1}{\beta})\frac{\partial^2 v'}{\partial (x')^2} + \frac{\nu}{UL}\frac{L^2}{\delta^2}(1+\frac{1}{\beta})\frac{\partial^2 v'}{\partial (y')^2}. \tag{1.48}$$

Inside the boundary layer, viscous forces balance inertia and pressure gradient forces. In other words, inertia and viscous forces are the same order, so

$$\frac{\nu}{UL}\frac{L^2}{\delta^2} = O(1) \Rightarrow \delta = O(R^{-1/2}L). \tag{1.49}$$

Now we drop the primes from the non-dimensional governing equations and with equation (1.49) we have

$$\frac{\partial u}{\partial x} + \frac{\partial v}{\partial y} = 0, \tag{1.50}$$

$$\frac{\partial u}{\partial t} + u\frac{\partial u}{\partial x} + v\frac{\partial u}{\partial y} = -\frac{\partial p}{\partial x} + \frac{1}{R}(1+\frac{1}{\beta})\frac{\partial^2 u}{\partial x^2} + (1+\frac{1}{\beta})\frac{\partial^2 u}{\partial y^2}, \tag{1.51}$$

$$\frac{1}{R}\left(\frac{\partial v}{\partial t} + u\frac{\partial v}{\partial x} + v\frac{\partial v}{\partial y}\right) = -\frac{\partial p}{\partial y} + \frac{1}{R^2}(1+\frac{1}{\beta})\left(\frac{\partial^2 v}{\partial x^2} + \frac{\partial^2 v}{\partial y^2}\right). \tag{1.52}$$

In the limit $R \to \infty$, the equations above reduce to

$$\frac{\partial u}{\partial x} + \frac{\partial v}{\partial y} = 0, \tag{1.53}$$

$$\frac{\partial u}{\partial t} + u\frac{\partial u}{\partial x} + v\frac{\partial u}{\partial y} = -\frac{\partial p}{\partial x} + (1+\frac{1}{\beta})\frac{\partial^2 u}{\partial y^2}, \tag{1.54}$$

$$-\frac{\partial p}{\partial y} = 0. \tag{1.55}$$

Notice that according to equation (1.55), the pressure is constant across the boundary layer. In terms of dimensional variables, the system of equations above assume the form:

$$\frac{\partial u}{\partial x} + \frac{\partial v}{\partial y} = 0, \tag{1.56}$$

$$\frac{\partial u}{\partial t} + u\frac{\partial u}{\partial x} + v\frac{\partial u}{\partial y} = -\frac{1}{\rho}\frac{\partial p}{\partial x} + \nu(1 + \frac{1}{\beta})\frac{\partial^2 u}{\partial y^2}, \tag{1.57}$$

$$-\frac{1}{\rho}\frac{\partial p}{\partial y} = 0. \tag{1.58}$$

1.1.10 Homotopy analysis method (HAM)

Zero-order deformation equation

The idea of the homotopy analysis [103] is very simple and straightforward. In most cases a nonlinear problem can be described by a set of governing equations and initial and/or boundary conditions. For brevity, let us consider here only one nonlinear equation in a general form

$$\mathcal{N}[u(\mathbf{r},t)] = 0, \tag{1.59}$$

where $\mathcal{N}$ is a nonlinear operator, $u(\mathbf{r},t)$ is an unknown function, $\mathbf{r}$ and t denote spatial and temporal independent variables respectively. Let $u_0(\mathbf{r},t)$ denote an initial guess of the exact solution $u(\mathbf{r},t)$, $\hbar \neq 0$ an auxiliary parameter, $H(\mathbf{r},t) \neq 0$ an auxiliary function, and $\mathcal{L}$ denote an auxiliary linear operator with the property

$$\mathcal{L}[f(\mathbf{r},t)] = 0 \text{ when } f(\mathbf{r},t) = 0. \tag{1.60}$$

Thus using $q \in [0,1]$ as an embedding parameter, we construct such a homotopy as

$$\mathcal{H}[\phi(\mathbf{r},t;q); u_0(\mathbf{r},t), H(\mathbf{r},t), \hbar, q] = (1-q)\mathcal{L}\{[\phi(\mathbf{r},t;q) - u_0(\mathbf{r},t)]\} - \hbar q H(\mathbf{r},t)\mathcal{N}[\phi(\mathbf{r},t);q)]. \tag{1.61}$$

It should be emphasized that the above homotopy contains the so-called auxiliary parameter $\hbar$ and the auxiliary function $H(\mathbf{r},t)$. The nonzero auxiliary parameter $\hbar$ and auxiliary function $H(\mathbf{r},t)$ are introduced for the first time in this way to construct a homotopy. So, such a kind of

homotopy is more general than traditional ones. The auxiliary parameter $\hbar$ and the auxiliary function $H(\mathbf{r},t)$ play important roles within the frame of the homotopy analysis method.

Let $q \in [0,1]$ denotes an embedding parameter. Enforcing the homotopy (1.61) to be zero, i.e.,

$$\mathcal{H}[\phi(\mathbf{r},t;q); u_0(\mathbf{r},t), H(\mathbf{r},t), \hbar, q] = 0, \tag{1.62}$$

we have the so-called zero-order deformation equation

$$(1-q)\mathcal{L}\{[\phi(\mathbf{r},t;q) - u_0(\mathbf{r},t)]\} = \hbar q H(\mathbf{r},t)\mathcal{N}[\phi(\mathbf{r},t);q)], \tag{1.63}$$

where $\phi(\mathbf{r},t;q)$ is the solution which depends upon not only the initial guess $u_0(\mathbf{r},t)$, the auxiliary linear operator $\mathcal{L}$, the auxiliary function $H(\mathbf{r},t)$ and the auxiliary parameter $\hbar$ but also the embedding parameter $q \in [0,1]$. When $q = 0$, the zero-order deformation equation (1.63) becomes

$$\mathcal{L}[\phi(\mathbf{r},t;0) - u_0(\mathbf{r},t)] = 0, \tag{1.64}$$

which gives, using the property (1.61),

$$\phi(\mathbf{r},t;0) = u_0(\mathbf{r},t). \tag{1.65}$$

When $q = 1$, since $\hbar = 0$ and $H(\mathbf{r},t) \neq 0$, the zero-order deformation equation (1.63) is equivalent to

$$\mathcal{N}[\phi(\mathbf{r},t);1)] = 0, \tag{1.66}$$

which is exactly the same as the original equation (1.59), provided

$$\phi(\mathbf{r},t;1) = u(\mathbf{r},t). \tag{1.67}$$

Thus, according to (1.65) and (1.67), as the embedding parameter q increases from 0 to 1, $\phi(\mathbf{r},t;1)$ varies (or deforms) continuously from the initial approximation $u_0(\mathbf{r},t)$ to the exact solution $u(\mathbf{r},t)$ of the original equation (1.59). Such a kind of continuous variation is called deformation in homotopy. This is the reason why we call (1.63) the zero-order deformation equation.

Define the so-called mth-order deformation derivatives

$$u_0^{[m]}(\mathbf{r},t) = \frac{\partial^m \phi(\mathbf{r},t;q)}{\partial q^m} \mid_{q=0} . \tag{1.68}$$

By Taylor's theorem, $\phi(\mathbf{r},t;q)$ can be expanded in a power series of q as follows:

$$\phi(\mathbf{r},t;q) = \phi(\mathbf{r},t;0) + \sum_{m=1}^{\infty} \frac{u_0^{[m]}(\mathbf{r},t)}{m!} q^m, \tag{1.69}$$

writing

$$u_m(\mathbf{r},t) = \frac{u_0^{[m]}(\mathbf{r},t)}{m!} = \frac{1}{m!} \frac{\partial^m \phi(\mathbf{r},t;q)}{\partial q^m} \mid_{q=0}, \tag{1.70}$$

and using (1.65), the power series (1.69) of $\phi(\mathbf{r},t;q)$ becomes

$$\phi(\mathbf{r},t;q) = u_0(\mathbf{r},t) + \sum_{m=1}^{\infty} u_m(\mathbf{r},t) q^m. \tag{1.71}$$

Note that we have great freedom to choose the initial guess $u_0(\mathbf{r},t)$, the auxiliary linear operator $\mathcal{L}$, the nonzero auxiliary parameter $\hbar$, and the auxiliary function $H(\mathbf{r},t)$. Assume that all of them are properly chosen so that:

1. The solution $\phi(\mathbf{r},t;q)$ of the zero-order deformation equation (1.63) exists for all $q \in [0,1]$.
2. The deformation derivative $u_0^{[m]}(\mathbf{r},t)$ exists for $m = 1, 2, 3, \cdots, \infty$.
3. The power series (1.71) of $\phi(\mathbf{r},t;q)$ converges at $q = 1$.

Then, from (1.67) and (1.71), we have under these assumptions the solution series

$$u(\mathbf{r},t) = u_0(\mathbf{r},t) + \sum_{m=1}^{\infty} u_m(\mathbf{r},t). \tag{1.72}$$

This expression provides us with a relationship between the exact solution $u(\mathbf{r},t)$ and the initial approximation $u_0(\mathbf{r},t)$ by means of the terms $u_m(\mathbf{r},t)$ which are determined by the so-called high-order deformation equations described below.

High-order deformation equation

For brevity, define the vector

$$\vec{u}_n = \{u_0(\mathbf{r},t), u_1(\mathbf{r},t), u_2(\mathbf{r},t), ..., u_m(\mathbf{r},t)\}.$$

According to the definition (1.70), the governing equation of $u_m(\mathbf{r},t)$ can be derived from the zero-order deformation equation (1.63). Differentiating the zero-order deformation equation (1.63) m times with respect to the embedding parameter q and then dividing it by $m!$ and finally setting $q = 0$, we have the so-called mth-order deformation equation

$$\mathcal{L}[u_m(\mathbf{r},t) - \chi_m u_{m-1}(\mathbf{r},t)] = \hbar H(\mathbf{r},t) R_m(\vec{u}_{m-1}, \mathbf{r},t), \tag{1.73}$$

where

$$\chi_m = \begin{cases} 0, & m \leq 1, \\ 1, & m > 1. \end{cases}, \tag{1.74}$$

and

$$R_m(\vec{u}_{m-1}, \mathbf{r},t) = \frac{1}{(m-1)!} \frac{\partial^{m-1} \mathcal{N}[\phi(\mathbf{r},t;q)]}{\partial q^{m-1}} \mid_{q=0} . \tag{1.75}$$

Substituting (1.71) into the above expression, we have

$$R_m(\vec{u}_{m-1}, \mathbf{r},t) = \frac{1}{(m-1)!} \left\{ \frac{\partial^{m-1}}{\partial q^{m-1}} \mathcal{N} \left[\sum_{n=0}^{\infty} u_n(\mathbf{r},t) q^n \right] \right\} \mid_{q=0} . \tag{1.76}$$

Note that the high-order deformation equation (1.73) is governed by the same linear operator $\mathcal{L}$, and the term $R_m(\vec{u}_{m-1}, \mathbf{r},t)$ can be expressed simply by (1.75) for any given nonlinear operator $\mathcal{N}$. According to the definition (1.75), the right-hand side of Equation (1.73) is only dependent upon $\vec{u}_{m-1}$. Thus, we gain $u_1(\mathbf{r},t), u_2(\mathbf{r},t), ...$ by means of solving the linear high-order deformation equation (1.73) one after the other in succession. The mth-order approximation of $u(\mathbf{r},t)$ is given by

$$u(\mathbf{r},t) \approx \sum_{k=0}^{m} u_k(\mathbf{r},t). \tag{1.77}$$

Chapter 2

Lie group study of non-Newtonion MHD flow with source/sink and thermal radiation effects

This chapter comprises of Lie group analysis of steady, incompressible, two-dimensional MHD Casson fluid flow with source/sink and thermal radiation effects through a homogenous porous medium. We divide this chapter into two sections. Section 1 consists of source/sink effects and section 2 consists of the thermal radiation effects. We formulate the system of boundary layer equations and normalize them through appropriate dimensionless variables. The detailed Lie group analysis of governing differential equations is presented. For physical interest of the fluid phenomenon we discuss one class of invariants for permeable stretching surface. Further we evaluate the analytical solutions and discuss the influence of different physical parameters on flow and heat transfer graphically. In the end, we express the findings for this study. Similarly, we have gone through section 2. In addition we also investigate the mass transfer phenomenon in section 2.

2.1 Lie group investigation of MHD Casson fluid flow with source/sink effects

2.1.1 Mathematical modeling

Consider the steady state laminar incompressible flow of a non-Newtonian Casson fluid with heat source and sink effects. The flow is assumed to be passing through a uniform porous medium with constant permeability k'. A uniform magnetic field of strength B_0 is applied parallel to the $\overline{y}$-axis. It is assumed that the fluid is electrically conducting and the magnetic Reynolds number is small so that the induced magnetic field is neglected. With Eq. (1.41) the governing equations of the flow and heat transfer are given by

$$\frac{\partial \overline{u}}{\partial \overline{x}} + \frac{\partial \overline{v}}{\partial \overline{y}} = 0, \tag{2.1}$$

$$\overline{u}\frac{\partial \overline{u}}{\partial \overline{x}} + \overline{v}\frac{\partial \overline{u}}{\partial \overline{y}} = \frac{\mu}{\rho}(1 + \frac{1}{\beta})\frac{\partial^2 \overline{u}}{\partial \overline{y}^2} - \frac{\nu}{k'}\overline{u} - \frac{\sigma B_0^2}{\rho}\overline{u}, \tag{2.2}$$

$$\overline{u}\frac{\partial T}{\partial \overline{x}} + \overline{v}\frac{\partial T}{\partial \overline{y}} = \frac{k}{\rho c_p}\frac{\partial^2 T}{\partial \overline{y}^2} + \frac{Q_0}{\rho c_p}(T - T_\infty), \tag{2.3}$$

where, $\beta = \frac{\mu_B\sqrt{2\pi_c}}{p_y}$ is the Casson fluid parameter, σ is the electrical conductivity, k' is the permeability of medium, $Q_0 > 0$ is the heat source and $Q_0 < 0$ is the heat sink, T is the temperature of the fluid, T_∞ is the ambient temperature, and $\overline{u}, \overline{v}$ are the velocity components in $\overline{x}$- and $\overline{y}$- directions respectively.

Introducing the following dimensionless variables

$$u(x,y) = \frac{\overline{u}(\overline{x},\overline{y})}{\sqrt{b\upsilon}},\ v(x,y) = \frac{\overline{v}(\overline{x},\overline{y})}{\sqrt{b\upsilon}},\ x = \sqrt{\frac{b}{\nu}}\overline{x},\ y = \sqrt{\frac{b}{\nu}}\overline{y},$$

$$\theta(x,y) = \frac{T(\overline{x},\overline{y}) - T_\infty}{(T_w - T_\infty)}. \tag{2.4}$$

Equations (2.1) – (2.3) transform as

$$\frac{\partial u}{\partial x} + \frac{\partial v}{\partial y} = 0, \tag{2.5}$$

$$u\frac{\partial u}{\partial x}+v\frac{\partial u}{\partial y}=(1+\frac{1}{\beta})\frac{\partial^2 u}{\partial y^2}-\frac{1}{K}u-Mu, \tag{2.6}$$

$$u\frac{\partial \theta}{\partial x}+v\frac{\partial \theta}{\partial y}=\frac{1}{\mathrm{Pr}}\frac{\partial^2 \theta}{\partial y^2}+Q\theta, \tag{2.7}$$

where $K=\frac{k'b}{\nu}$ is the permeability parameter, $M=\frac{\sigma B_0^2}{\rho b}$ is the Hartman number, $\mathrm{Pr}=\frac{\mu c_p}{\kappa}$ is the Prandtl number and $Q=\frac{Q_0}{b\rho c_p}$ is the dimensionless heat source or sink parameter.

Introducing the stream function ψ defined by $u=\partial\psi/\partial y$ and $v=-\partial\psi/\partial x$, Eqs. (2.5)-(2.7) take the following forms

$$(1+\frac{1}{\beta})\frac{\partial^3\psi}{\partial y^3}-\frac{\partial\psi}{\partial y}\frac{\partial^2\psi}{\partial x\partial y}+\frac{\partial\psi}{\partial x}\frac{\partial^2\psi}{\partial y^2}-(M+\frac{1}{K})\frac{\partial\psi}{\partial y}=0, \tag{2.8}$$

$$\frac{1}{\mathrm{Pr}}\frac{\partial^2\theta}{\partial y^2}-\frac{\partial\psi}{\partial y}\frac{\partial\theta}{\partial x}+\frac{\partial\psi}{\partial x}\frac{\partial\theta}{\partial y}+Q\theta=0. \tag{2.9}$$

2.1.2 Lie group analysis

A sophisticated and powerful method to obtain the particular solutions of partial differential equations is based on the study of their invariance with respect to one-parameter Lie group of point transformation. A symmetry of a differential equation is an invertible transformation of the dependent and independent variables that maps the equation to itself. Amongst symmetries of differential equations, those depending continuously on a small parameter and forming a local one-parameter group of transformation can be calculated algorithmically through a procedure due to Sophus Lie [13]. One of the most useful and striking properties of symmetries is that they map solutions to solutions. For partial differentials, symmetries allow the reduction of the number of independent variables. Consider the one-parameter Lie group of infinitesimal transformations in (x,y,ψ,θ) given by

$$\begin{aligned}
x^* &= x+\epsilon\xi(x,y,\psi,\theta)+O(\epsilon^2),\\
y^* &= y+\epsilon\tau(x,y,\psi,\theta)+O(\epsilon^2),\\
\psi^* &= \psi+\epsilon\Gamma(x,y,\psi,\theta)+O(\epsilon^2),\\
\theta^* &= \theta+\epsilon\Omega(x,y,\psi,\theta)+O(\epsilon^2),
\end{aligned} \tag{2.10}$$

where ϵ is the Lie group parameter. By following Eq. (1.2) the infinitesimal generator for the problem is

$$\vec{V} = \xi(x, y, \psi, \theta)\partial_x + \tau(x, y, \psi, \theta)\partial_y + \Gamma(x, y, \psi, \theta)\partial_\psi + \Omega(x, y, \psi, \theta)\partial_\theta. \tag{2.11}$$

We wish to find all possible coefficients ξ, τ, Γ and Ω so that the corresponding one-parameter group $\exp(\epsilon\vec{V})$ is a symmetry group of the system (2.8)-(2.9). According to the Eq. (1.3) we need to know the third prolongation of $\vec{V}$ as

$$\overset{3}{\mathrm{Pr}}\,\vec{V} = \vec{V} + \Gamma^x\partial_{\Psi_x} + \Gamma^y\partial_{\Psi_y} + \Omega^x\partial_{\theta_x} + \Omega^y\partial_{\theta_y} + \Gamma^{xy}\partial_{\Psi_{xy}} + \Gamma^{yy}\partial_{\Psi_{yy}} + \Omega^{yy}\partial_{\theta_{yy}} + \Gamma^{yyy}\partial_{\Psi_{yyy}}, \tag{2.12}$$

where coefficients with derivatives are written as

$$\begin{aligned}
\Gamma^x &= D_x(\Gamma - \xi\Psi_x - \tau\Psi_y) + \xi\Psi_{xx} + \tau\Psi_{xy}, \\
\Gamma^y &= D_y(\Gamma - \xi\Psi_x - \tau\Psi_y) + \xi\Psi_{xy} + \tau\Psi_{yy}, \\
\Omega^x &= D_x(\Omega - \xi\theta_x - \tau\theta_y) + \xi\theta_{xx} + \tau\theta_{xy}, \\
\Omega^y &= D_y(\Omega - \xi\theta_x - \tau\theta_y) + \xi\theta_{xy} + \tau\theta_{yy}, \\
\Gamma^{xy} &= D_xD_y(\Gamma - \xi\Psi_x - \tau\Psi_y) + \xi\Psi_{xxy} + \tau\Psi_{xyy}, \\
\Gamma^{yy} &= D_y^2(\Gamma - \xi\Psi_x - \tau\Psi_y) + \xi\Psi_{xyy} + \tau\Psi_{yyy}, \\
\Omega^{yy} &= D_y^2(\Omega - \xi\theta_x - \tau\theta_y) + \xi\theta_{xyy} + \tau\theta_{yyy}, \\
\Gamma^{yyy} &= D_y^3(\Gamma - \xi\Psi_x - \tau\Psi_y) + \xi\Psi_{xyyy} + \tau\Psi_{yyyy},
\end{aligned} \tag{2.13}$$

and

$$D_x\Gamma = \Gamma_x + \Gamma_\Psi\Psi_x + \Gamma_\theta\theta_x. \tag{2.14}$$

Substituting the third order prolongation (2.12) with expressions (2.13) to the system (2.8)-(2.9) and separating by powers of the derivatives of Ψ and θ as ξ, τ, Γ and Ω are independent of the derivatives of Ψ, lead to the over determined system of linear homogeneous partial differential

equations

$$\begin{aligned}
\xi_y &= 0, \xi_\psi = 0, \xi_\theta = 0, \tau_y = 0, \tau_\psi = 0, \tau_\theta = 0, \\
\Gamma_x &= 0, \Gamma_y = 0, \Gamma_{\psi\psi} = 0, \Gamma_\theta = 0, \\
\Omega_x &= 0, \Omega_y = 0, \Omega_\psi = 0, \Omega_{\theta\theta} = 0, \\
\xi_x &= \Gamma_\psi, \Omega - \theta\Omega_\theta = 0.
\end{aligned} \tag{2.15}$$

By solving the above all equations we find the following solutions for ξ, τ, Γ and Ω

$$\xi = c_3 + c_4 x,\ \tau = g(x),\ \Gamma = c_1 + c_4\psi,\ \Omega = c_2\theta. \tag{2.16}$$

There are four finite parameter Lie group symmetries represented by parameters c_1, c_2, c_3 and c_4 and one infinite symmetry $g(x)$. Parameter c_1 corresponds to the translation in the variable ψ, c_2 corresponds to the scaling in θ, c_3 corresponds to the translation in x and c_4 corresponds to the scaling in x and ψ.

The infinitesimal generators of an $r-$parameter Lie group, being solutions of a linear system of partial differential equations, span an $r-$dimensional vector space; by introducing an operation of commutation between two infinitesimal generators. Here we have a $5-$dimensional vector space of infinitesimal generators closed under the operation of commutation, i.e., $5-$dimensional Lie algebra, the basis of the corresponding Lie algebra as follows

$$V_1 = \partial_\psi, V_2 = \theta\partial_\theta, V_3 = \partial_x, V_4 = x\partial_x + \psi\partial_\psi, V_5 = \partial_y. \tag{2.17}$$

In dealing with Lie algebras of transformations admitted by differential equations, two classes play a special role, the solvable and the Abelian Lie algebras. Because we have the Lie algebra of the system (2.8)-(2.9) we want to know if the general solution of the system of differential equations can be found by quadratures. This thing is possible if the Lie group is solvable. A Lie algebra is solvable if there exists a series as we defined in chapter 1. The requirement for solvability is equivalent to the existence of a basis $\{V_1, V_2, ..., V_5\}$ of Lie algebra such that by

Eq. (1.13) we can develop the commutator table

[,]	V_1	V_2	V_3	V_4	V_5
V_1	0	0	0	0	V_1
V_2	0	0	0	0	-V_2
V_3	0	0	0	0	0
V_4	0	0	0	0	-V_4
V_5	-V_1	V_2	0	V_4	0

Table 2.1: Commutator table

By straightforward observation of commutator table we found the following Abelian Lie algebra

$$\begin{aligned} [V_\alpha, V_\beta] &= 0, \text{ as } \alpha = \beta, [V_1, V_2] = 0, [V_1, V_3] = 0, [V_1, V_4] = 0, \\ [V_2, V_3] &= 0, [V_2, V_4] = 0, [V_3, V_4] = 0, [V_3, V_5] = 0. \end{aligned}$$

Group invariant solutions

A solution of the system of partial differential equations is said to be $\mathcal{G}$-invariant if it is unchanged by all the group transformations in $\mathcal{G}$. In general, to each r-parameter subgroup $\mathcal{H}$ of the full symmetry group $\mathcal{G}$ of a system of differential equations, there will correspond a family of group-invariant solutions. Since there are almost always an infinite number of such subgroups, it is not usually feasible to list all possible group-invariant solutions to the system. We need an effective systematic means of classifying these solutions, leading to an optimal system of group-invariant solutions from which every other solution can be derived. Since elements $g \in G$ not in the subgroup $\mathcal{H}$ will transform an $\mathcal{H}$-invariant solution to some other group-invariant solution, only those solutions not so related need to be listed in our optimal system.

An optimal system of r-parameter subgroups is a list of conjugancy inequivalent r-parameter subgroups with the property that any other subgroup is conjugate to precisely one subgroup in the list (conjugacy map: $h \rightarrow ghg^{-1}$) [13]. By using the definition of adjoint representation from chapter 1, we can reconstruct the adjoint representation adG of the Lie group by summing the Lie series (1.14) obtaining the adjoint table

Ad	V_1	V_2	V_3	V_4	V_5
V_1	V_1	V_2	V_3	V_4	$V_5 - \varepsilon V_1$
V_2	V_1	V_2	V_3	V_4	$V_5 + \varepsilon V_2$
V_3	V_1	V_2	V_3	V_4	V_5
V_4	V_1	V_2	V_3	V_4	$V_5 + \varepsilon V_4$
V_5	$e^{\varepsilon} V_1$	$[\cosh\varepsilon - \sinh\varepsilon] V_2$	V_3	$[\cosh\varepsilon - \sinh\varepsilon] V_4$	V_5

Table 2.2: Adjoint table

The optimal system of our equations (2.8)-(2.9) is provided by those generated by

$$
\begin{array}{lll}
I_1)\ V_1 + V_3 & I_2)\ V_1 + V_5 & I_3)\ V_2 + V_3 \\
I_4)\ V_2 + V_4 & I_5)\ V_2 + V_5 & I_6)\ V_4 + V_5 \\
I_7)\ V_1 + V_2 + V_3 & I_8)\ V_1 + V_2 + V_5 & I_9)\ V_i, (i = 1, 2, ...5)
\end{array}
$$

Further we will concentrate our attention on the classification of the group-invariant solutions. The system of invariants can be used to reduce the order of the original equations - constructing the reduced order system of equations. Doing this one can hope to find simple equations that can be integrated. Since differential equations can admit more than one symmetry, there are different ways to choose a set of similarity variables by starting from different symmetries. It is also possible to achieve a multiple reduction of variables by using multiple–parameter groups of transformations. When this is possible, there are essentially two ways to obtain such a multiple reduction of independent variables: repeating step by step the procedure used in the case of one–parameter Lie groups for each subgroup considered, or performing the reduction together. Reducing step by step the number of variables means performing the following:

1. take a generator of a subgroup (say, $\vec{V}$, written in terms of the variables involved in the system) and build the associated similarity reduction.

2. write the original system of differential equations in terms of the similarity variables and similarity functions, thus obtaining the reduced system.

3. if a further reduction is wanted, go to step 1 and so on.

This method works only if each considered subgroup is possessed by the system where the similarity reduction is performed. Of course, this is true for the first subgroup considered, but for the subsequent steps this is true only if the subgroup (written in terms of the similarity variables) is inherited by the reduced system [13,100]. Here we follow the aforementioned procedure to

reduce the governing partial differential equations into ordinary differential equations. For our system (2.8)-(2.9) we find nine group invariants which lead to group invariant solutions.

I_1) The invariants are $y = \eta, \psi = x + f(\eta), \theta = \theta(\eta)$, now our system becomes

$$(1 + \frac{1}{\beta})f'''(\eta) + f''(\eta) - \left(M + \frac{1}{K}\right) f'(\eta) = 0, \tag{2.18}$$

$$\theta''(\eta) + \Pr \theta'(\eta) + \Pr Q\theta(\eta) = 0. \tag{2.19}$$

The solution of the above equations is

$$f(\eta) = -\frac{a_1}{d} + a_2 e^{(\frac{-1+\sqrt{1+4ad}}{2a})\eta} + a_3 e^{(\frac{-1-\sqrt{1+4ad}}{2a})\eta}, \tag{2.20}$$

$$\theta(\eta) = b_1 e^{(\frac{-\Pr+\sqrt{\Pr^2-4Q\Pr}}{2})\eta} + b_2 e^{(\frac{-\Pr-\sqrt{\Pr^2-4Q\Pr}}{2})\eta}, \tag{2.21}$$

where a_1, a_2, a_3, b_1 and b_2 are integration constants, and $a = 1 + \frac{1}{\beta}, d = M + \frac{1}{K}$.

I_2) For this case invariants are $x = \eta, \psi = y + f(\eta), \theta = \theta(\eta)$. After using these invariants first equation identically satisfies but second equation becomes

$$\theta'(\eta) - Q\theta(\eta) = 0, \text{implies } \theta(\eta) = a_1 e^{-Q\eta}. \tag{2.22}$$

I_3) Invariants are $y = \eta, \psi = f(\eta), \theta = e^x\theta(\eta)$, now our system will be reduced as

$$(1 + \frac{1}{\beta})f'''(\eta) - \left(M + \frac{1}{K}\right) f'(\eta) = 0, \text{implies}$$

$$f(\eta) = -\frac{a_1}{d} + a_2 e^{\sqrt{\frac{d}{a}}\eta} + a_3 e^{\bar{\sqrt{\frac{d}{a}}}\eta}. \tag{2.23}$$

$$\theta''(\eta) - \Pr[a_2\sqrt{\frac{d}{a}}e^{\sqrt{\frac{d}{a}}\eta} - \sqrt{\frac{d}{a}}a_3 e^{\bar{\sqrt{\frac{d}{a}}}\eta}]\theta(\eta) + \Pr Q\theta(\eta) = 0.$$

Above equation can be solved numerically.

I_4) Here the set of invariants are $y = \eta, \psi = xf(\eta), \theta = x\theta(\eta)$. Further our equations are

$$(1 + \frac{1}{\beta})f'''(\eta) - (f'(\eta))^2 + f(\eta)f''(\eta) - \left(M + \frac{1}{K}\right) f'(\eta) = 0, \tag{2.24}$$

$$\theta''(\eta) + \Pr f(\eta)\theta'(\eta) - \Pr f'(\eta)\theta(\eta) + \Pr Q\theta(\eta) = 0. \tag{2.25}$$

The solution of first equation will be solved later for V_4, and second equation can be solved numerically.

I_5) Invariants are $x = \eta, \psi = f(\eta), \theta = e^y\theta(\eta)$. By using these invariants we observe no significant information about $f(\eta)$ and $\theta(\eta)$.

I_6) Following invariants are calculated $\eta = \frac{e^y}{x}, \psi = xf(\eta), \theta = \theta(\eta)$, now our system will be reduced as

$$(1+\frac{1}{\beta})[\eta^2 f'''(\eta)+3\eta f''(\eta)+f'(\eta)]+f(\eta)f'(\eta)-\eta(f'(\eta))^2+\eta f(\eta)f''(\eta)-\left(M+\frac{1}{K}\right)f'(\eta)=0, \tag{2.26}$$

$$\eta^2\theta''(\eta) + \Pr f(\eta)\theta'(\eta) + \eta\theta'(\eta) + \Pr Q\theta(\eta) = 0. \tag{2.27}$$

The above system can be solved numerically.

I_7) This case is observed similar as I_3.

I_8) Following invariants are calculated $x = \eta, \psi = y + f(\eta), \theta = e^y\theta(\eta)$. In this case first equation identically satisfied and second becomes

$$\theta'(\eta) - (\frac{1}{\Pr} + Q)\theta(\eta) = 0, \text{implies } \theta(\eta) = a_1 e^{-(\frac{1}{\Pr}+Q)\eta}. \tag{2.28}$$

I_9) From these invariants we are interested to represent the solutions in the form of physical parameters of fluid. For that we will focus on V_4.

Stretching sheet case

To observe the influence of physical parameters on flow and heat transfer we consider the permeable stretching sheet case. In which the plate with constant permeability is immersed in the fluid at $\overline{y} = 0$. The flow is assumed to be passing through a uniform porous medium with constant permeability k'. The $\overline{x}$-coordinate is taken along the stretching surface and the $\overline{y}$-coordinate normal to the surface. The boundary conditions for this case will be as follows

$$\overline{u}(\overline{x},\overline{y}) = b\overline{x},\ \overline{v}(\overline{x},\overline{y}) = -v_w,\ T(\overline{x},\overline{y}) = T_w \text{ at } \overline{y} = 0, \tag{2.29}$$

$$\overline{u}(\overline{x},\overline{y}) = 0,\ T(\overline{x},\overline{y}) = T_\infty \text{ at } \overline{y} \to \infty, \tag{2.30}$$

where T_w the wall temperature, v_w the suction velocity and b is the stretching parameter. After using the (2.4) the corresponding boundary conditions take the form

$$u(x,y) = x, v(x,y) = \frac{-v_w}{\sqrt{b\upsilon}}, \theta(x,y) = 1 \text{ at } y = 0, \tag{2.31}$$

$$u(x,y) = 0,\ \theta(x,y) = 0 \text{ as } y \to \infty. \tag{2.32}$$

Similarly we can employ stream function on our boundary conditions that becomes

$$\frac{\partial \psi}{\partial y} = x,\ \frac{\partial \psi}{\partial x} = S,\ \theta(x,y) = 1, \text{at } y = 0, \tag{2.33}$$

$$\frac{\partial \psi}{\partial y} = 0,\ \theta(x,y) = 0, \quad \text{as } y \to \infty, \tag{2.34}$$

where $S = \frac{v_w}{\sqrt{b\upsilon}}$, A positive value of S represents suction and negative value of S represents injection.

For this particular invariant $y = \eta$, $\psi = xf(\eta)$, $\theta = \theta(\eta)$, our system becomes

$$(1 + \frac{1}{\beta})f'''(\eta) + f(\eta)f''(\eta) - f'(\eta)^2 - \left(M + \frac{1}{K}\right) f'(\eta) = 0, \tag{2.35}$$

$$\theta''(\eta) + \Pr f(\eta)\theta'(\eta) = 0, \tag{2.36}$$

$$f(0) = S, f'(0) = 1, f'(\infty) = 0, \tag{2.37}$$

$$\theta(0) = 1, \theta(\infty) = 0. \tag{2.38}$$

In order to obtain the solution of Eq. (2.35), we consider

$$f(\eta) = A + Be^{-\alpha\eta}. \tag{2.39}$$

Since the nature of the problem is exponential decaying, we consider the solution like Eq. (2.39), where the constants A and B can be found by using conditions (2.37), then $f(\eta)$ can be written as

$$f(\eta) = S + \frac{1}{\alpha}(1 - e^{-\alpha\eta}), \tag{2.40}$$

where

$$\alpha = \frac{S + \sqrt{S^2 + 4(1 + \frac{1}{\beta})\left(M + \frac{1}{K}\right)}}{2(1 + \frac{1}{\beta})}. \tag{2.41}$$

Substituting Eq. (2.40) in Eq. (2.36), we get

$$\theta''(\eta) + [\Pr S + \frac{\Pr}{\alpha} - \frac{\Pr}{\alpha} e^{-\alpha\eta}]\theta'(\eta) + \Pr Q\theta(\eta) = 0. \tag{2.42}$$

After setting $\xi = -\frac{\Pr}{\alpha^2} e^{-\alpha\eta}$, Eq. (2.42) becomes

$$\xi\theta''(\xi) + (1 - \frac{\Pr}{\alpha^2}(1 + \alpha S) - \xi)\theta'(\xi) + \frac{\Pr Q}{\alpha^2 \xi}\theta(\xi) = 0, \tag{2.43}$$

and boundary conditions will be

$$\theta(\frac{-\Pr}{\alpha^2}) = 1, \theta(0) = 0,$$

where primes denote differentiation with respect to ξ.

Using the transformation $\theta(\xi) = \xi^\gamma F(\xi)$, Eq. (2.43) becomes

$$\xi F''(\xi) + (1 - A - \xi)F'(\xi) - \gamma F(\xi) = 0, \tag{2.44}$$

where

$$\gamma = \frac{\alpha \Pr S + \Pr - \sqrt{(\alpha \Pr S + \Pr)^2 - 4\alpha^2 \Pr Q}}{2\alpha^2}, \tag{2.45}$$

$$A = \frac{\sqrt{(\alpha \Pr S + \Pr)^2 - 4\alpha^2 \Pr Q}}{\alpha^2}. \tag{2.46}$$

The corresponding boundary conditions become

$$F(0) = 0, F\left(\frac{-\Pr}{\alpha^2}\right) = \left(\frac{-\Pr}{\alpha^2}\right)^{-\gamma}. \tag{2.47}$$

Equation (2.44) is the standard confluent Hypergeometric Equation, whose solution is

$$F(\xi) = \frac{(\frac{-\Pr}{\alpha^2})^{-\gamma - A}\ \xi^A\ {}_1F_1(\gamma + A; 1 + A; \xi)}{{}_1F_1(\gamma + A; 1 + A; \frac{-\Pr}{\alpha^2})}, \tag{2.48}$$

where ${}_1F_1(a;b;z)$ is Kummer's function defined as [30]

$$ {}_1F_1(a;b;z) = \sum_{n=0}^{\infty} \frac{(a)_n}{(b)_n} \frac{z^n}{n!}, b \neq 0, -1, -2..., $$

where $(a)_n$ denoting the Pochhammer symbol defined in terms of the gamma function by

$$ (a)_n = a(a+1)(a+2)...(a+n-1) = \frac{\Gamma(a+n)}{\Gamma(a)}. $$

The solution of (2.36) can be rewritten, in terms of η as

$$ \theta(\eta) = \frac{e^{-\alpha(\gamma+A)\eta}\ {}_1F_1(\gamma+A;1+A;\frac{-\mathrm{Pr}}{\alpha^2}e^{-\alpha\eta})}{{}_1F_1(\gamma+A;1+A;\frac{-\mathrm{Pr}}{\alpha^2})}, $$

$$ \begin{aligned} \theta'(\eta) &= -\frac{e^{-\alpha(\gamma+A)\eta}\ \frac{\mathrm{Pr}}{\alpha}e^{-\alpha\eta}}{{}_1F_1(\gamma+A;1+A;\frac{-\mathrm{Pr}}{\alpha^2})}\alpha(A+\gamma){}_1F_1(\gamma+A;1+A;\frac{-\mathrm{Pr}}{\alpha^2}e^{-\alpha\eta}) \\ &\quad +\frac{\mathrm{Pr}}{\alpha}e^{-\alpha\eta}\ {}_1F_1(1+\gamma+A;2+A;\frac{-\mathrm{Pr}}{\alpha^2}e^{-\alpha\eta}), \end{aligned} \tag{2.49} $$

$$ \theta'(0) = -\alpha(A+\gamma) + \frac{(A+\gamma)\,\mathrm{Pr}}{\alpha(A+1)} \frac{{}_1F_1(1+\gamma+A;2+A;\frac{-\mathrm{Pr}}{\alpha^2})}{{}_1F_1(\gamma+A;1+A;\frac{-\mathrm{Pr}}{\alpha^2})}. \tag{2.50} $$

The skin friction coefficient and the local Nusselt number are defined as:

$$ \begin{aligned} C_f &= \frac{\left(\mu_B + \frac{p_y}{\sqrt{2\pi_c}}\right)}{\rho(b\bar{x})^2} \left(\frac{\partial \bar{u}}{\partial \bar{y}}\right)_{\bar{y}=0}, \\ Nu_x &= \frac{\bar{x}}{(T_w - T_\infty)} \left(\frac{\partial T}{\partial \bar{y}}\right)_{\bar{y}=0}. \end{aligned} \tag{2.51} $$

Using Eqs. (2.4) and (2.51), the dimensionless forms of skin friction, and the local Nusselt number, respectively, become

$$ \mathrm{Re}_x^{1/2}\, C_f = -\left(1 + \frac{1}{\beta}\right) f''(0), $$

$$ \mathrm{Re}_x^{-1/2}\, Nu_x = -\theta'(0). \tag{2.52} $$

2.1.3 Flow characteristics

In this section the effects of various parameters on velocity and temperature profiles are discussed. Figure 2.1 depicts the effects of Casson fluid parameter β on velocity profile. It is quite clear that there is a decrease in velocity with an increase in Casson fluid parameter β. In Figure 2.2, the influence of magnetic field parameter M on velocity profile $f'(\eta)$ are shown. It is observed that with an increase in magnetic field parameter M, the thickness of momentum boundary layer decreases. This is mainly due to the fact that application of magnetic field to an electrically conducting fluid gives rise to Lorentz force, which causes the fluid to decelerate. Figure 2.3 interprets that velocity increases on increasing K. This is due to the fact that as the permeability parameter increases, a decrease in the resistance of the porous medium occurs which speeds up the flow. In Figure 2.4 the effect of suction parameter S on velocity field $f'(\eta)$ is shown. An increase in suction parameter S causes the velocity profile to decrease.

The effect of various parameters on temperature profile $\theta(\eta)$ are presented in Figures 2.5 – 2.11. The effects of source ($Q > 0$) and sink ($Q < 0$) on temperature profile are shown in Figures 2.5 and 2.6. It is noticed that in case of source the temperature increases with increase in the value of heat generation parameter. However a decrease in temperature profile is noticed in case of sink. Figure 2.7 illustrates that the thickness of thermal boundary layer increases with increasing the Casson fluid parameter β. With an increase in magnetic field parameter M, the resistive force becomes stronger which increases the temperature profile as shown in Figure 2.8. The influence of permeability parameter K on $\theta(\eta)$ is depicted in Figure 2.9. A decrease in temperature profile is noticed with an increase in permeability parameter. Figure 2.10 shows that the temperature decreases as the suction parameter S increases. From Figure 2.11 it is observed that thickness of the thermal boundary layer decreases with increasing Prandtl number Pr.

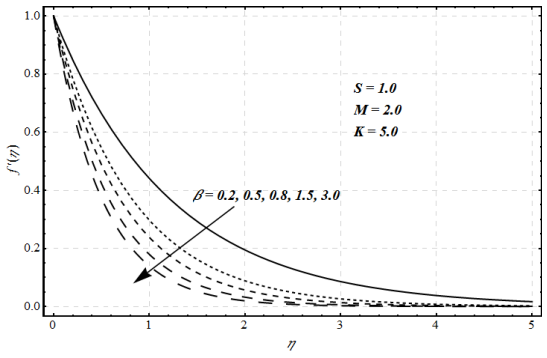

Figure 2.1: Effect of β on $f'(\eta)$

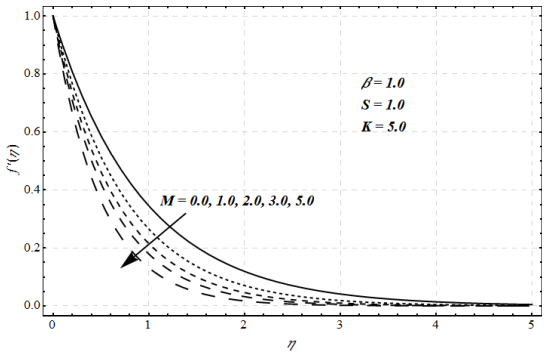

Figure 2.2: Effect of M on $f'(\eta)$

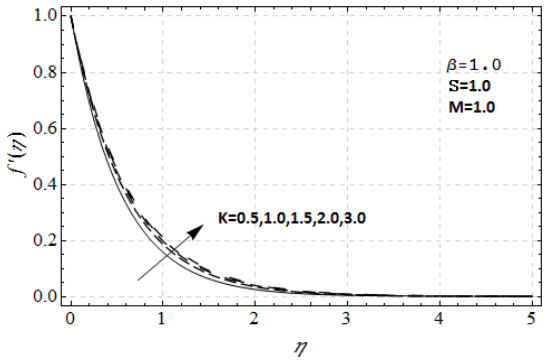

Figure 2.3: Effect of K on $f'(\eta)$

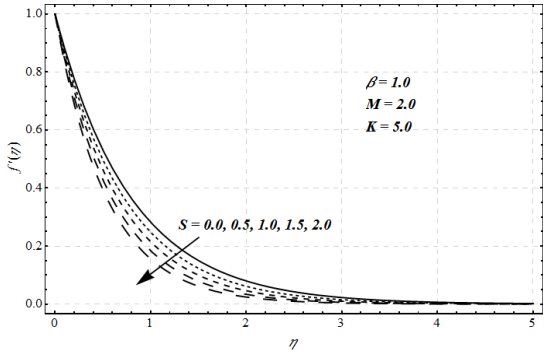

Figure 2.4: Effect of S on $f'(\eta)$

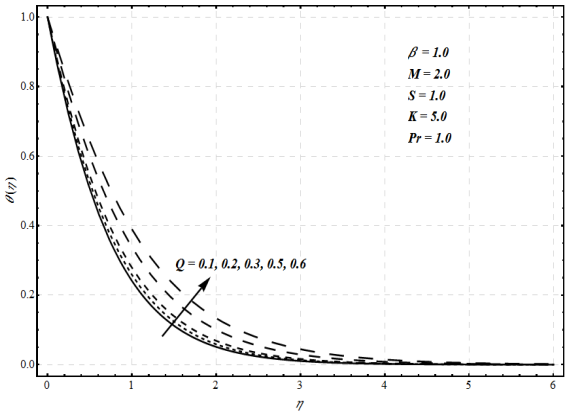

Figure 2.5: Effect of $(Q > 0)$ on $\theta(\eta)$

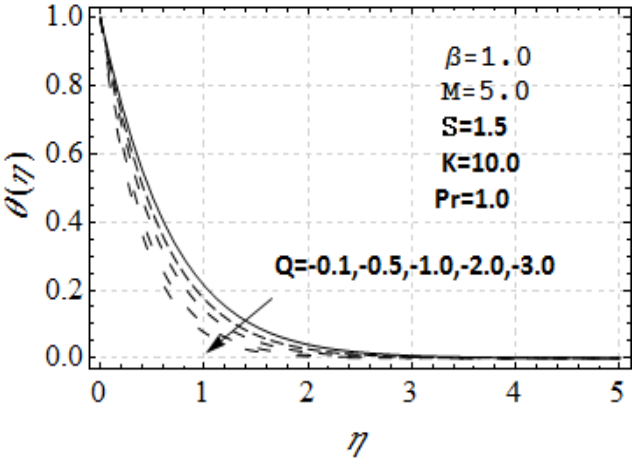

Figure 2.6: Effect of $(Q < 0)$ on $\theta(\eta)$

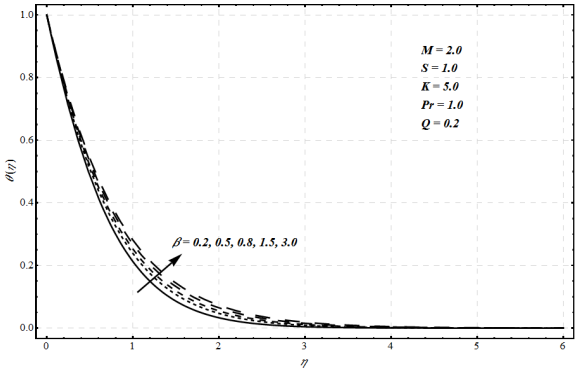

Figure 2.7: Effect of β on $\theta(\eta)$

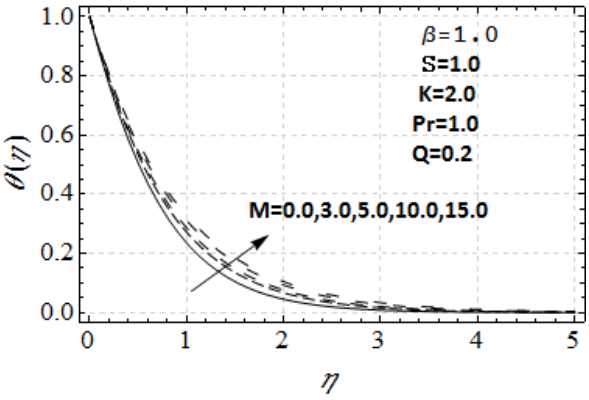

Figure 2.8: Effect of M on $\theta(\eta)$

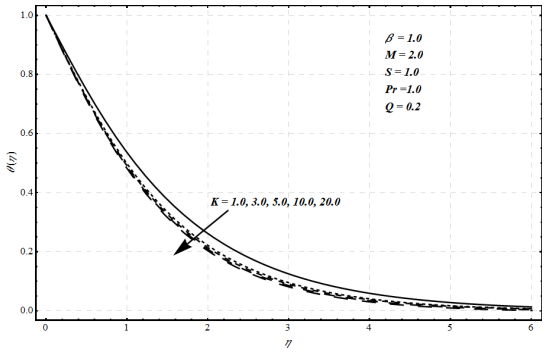

Figure 2.9: Effect of K on $\theta(\eta)$

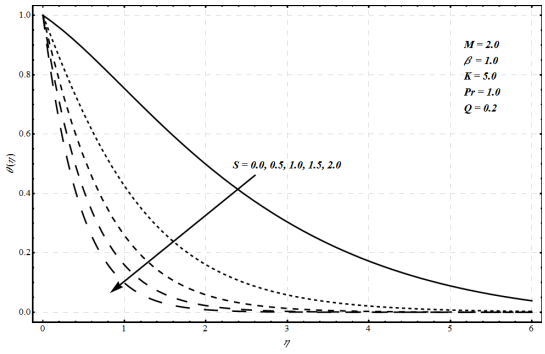

Figure 2.10: Effect of S on $\theta(\eta)$

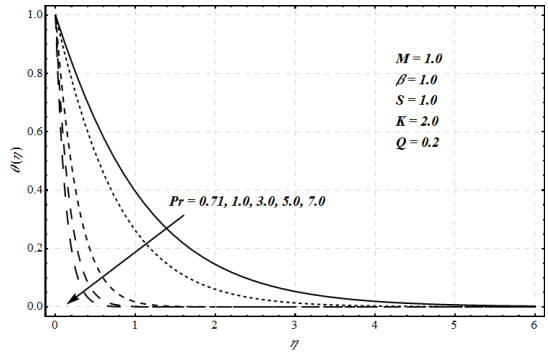

Figure 2.11: Effect of Pr on $\theta(\eta)$

In order to validate our study, we have made a comparison of values of $-f''(0)$ with those reported earlier [102] and presented in Table 2.3. By keeping $S = 0$, $\beta = \infty$ and $K = \infty$, we have found that the values obtained in this study are in good agreement with those reported earlier [102]. Table 2.4 presents the values of $-(1 + \frac{1}{\beta})f''(0)$ for various values of Casson fluid parameter β, Magnetic field parameter M, permeability parameter K and suction parameter S. It is noticed that the skin friction coefficient decreases with β and K and increases with M and S. Further for the comparison of the value of $-\theta'(0)$ we have taken $M = 0, S = 0, \beta = \infty, K = \infty$ and $\Pr = 1$ and obtained the value as $\frac{1}{1+e}$ which exactly matches with that reported in [30]. Table 2.5 shows that the local Nusselt number $-\theta'(0)$ increases with permeability parameter

K, Prandtl number Pr and suction parameter S, and decreases with Casson fluid parameter β and magnetic field parameter M. Table 2.6 indicates that the local Nusselt number $-\theta'(0)$ increases with heat sink ($Q < 0$) and decreases with heat source ($Q > 0$).

M	$-f''(0)$ Present	$-f''(0)$ [102]
0.0	1.0000000	1.00000
0.2	1.09545	1.09545
0.5	1.22474	1.22475
1.0	1.4142136	1.41421
1.2	1.48324	1.48324
1.5	1.58114	1.58114
2.0	1.7320508	1.73205
2.2	1.78885	
2.5	1.87083	
3.0	2.0000000	

Table 2.3: A comparison of $-f''(0)$ obtained by the analytical method with the Cortell studies [102] when we fixed $S = 0, K = \infty$ & $\beta = \infty$

β	M	K	S	$-(1+\frac{1}{\beta})f''(0)$
0.5	1.0	0.5	1.0	4.0
1.0				3.37228
1.5				3.12996
2.0				3.0
0.5	0.5	0.5	1.0	3.77872
	1.0			4.0
	1.5			4.2081
	2.0			4.40512
0.5	1.0	0.5	1.0	4.0
		1.0		3.54138
		1.5		3.37228
		2.0		3.28388
0.5	1.0	0.5	0.5	3.72311
			1.0	4.0
			1.5	4.29436
			2.0	4.60555

Table 2.4: Effects of various parameters on $-\left(1+\frac{1}{\beta}\right)f''(0)$

β	M	K	Pr	S	Q	$-\theta'(0)$
0.5	1.0	0.5	0.71	1.0	0.1	1.80982
1.0						1.74601
1.5						1.71045
2.0						1.68876
0.5	0.5	0.5	0.71	1.0	0.1	1.82049
	1.0					1.80982
	1.5					1.79835
	2.0					1.78671
0.5	1.0	0.5	0.71	1.0	0.1	1.80982
		1.0				1.82913
		1.5				1.83254
		2.0				1.83306
0.5	1.0	0.5	0.71	1.0	0.1	1.80982
			1.0			2.46103
			2.0			4.26035
			3.0			5.29138
0.5	1.0	0.5	0.71	0.5	0.1	1.16068
				1.0		1.80982
				1.5		2.46935
				2.0		3.13938

Table 2.5: Effects of various parameters on $-\theta'(0)$

β	M	K	Pr	S	Q	$-\theta'(0)$
0.5	1.0	0.5	0.71	0.5	0.1	1.16068
					0.2	1.62776
					0.3	1.4196
					0.4	1.16736
					-0.1	-1.16068
					-0.2	-1.62776
					-0.3	-1.4196
					-0.4	-1.16736

Table 2.6: Effects of heat source and sink on $-\theta'(0)$

2.1.4 Findings

The optimal system lead us to find the nine group invariant solutions. For one particular invariant we solved the governing system of ordinary differential equations by considering permeable stretching sheet case to observe the influence of physical parameters on fluid and heat transfer phenomenon. Further, the solution of that particular invariant are also presented through

graphs and tables. The following observations have been found from permeable stretching sheet case:

A decrease in thickness of momentum boundary layer is observed with increase in Casson fluid parameter, magnetic field parameter and suction parameter. An increase in fluid velocity is noticed with increase in permeability parameter. The thermal boundary layer thickness increases with Casson fluid parameter, magnetic field parameter and heat source ($Q > 0$). A decreasing effect is noticed on temperature with increase in permeability parameter, suction parameter, heat sink ($Q < 0$) and Prandtl number. Skin friction increases with magnetic field parameter and suction parameter, and decreases with Casson fluid parameter and permeability parameter. The permeability parameter, suction parameter, and Prandtl number have increasing effects on local Nusselt number where Nu_x decreases with Casson fluid parameter, heat source ($Q > 0$) and magnetic field parameter.

2.2 Lie group investigation of MHD flow with the thermal radiation effects

2.2.1 Mathematical modeling

In this section we consider a two-dimensional laminar flow of an incompressible Casson fluid flow and heat transfer through a porous medium in the presence of thermal radiation effects instead of source/sink effects. In addition we are also interested in observing the mass transfer phenomenon.

The governing system along with equations of the Casson fluid flow Eq. (1.41), heat and mass transfer are given by

$$\frac{\partial \overline{u}}{\partial \overline{x}} + \frac{\partial \overline{v}}{\partial \overline{y}} = 0, \tag{2.53}$$

$$\overline{u}\frac{\partial \overline{u}}{\partial \overline{x}} + \overline{v}\frac{\partial \overline{u}}{\partial \overline{y}} = \frac{\mu}{\rho}(1 + \frac{1}{\beta})\frac{\partial^2 \overline{u}}{\partial \overline{y}^2} - \frac{\nu}{k'}\overline{u} - \frac{\sigma B_0^2}{\rho}\overline{u}, \tag{2.54}$$

$$\overline{u}\frac{\partial T}{\partial \overline{x}} + \overline{v}\frac{\partial T}{\partial \overline{y}} = \frac{k}{\rho c_p}\frac{\partial^2 T}{\partial \overline{y}^2} + \frac{16\sigma_1 T_\infty^3}{3\rho c_p k_1}\frac{\partial^2 T}{\partial \overline{y}^2}, \tag{2.55}$$

$$\overline{u}\frac{\partial C}{\partial \overline{x}} + \overline{v}\frac{\partial C}{\partial \overline{y}} = D\frac{\partial^2 C}{\partial \overline{y}^2}, \tag{2.56}$$

where σ_1 and k_1 are the Stefen-Boltzmann constant and the mean absorption coefficient respectively. T and T_∞ are fluid and ambient temperatures respectively, C is concentration of fluid, D mass diffusivity, $\overline{u}, \overline{v}$ are the velocity components in $\overline{x}$- and $\overline{y}$- directions respectively.

Introducing the following similarity transformations:

$$u(x,y) = \frac{\overline{u}(\overline{x},\overline{y})}{\sqrt{b\upsilon}},\ v(x,y) = \frac{\overline{v}(\overline{x},\overline{y})}{\sqrt{b\upsilon}},\ x = \sqrt{\frac{b}{\nu}}\overline{x},\ y = \sqrt{\frac{b}{\nu}}\overline{y}, \tag{2.57}$$

$$\theta(x,y) = \frac{T(\overline{x},\overline{y}) - T_\infty}{(T_w - T_\infty)},\ \phi(x,y) = \frac{C(\overline{x},\overline{y}) - C_\infty}{(C_w - C_\infty)}. \tag{2.58}$$

Using the transformations $(2.57) - (2.58)$ in Eqs. $(2.53) - (2.56)$, we have

$$\frac{\partial u}{\partial x} + \frac{\partial v}{\partial y} = 0, \tag{2.59}$$

$$u\frac{\partial u}{\partial x} + v\frac{\partial u}{\partial y} = (1 + \frac{1}{\beta})\frac{\partial^2 u}{\partial y^2} - \frac{1}{K}u - Mu, \tag{2.60}$$

$$u\frac{\partial \theta}{\partial x} + v\frac{\partial \theta}{\partial y} = \frac{1}{\mathrm{Pr}}\left(1 + \frac{4}{3Nr}\right)\frac{\partial^2 \theta}{\partial y^2}, \tag{2.61}$$

$$u\frac{\partial \phi}{\partial x} + v\frac{\partial \phi}{\partial y} = \frac{1}{Sc}\frac{\partial^2 \phi}{\partial y^2}, \tag{2.62}$$

where $Nr = \frac{\kappa\kappa_1}{4\sigma_1 T_\infty^3}$ is radiation parameter and $Sc = \frac{\upsilon}{b}$ is Schmidt number. Now by introducing stream function

$$u = \frac{\partial \psi}{\partial y}, \qquad \text{and} \quad v = -\frac{\partial \psi}{\partial x}. \tag{2.63}$$

By using stream function the Eq. (2.59) will become identically zero and the system (2.60)-(2.62) take the forms

$$(1 + \frac{1}{\beta})\frac{\partial^3 \psi}{\partial y^3} - \frac{\partial \psi}{\partial y}\frac{\partial^2 \psi}{\partial x \partial y} + \frac{\partial \psi}{\partial x}\frac{\partial^2 \psi}{\partial y^2} - (M + \frac{1}{K})\frac{\partial \psi}{\partial y} = 0, \tag{2.64}$$

$$\frac{1}{\mathrm{Pr}}\left(1 + \frac{4}{3Nr}\right)\frac{\partial^2 \theta}{\partial y^2} - \frac{\partial \psi}{\partial y}\frac{\partial \theta}{\partial x} + \frac{\partial \psi}{\partial x}\frac{\partial \theta}{\partial y} = 0, \tag{2.65}$$

$$\frac{1}{Sc}\frac{\partial^2 \phi}{\partial y^2} - \frac{\partial \psi}{\partial y}\frac{\partial \phi}{\partial x} + \frac{\partial \psi}{\partial x}\frac{\partial \phi}{\partial y} = 0. \tag{2.66}$$

2.2.2 Lie group analysis

The infinitesimals of the Lie group of transformations leaving a given system of differential equations invariant can be found by means of the straightforward algorithm discussed in previous section. Consider the one-parameter Lie group of infinitesimal transformations in $(x, y, \psi, \theta, \phi)$ given by

$$\begin{aligned} x^* &= x + \epsilon\xi(x, y, \psi, \theta, \phi) + O(\epsilon^2), \\ y^* &= y + \epsilon\tau(x, y, \psi, \theta, \phi) + O(\epsilon^2), \\ \psi^* &= \psi + \epsilon\Gamma(x, y, \psi, \theta, \phi) + O(\epsilon^2), \\ \theta^* &= \theta + \epsilon\Omega(x, y, \psi, \theta, \phi) + O(\epsilon^2), \\ \phi^* &= \phi + \epsilon\Phi(x, y, \psi, \theta, \phi) + O(\epsilon^2). \end{aligned} \tag{2.67}$$

Equations $(2.64) - (2.66)$ are nonlinear partial differential equation with three dependent variables (ψ, θ, ϕ) and two independent variables (x, y). Lie group analysis is required so that Eqs. $(2.64) - (2.66)$ remain invariant under these transformations which yields an over-determined, linear system of equations for infinitesimals ξ, τ, Γ, Ω, Φ.

The infinitesimal group generator is defined by

$$\begin{aligned} \overrightarrow{V} &= \xi(x, y, \psi, \theta, \phi)\frac{\partial}{\partial x} + \tau(x, y, \psi, \theta, \phi)\frac{\partial}{\partial y} + \Gamma(x, y, \psi, \theta, \phi)\frac{\partial}{\partial \Psi} \\ &\quad + \Omega(x, y, \psi, \theta, \phi)\frac{\partial}{\partial \theta} + \Phi(x, y, \psi, \theta, \phi)\frac{\partial}{\partial \phi}. \end{aligned} \tag{2.68}$$

After following the procedure defined in previous section to calculate the infinitesimals we have

$$\xi = c_1 + c_2 x,\ \tau = f_1(x),\ \Gamma = c_3 + c_2\psi,\ \Omega = c_4 + c_5\theta,\ \Phi = c_6 + c_7\phi, \tag{2.69}$$

where $c_i (i = 1, 2, ..., 7)$, are arbitrary constants and $f_1(x)$ is arbitrary function of x.

There are seven finite parameter Lie group symmetries represented by parameters c_i, and one infinite symmetry $f_1(x)$. Parameter c_1 corresponds to the translation in the variable x, c_2 corresponds to the scaling in ψ and x, c_3 corresponds to the translation in ψ, c_4 corresponds to the translation in θ, c_5 corresponds to scaling in θ, and c_6 and c_7 correspond to translation

and scaling in ϕ respectively.

Here we have a 8−dimensional vector space of infinitesimal generators closed under the operation of commutation, i.e., 8−dimensional Lie algebra, the basis of the corresponding Lie algebra is as follows

$$V_1 = \partial_x, V_2 = x\partial_x + \psi\partial_\psi, V_3 = \partial_\psi, V_4 = \partial_\theta, V_5 = \theta\partial_\theta, V_6 = \partial_\phi, V_7 = \phi\partial_\phi, V_8 = \partial_y. \qquad (2.70)$$

The requirement for solvability is equivalent to the existence of a basis $\{V_1, V_2, ..., V_8\}$ of Lie algebra such that by Eq. (1.13) we can develop the commutator table

[,]	V_1	V_2	V_3	V_4	V_5	V_6	V_7	V_8
V_1	0	0	V_1	0	0	0	0	0
V_2	0	0	-V_2	0	0	0	0	0
V_3	-V_1	V_2	0	V_4	0	0	0	0
V_4	0	0	-V_4	0	0	0	0	0
V_5	0	0	0	0	0	-V_5	0	0
V_6	0	0	0	0	V_5	0	0	0
V_7	0	0	0	0	0	0	0	V_7
V_8	0	0	0	0	0	0	V_7	0

Table 2.7: Commutator table

By a straightforward observation of the commutator table we found the following Abelian Lie algebra

$$\begin{aligned}
[V_s, V_t] &= 0, \text{ as } s = t, [V_1, V_2] = 0, [V_1, V_4] = 0, [V_1, V_5] = 0, \\
[V_1, V_6] &= 0, [V_1, V_7] = 0, [V_1, V_8] = 0, [V_2, V_4] = 0, [V_2, V_5] = 0, \\
[V_2, V_6] &= 0, [V_2, V_7] = 0, [V_2, V_8] = 0, [V_3, V_5] = 0, [V_3, V_6] = 0, \\
[V_3, V_7] &= 0, [V_3, V_8] = 0, [V_4, V_5] = 0, [V_4, V_6] = 0, [V_4, V_7] = 0, \\
[V_4, V_8] &= 0, [V_5, V_7] = 0, [V_5, V_8] = 0, [V_6, V_7] = 0, [V_6, V_8] = 0.
\end{aligned}$$

We can reconstruct the following adjoint representation adG of the Lie group by summing the

Lie series (1.14).

Ad	V_1	V_2	V_3	V_4
V_1	V_1	V_2	$V_3 - \varepsilon V_1$	V_4
V_2	$V_1 e^{\varepsilon}$	V_2	$V_3 + \varepsilon V_2$	V_4
V_3	V_1	$V_2[\cosh\varepsilon - \sinh\varepsilon]$	V_3	$V_4[\cosh\varepsilon - \sinh\varepsilon]$
V_4	V_1	V_2	$V_4 e^{\varepsilon}$	V_4
V_5	V_1	V_2	V_3	V_4
V_6	V_1	V_2	V_3	V_4
V_7	V_1	V_2	V_3	V_4
V_8	V_1	V_2	V_3	V_4

Ad	V_5	V_6	V_7	V_8
V_1	V_5	V_6	V_7	V_8
V_2	V_5	V_6	V_7	V_8
V_3	V_5	V_6	V_7	V_8
V_4	V_5	V_6	V_7	V_8
V_5	V_5	$V_6 + \varepsilon V_5$	V_7	V_8
V_6	$V_5[\cosh\varepsilon - \sinh\varepsilon]$	V_6	V_7	$V_8 + \varepsilon V_7$
V_7	V_5	V_6	V_7	V_8
V_8	V_5	V_6	$V_7[\cosh\varepsilon - \sinh\varepsilon]$	V_8

Table 2.8: Adjoint table

Following the procedure of the previous section, the optimal system of our equations (2.64)-(2.66) is given by

$I_1)\ V_1 + V_3$ $I_2)\ V_1 + V_4$ $I_3)\ V_1 + V_5$
$I_4)\ V_1 + V_6$ $I_5)\ V_1 + V_7$ $I_6)\ V_2 + V_4$
$I_7)\ V_2 + V_5$ $I_8)\ V_2 + V_6$ $I_9)\ V_2 + V_7$
$I_{10})\ V_2 + V_8$ $I_{11})\ V_3 + V_8$ $I_{12})\ V_4 + V_8$
$I_{13})\ V_5 + V_8$ $I_{14})\ V_6 + V_8$ $I_{15})\ V_7 + V_8$
$I_{16})\ V_1 + V_3 + V_4$ $I_{17})\ V_1 + V_3 + V_5$ $I_{18})\ V_1 + V_3 + V_6$
$I_{19})\ V_1 + V_3 + V_7$ $I_{20})\ V_1 + V_3 + V_8$ $I_{21})\ V_1 + V_4 + V_8$
$I_{22})\ V_1 + V_5 + V_8$ $I_{23})\ V_1 + V_6 + V_8$ $I_{24})\ V_1 + V_7 + V_8$
$I_{25})\ V_3 + V_4 + V_8$ $I_{26})\ V_3 + V_5 + V_8$ $I_{27})\ V_3 + V_6 + V_8$
$I_{28})\ V_3 + V_7 + V_8$ $I_{29})\ V_i (i = 1, 2, 3...8)$

Here we follow the procedure of the previous section to reduce the governing partial differential equations into ordinary differential equations. For our system (2.64)-(2.66) we find the following twenty nine group invariants which lead to group invariant solutions.

I_1) Invariants are $y = \eta, \psi = x + f(\eta), \theta = \theta(\eta), \phi = \phi(\eta)$. The system reduced into the following form

$$(1 + \frac{1}{\beta})f'''(\eta) + f''(\eta) - \left(M + \frac{1}{K}\right) f'(\eta) = 0, \tag{2.71}$$

$$\left(1 + \frac{4}{3Nr}\right) \theta''(\eta) + \Pr \theta'(\eta) = 0, \tag{2.72}$$

$$\phi''(\eta) + Sc\phi'(\eta) = 0. \tag{2.73}$$

The solution of flow Eq. (2.71) is same as in I_1 of section 1.2.2 and the solution of above other equations are

$$\begin{aligned} \theta(\eta) &= a_1 + a_2 e^{-\frac{\Pr}{n}\eta}, \text{ where } n = 1 + \frac{4}{3Nr}, \\ \phi(\eta) &= b_1 + b_2 e^{-Sc\eta}, \end{aligned}$$

where a_1, a_2, b_1 and b_2 are constants.

I_2) The set of invariants are $y = \eta, \psi = f(\eta), \theta = x + \theta(\eta), \phi = \phi(\eta)$. Then the system becomes

$$(1 + \frac{1}{\beta})f'''(\eta) - \left(M + \frac{1}{K}\right) f'(\eta) = 0, \tag{2.74}$$

$$\left(1 + \frac{4}{3Nr}\right) \theta''(\eta) - \Pr f'(\eta) = 0, \tag{2.75}$$

$$\phi''(\eta) - Scf'(\eta) = 0. \tag{2.76}$$

The solution of flow Eq. (2.74) observed similar as in I_3 (previous section), other equations reveals the solution as

$$\theta(\eta) = \frac{a_5}{n} + \frac{a_4}{n}\eta + \frac{\Pr a_2}{nm} e^{m\eta} - \frac{\Pr a_3}{nm} e^{-m\eta},$$

$$\phi(\eta) = a_7 + a_6\eta + \frac{Sca_2}{m} e^{m\eta} - \frac{Sca_3}{m} e^{-m\eta},$$

where $m = \frac{M + \frac{1}{K}}{1 + \frac{1}{\beta}}$.

I_3) The invariants are $y = \eta, \psi = f(\eta), \theta = e^x\theta(\eta), \phi = \phi(\eta)$. The flow and mass transfer equations appeared same as in I_2 but the heat equation can be solved numerically which

becomes

$$\left(1+\frac{4}{3Nr}\right)\theta''(\eta)-\Pr f'(\eta)\theta(\eta)=0. \tag{2.77}$$

I_4) The invariants are $y=\eta,\psi=f(\eta),\theta=\theta(\eta),\phi=x+\phi(\eta)$. The flow and mass transfer equations appeared same as in I_2 but the heat equation becomes

$$\theta''(\eta)=0,\ \text{implies}\ \theta(\eta)=a_1+a_2\eta. \tag{2.78}$$

I_5) Here the invariants are $y=\eta,\psi=f(\eta),\theta=\theta(\eta),\phi=e^x\phi(\eta)$. The flow equation reduced to same as in I_2 and heat transfer equations appeared same as in I_4 but the mass transfer equation can be solved numerically which becomes

$$\phi''(\eta)-Scf'(\eta)\phi(\eta)=0. \tag{2.79}$$

I_6) The invariants are $y=\eta,\psi=xf(\eta),\theta=\ln x+\theta(\eta),\phi=\phi(\eta)$. The system becomes

$$(1+\frac{1}{\beta})f'''(\eta)+f(\eta)f''(\eta)-f'(\eta)^2-\left(M+\frac{1}{K}\right)f'(\eta)=0, \tag{2.80}$$

$$\left(1+\frac{4}{3Nr}\right)\theta''(\eta)+\Pr f(\eta)\theta'(\eta)-\Pr f'(\eta)=0, \tag{2.81}$$

$$\phi''(\eta)+Scf(\eta)\phi'(\eta)=0. \tag{2.82}$$

The Eq. (2.80) and Eq. (2.82) will be solved later in detail for V_2 and Eq. (2.81) can be solved numerically.

I_7) The invariants are $y=\eta,\psi=xf(\eta),\theta=x\theta(\eta),\phi=\phi(\eta)$. The flow and mass transfer equations observed the same as in I_6 but heat transfer can be solved numerically which becomes

$$\left(1+\frac{4}{3Nr}\right)\theta''(\eta)+\Pr f(\eta)\theta'(\eta)-\Pr f'(\eta)\theta(\eta)=0. \tag{2.83}$$

I_8) Here the invariants are: $y=\eta,\psi=xf(\eta),\theta=\theta(\eta),\phi=\ln x+\phi(\eta)$. The flow equation is the same as in I_6 and heat equation will be solved later for V_2, but mass transfer equation

can be solved numerically i.e.,

$$\phi''(\eta) + Scf(\eta)\phi'(\eta) - Scf'(\eta) = 0. \tag{2.84}$$

I_9) The invariants are $y = \eta, \psi = xf(\eta), \theta = \theta(\eta), \phi = x\phi(\eta)$. The flow and heat transfer equations will be solved for V_2 but mass transfer can be solved numerically, which become

$$\phi''(\eta) + Scf(\eta)\phi'(\eta) - Scf'(\eta)\phi(\eta) = 0. \tag{2.85}$$

I_{10}) The invariants are $\eta = \frac{e^y}{x}, \psi = xf(\eta), \theta = \theta(\eta), \phi = \phi(\eta)$. After using them we have the following system which can be solved numerically

$$(1 + \frac{1}{\beta})\left[\eta^2 f''' + 3\eta f'' + f'\right] + ff' + \eta ff'' - \eta f'^2 - \left(M + \frac{1}{K}\right) f' = 0, \tag{2.86}$$

$$\left(1 + \frac{4}{3Nr}\right)[\eta\theta'' + \theta'] + \Pr f\theta' = 0, \tag{2.87}$$

$$\eta\phi'' + (1 + Scf)\phi' = 0. \tag{2.88}$$

I_{11}) Here the invariants are $x = \eta, \psi = y + f(\eta), \theta = \theta(\eta), \phi = \phi(\eta)$. Using these invariants, flow equation identically satisfied, and the other two equations are

$$\theta'(\eta) - \frac{n}{\Pr}\theta(\eta) = 0, \text{ implies } \theta(\eta) = a_1 e^{\frac{n}{\Pr}\eta}, \tag{2.89}$$

$$\phi'(\eta) - \frac{1}{Sc}\phi(\eta) = 0, \text{ implies } \phi(\eta) = b_1 e^{\frac{1}{Sc}\eta}. \tag{2.90}$$

I_{12}) Here the invariants are $x = \eta, \psi = f(\eta), \theta = y + \theta(\eta), \phi = \phi(\eta)$. These invariants give us no result.

I_{13}) The invariants are $x = \eta, \psi = f(\eta), \theta = e^y\theta(\eta), \phi = \phi(\eta)$. These invariants give us no result.

I_{14}) The invariants are $x = \eta, \psi = f(\eta), \theta = \theta(\eta), \phi = y + \phi(\eta)$. These invariants give us no result.

I_{15}) The invariants are $x = \eta, \psi = f(\eta), \theta = \theta(\eta), \phi = e^y\phi(\eta)$. These invariants give us no result.

I_{16}) Here the set of invariants are $y = \eta, \psi = x + f(\eta), \theta = x + \theta(\eta), \phi = \phi(\eta)$. The flow and mass transfer equations are observed to be the same as I_1. But the heat equation becomes

$$\left(1 + \frac{4}{3Nr}\right)\theta'' + \Pr\theta' - \Pr f' = 0. \tag{2.91}$$

The solution of this equation will be

$$\theta(\eta) = \frac{\Pr a_2}{nn_1 + \Pr}e^{n_1\eta} - \frac{\Pr a_3}{nn_1 - \Pr}e^{-n_2\eta} + a_4 + a_5 e^{-\frac{\Pr}{n}\eta},$$

where $n_1 = \frac{-1+\sqrt{1+4am}}{2a}, n_2 = \frac{-1-\sqrt{1+4am}}{2a}, a = 1 + \frac{1}{\beta}, m = M + \frac{1}{K}$.

I_{17}) Here the set of invariants are $y = \eta, \psi = x + f(\eta), \theta = e^x\theta(\eta), \phi = \phi(\eta)$. The flow and mass transfer equations are the same as in I_1. But the heat equation can be solved numerically which becomes

$$\left(1 + \frac{4}{3Nr}\right)\theta'' + \Pr\theta' - \Pr f'\theta = 0. \tag{2.92}$$

I_{18}) Here the set of invariants are $y = \eta, \psi = x + f(\eta), \theta = \theta(\eta), \phi = x + \phi(\eta)$. The flow and heat transfer equations are observed the same as in I_1. But the mass transfer equation becomes

$$\phi'' + Sc\phi' - Scf' = 0, \tag{2.93}$$

which implies

$$\phi(\eta) = \frac{Sca_2}{n_1 + Sc}e^{n_1\eta} - \frac{Sca_3}{n_1 - Sc}e^{-n_2\eta} + a_4 + a_5 e^{-Sc\eta}.$$

I_{19}) Here the set of invariants are $y = \eta, \psi = x + f(\eta), \theta = \theta(\eta), \phi = e^x\phi(\eta)$. The flow and heat transfer equations are the same as in I_1. But the mass transfer equation can be solved numerically which becomes

$$\phi'' + Sc\phi' - Scf'\phi = 0. \tag{2.94}$$

I_{20}) Here the set of invariants are $y - x = \eta, \psi = x + f(\eta), \theta = \theta(\eta), \phi = \phi(\eta)$. Here the system reduced similar as I_1.

After a keen observation we conclude that the invariants I_{21}, I_{22}, I_{23} and I_{24} are similar as I_2, I_3, I_4, I_5 respectively. And invariants I_{25}, I_{26}, I_{27} and I_{28} give us no results.

I_{29}) From these invariants we are interested in representing the solutions in form of physical parameters of fluid. For that we will focus on V_2.

Stretching sheet case

We will consider the stretching sheet case here. The plate with constant permeability is immersed in the fluid at $\overline{y} = 0$. The flow is passing through a uniform porous medium with constant permeability k'. The $\overline{y}-$coordinate is normal to the surface and $\overline{x}$-coordinate is being taken along the stretching surface. Now our boundary conditions will be as follows

$$\begin{aligned} \overline{u}(\overline{x},\overline{y}) &= b\overline{x},\ \overline{v}(\overline{x},\overline{y}) = 0 \text{ at } \overline{y} = 0, \\ \overline{u}(\overline{x},\overline{y}) &= 0, \text{ as } \overline{y} \to \infty, \end{aligned} \tag{2.95}$$

$$\begin{aligned} T(\overline{x},\overline{y}) &= T_w\ ,\ C(\overline{x},\overline{y}) = C_w \text{ at } \overline{y} = 0, \\ T(\overline{x},\overline{y}) &= T_\infty\ ,\ C(\overline{x},\overline{y}) = C_\infty \text{ as } \overline{y} \to \infty, \end{aligned} \tag{2.96}$$

where T_w wall temperature, C_w species concentration at the surface, C_∞ is free stream concentration of the species, and b is stretching parameter.

After using the similarity transformations (2.57)-(2.58) our boundary conditions become

$$\begin{aligned} u(x,y) &= x,\ v(x,y) = 0, \text{at } y = 0, \\ u(x,y) &= 0, \text{ as } y \to \infty, \end{aligned} \tag{2.97}$$

$$\begin{aligned} \theta(x,y) &= 1,\ \phi(x,y) = 1 \ \text{ at } y = 0, \\ \theta(x,y) &= 0,\ \phi(x,y) = 0 \text{ as } y \to \infty. \end{aligned} \tag{2.98}$$

And in form of stream functions Eqs. (2.97)-(2.98) will have the following form

$$\frac{\partial\psi(x,0)}{\partial y} = x, \frac{\partial\psi(x,0)}{\partial x} = 0, \frac{\partial\psi(x,\infty)}{\partial y} = 0, \tag{2.99}$$

$$\theta(x,0) = 1,\ \phi(x,0) = 1, \theta(x,\infty) = 0,\ \phi(x,\infty) = 0. \tag{2.100}$$

For these particular invariants $y = \eta$, $\psi = xf(\eta)$, $\theta = \theta(\eta)$, $\phi = \phi(\eta)$ our governing system will

take the following form

$$(1+\frac{1}{\beta})f'''(\eta)+f(\eta)f''(\eta)-f'(\eta)^2-\left(M+\frac{1}{K}\right)f'(\eta)=0, \tag{2.101}$$

$$\left(1+\frac{4}{3Nr}\right)\theta''(\eta)+\Pr f(\eta)\theta'(\eta)=0, \tag{2.102}$$

$$\phi''(\eta)+Scf(\eta)\phi'(\eta)=0, \tag{2.103}$$

$$f(0)=0, f'(0)=1, f'(\infty)=0, \tag{2.104}$$

$$\theta(0)=1, \theta(\infty)=0, \phi(0)=1, \phi(\infty)=0. \tag{2.105}$$

The skin friction coefficient, the local Nusselt number and the local Sherwood number are defined as:

$$\begin{aligned} C_f &= \frac{\left(\mu_B+\frac{p_y}{\sqrt{2\pi_c}}\right)}{\rho(b\bar{x})^2}\left(\frac{\partial\bar{u}}{\partial\bar{y}}\right)_{\bar{y}=0}, \\ Nu_x &= \frac{\bar{x}}{(T_w-T_\infty)}\left(\frac{\partial T}{\partial\bar{y}}\right)_{\bar{y}=0}, \\ Sh_x &= \frac{\bar{x}}{(C_w-C_\infty)}\left(\frac{\partial C}{\partial\bar{y}}\right)_{\bar{y}=0}. \end{aligned} \tag{2.106}$$

Using $(2.57)-(2.58)$ and (2.106), the dimensionless form of skin friction, local Nusselt number and local Sherwood number become

$$\begin{aligned} \mathrm{Re}_x^{1/2}\,C_f &= -\left(1+\frac{1}{\beta}\right)f''(0), \\ \mathrm{Re}_x^{-1/2}\,Nu_x &= -\theta'(0), \\ \mathrm{Re}_x^{-1/2}\,Sh_x &= -\phi'(0). \end{aligned} \tag{2.107}$$

In order to solve the non-linear Eqs. $(2.101)-(2.103)$ with boundary conditions $(2.104)-(2.105)$, an analytical technique known as Homotopy Analysis Method (HAM) is used [103]. According to the nature of problem, following set of initial guesses and auxiliary linear operators for $f(\eta)$,

$\theta(\eta)$ and $\phi(\eta)$ are used

$$f_0(\eta) = 1 - \exp(-\eta), \quad \theta_0(\eta) = \exp(-\eta), \quad \phi_0(\eta) = \exp(-\eta), \tag{2.108}$$

$$\mathcal{L}_f = \frac{d^3 f}{d\eta^3} - \frac{df}{d\eta}, \quad \mathcal{L}_\theta = \frac{d^2\theta}{d\eta^2} + \frac{d\theta}{d\eta}, \quad \mathcal{L}_\phi = \frac{d^2\phi}{d\eta^2} + \frac{d\phi}{d\eta}. \tag{2.109}$$

The series solutions obtained by HAM for Eqs. $(2.101)-(2.103)$ subject to boundary conditions $(2.104)-(2.105)$ can be written as

$$f(\eta) = \sum_{m=0}^{\infty} f_m(\eta), \quad \theta(\eta) = \sum_{m=0}^{\infty} \theta_m(\eta), \quad \phi(\eta) = \sum_{m=0}^{\infty} \phi_m(\eta), \tag{2.110}$$

where

$$f_m(\eta) = \frac{1}{m!}\frac{\partial^m F(\eta;q)}{\partial q^m}\bigg|_{q=0}, \theta_m(\eta) = \frac{1}{m!}\frac{\partial^m \theta(\eta;q)}{\partial q^m}\bigg|_{q=0},$$
$$\phi_m(\eta) = \frac{1}{m!}\frac{\partial^m \phi(\eta;q)}{\partial q^m}\bigg|_{q=0}. \tag{2.111}$$

The further detail of this method was discussed in chapter 1.

2.2.3 Convergence of the solutions

It is observed that the series solution (2.110) contains the auxiliary parameters $\hbar_f$, $\hbar_\theta$ and $\hbar_\phi$ with the help of which the convergence region and rate of approximation of series solutions can be controlled and adjusted. To get an idea of the admissible ranges of $\hbar_f$, $\hbar_\theta$ and $\hbar_\phi$ in which the series solution converge, the so-called $\hbar$-curves are plotted at the $20th$ order of approximation. The range for the admissible values of $\hbar_f$, $\hbar_\theta$ and $\hbar_\phi$ are $-0.5 < \hbar_f < -0.1$, $-0.5 < \hbar_\theta < -0.2$ and $-0.5 < \hbar_\phi < -0.1$ as shown in Figure 2.12.

To accelerate the convergence of the series solutions (2.110), the homotopy-Pad´e approximation is utilized, and the tabulated results for $f''(0)$, $\theta'(0)$ and $\phi'(0)$ at $\hbar_f = -0.35$, $\hbar_\theta = -0.35$, $\hbar_\phi = -0.45$ are presented in Table 2.9. It is quite evident that the value of $f''(0)$ converge up to 6 decimal places after 6th order of approximation and the values of $\theta'(0)$ and $\phi'(0)$ are convergent after $8th$ order of approximation.

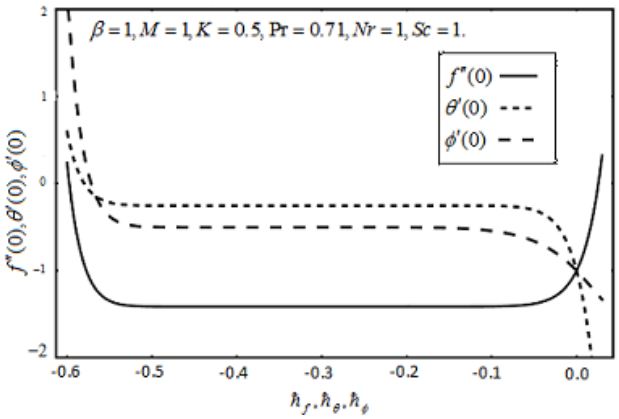

Figure 2.12: The $\hbar$-curves of at 20th-order of approximations

Pad′e Approximation	$-f''(0)$	$-\theta'(0)$	$-\phi'(0)$
$[2,2]$	1.413790	0.252893	0.493297
$[4,4]$	1.414210	0.25365	0.501131
$[6,6]$	1.414210	0.253648	0.501254
$[8,8]$	1.414210	0.253648	0.501250
$[10,10]$	1.414210	0.253648	0.501250

Table 2.9: Convergence table for the $[m/m]$ homotopy Pad´e approximation of $f''(0)$, $\theta'(0)$ and $\phi'(0)$ when $\beta = 1.0$, $M = 1.0$, $K = 0.5$, $Pr = 1.0, Nr = 1.0$ and $Sc = 1.0$ are kept fixed

2.2.4 Flow characteristics

In this section, the effects of various parameters on velocity, temperature, and concentration profiles are presented through graphs and tables. The influence of magnetic field parameter M and Casson fluid parameter revealed the same effects as observed in previous section. Figure 2.13 depicts the effects of permeability parameter on velocity profile. The velocity increases with increasing K because as the permeability parameter increases, a decrease in the resistance of porous medium is observed which speeds up the flow.

The effects of various physical parameters on temperature profile $\theta(\eta)$ are presented in Figures 2.14−2.17. Figure 2.14 illustrates that the thermal boundary layer thickness increases with

increase in Casson fluid parameter β. The effects of magnetic field parameter M on temperature profile are increasing as shown in Figure 2.15. The influence of permeability parameter K on $\theta(\eta)$ is depicted in Figure 2.16. A decrease in temperature profile is noticed with increase in permeability parameter. Figure 2.17 illustrates that thermal boundary layer thickness decreases with increase in Prandtl number Pr. On the other hand, Figure 2.18 demonstrates that thermal radiation parameter Nr enhances fluid temperature.

In Figure 2.19, the influence of Casson fluid parameter β on concentration profile $\phi(\eta)$ are shown. An increase in concentration profile is observed with increase in β. The concentration boundary layer increases with magnetic field parameter M and decreases with permeability parameter K and Schmidt number Sc as shown in Figures 2.20, 2.21 and 2.22 respectively.

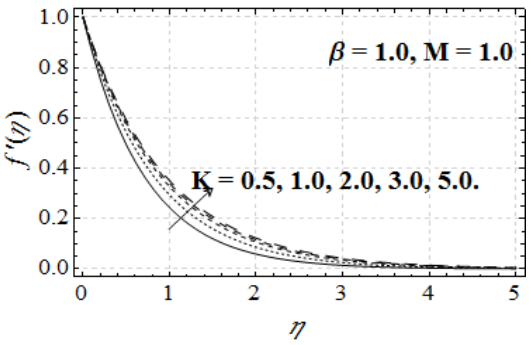

Figure 2.13: Effect of K on $f\prime(\eta)$

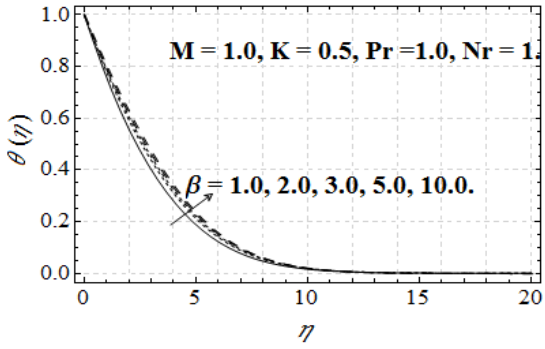

Figure 2.14: Effect of β on $\theta(\eta)$

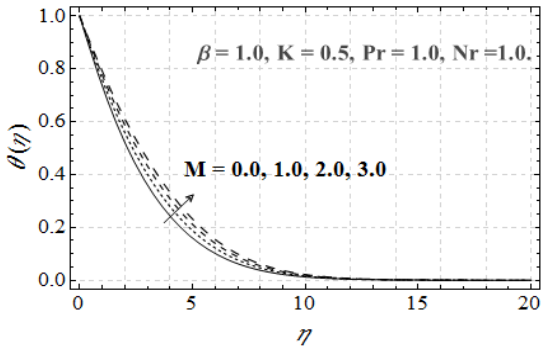

Figure 2.15: Effect of M on $\theta(\eta)$

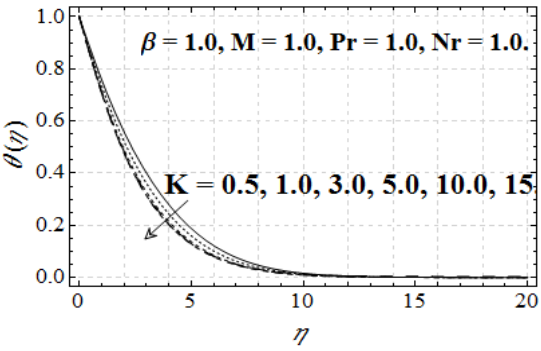

Figure 2.16: Effect of K on $\theta(\eta)$

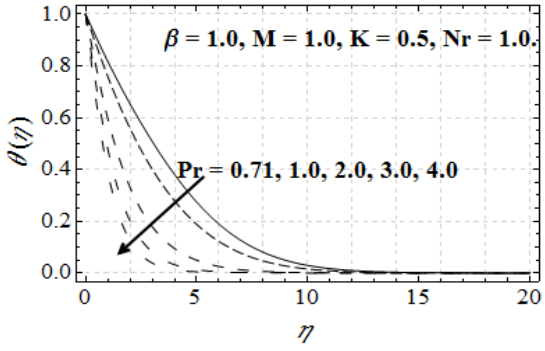

Figure 2.17: Effect of Pr on $\theta(\eta)$

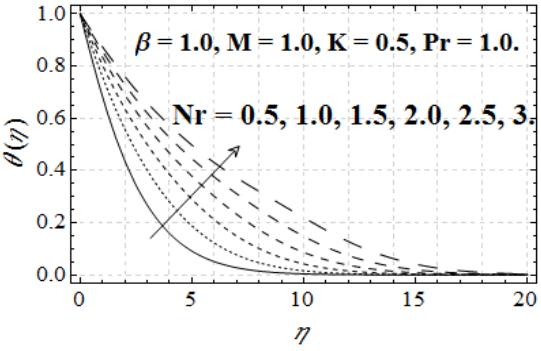

Figure 2.18: Effect of Nr on $\theta(\eta)$

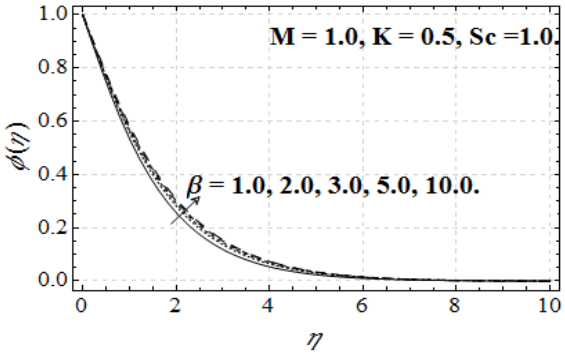

Figure 2.19: Effect of β on $\phi(\eta)$

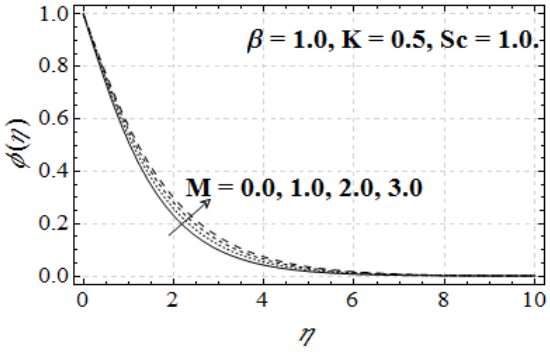

Figure 2.20: Effect of M on $\phi(\eta)$

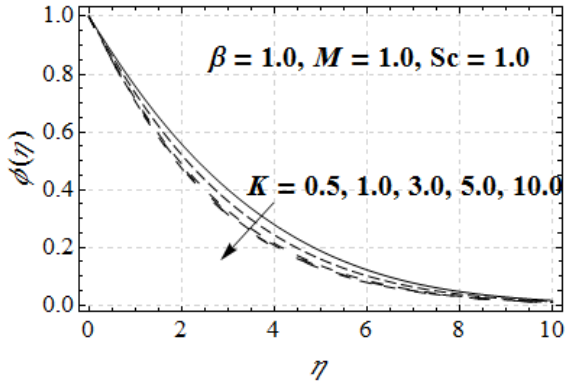

Figure 2.21: Effect of K on $\phi(\eta)$

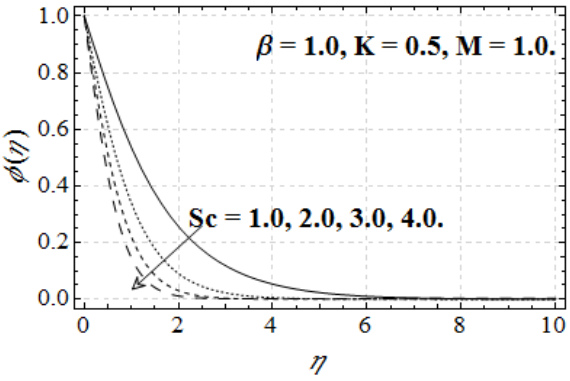

Figure 2.22: Effect of Sc on $\phi(\eta)$

Table 2.10 presents the values of $-(1+\frac{1}{\beta})f''(0)$ for various values of Casson fluid parameter β, Magnetic field parameter M and permeability parameter K. The skin friction coefficient decreases with β and K and increases with M. Table 2.11 shows that the local Nusselt number $-\theta'(0)$ increases with permeability parameter K and Prandtl number Pr and decreases with Casson fluid parameter β, magnetic field parameter M and radiation parameter Nr. In Table 2.12 the effects of pertinent parameters on local Sherwood number are demonstrated. It is seen that $-\phi'(0)$ augments with permeability parameter and Schmidt number Sc and decreases with Casson fluid parameter β, magnetic field parameter M.

β	M	K	$-(1+\frac{1}{\beta})\ f''(0)$
0.5	1.0	0.5	3.46410
1.0			2.82843
1.5			2.58199
2.0			2.44949
0.5	0.5	0.5	3.24037
	1.0		3.46410
	1.5		3.67423
	2.0		3.87298
0.5	1.0	0.5	3.46410
		1.0	3.00000
		1.5	2.82843
		2.0	2.73861

Table 2.10: Effects of various parameters on $-(1+\frac{1}{\beta})f''(0)$ when $h_f = 0.35$

β	M	K	Pr	Nr	$-\theta'(0)$
0.5	1.0	0.5	0.71	1.0	0.218459
1.0					0.188432
1.5					0.175448
2.0					0.168150
0.5	0.5	0.5	0.71	1.0	0.228523
	1.0				0.218459
	1.5				0.209624
	2.0				0.201784
0.5	1.0	0.5	0.71	1.0	0.218459
		1.0			0.240133
		1.5			0.248948
		2.0			0.253742
0.5	1.0	0.5	0.71	1.0	0.218459
			1.0		0.289864
			2.0		0.492932
			3.0		0.655593
0.5	1.0	0.5	0.71	0.5	0.288460
				1.0	0.218459
				1.5	0.176120
				2.0	0.147643

Table 2.11: Effects of various parameters on $-\theta'(0)$ when $h_f = 0.35, h_\theta = 0.45$

β	M	K	Sc	$-\phi'(0)$
0.5	1.0	0.5	0.71	0.429091
1.0				0.384405
1.5				0.363575
2.0				0.351450
0.5	0.5	0.5	0.71	0.443042
	1.0			0.429092
	1.5			0.416431
	2.0			0.404862
0.5	0.5	0.5	0.71	0.429092
		1.0		0.458545
		1.5		0.469915
		2.0		0.475961
0.5	0.5	0.5	0.71	0.429092
			1.0	0.550535
			2.0	0.877907
			3.0	1.13143

Table 2.12: Effects of various parameters on $-\phi'(0)$ when $h_f = 0.35, h_\phi = 0.45$

2.2.5 Findings

We find the twenty nine group invariant solutions by using the optimal system. For one particular invariant we solved the governing system of ordinary differential equations by considering permeable stretching sheet case to observe the influence of physical parameters on fluid and heat transfer phenomenon. The solution of that particular invariant are also presented through graphs and tables. The following observations have been made from stretching sheet case:

A decrease in momentum boundary layer thickness is observed with increase in Casson fluid parameter β and magnetic field parameter M. An increase in fluid velocity is noticed with increase in permeability parameter K. The thermal boundary layer thickness increases with Casson fluid parameter β, magnetic field parameter M and radiation parameter Nr. A decreasing effect is noticed on temperature with increase in permeability parameter K and Prandtl number Pr. The concentration increases with Casson fluid parameter β and magnetic field parameter M and decreases with permeability parameter K and Schmidt number Sc. Skin friction increases with magnetic field parameter M and decreases with Casson fluid parameter β and permeability parameter K. The permeability parameter K and Prandtl number Pr has increasing effects on local Nusselt number and it decreases with Casson fluid parameter β,

magnetic field parameter M and radiation parameter Nr. Local Sherwood number increases with K and Sc and decreases with β and M.

Chapter 3

Lie group study of unsteady MHD non-Newtonian fluid flow with viscous dissipation effects

This chapter comprises of some extension work of previous chapter. In this chapter we consider the MHD, unsteady flow of Casson fluid with viscous dissipation effects. The governing partial differential equations are made dimensionless after using appropriate similarity transformations. Further, group theoretical method is applied to analyze the governing system of partial differential equations. For the physical interest of fluid parameters we discuss one particular invariant for unsteady stretching sheet case in detail with graphs and tables.

3.1 Mathematical modeling

Consider an unsteady two-dimensional laminar flow of an incompressible Casson fluid. A uniform transverse magnetic field of strength B_0 is applied parallel to y-axis. It is also assumed that the fluid is electrically conducting and the magnetic Reynolds number is small so that the induced magnetic field is neglected. No electric field is assumed to exist. The rheological equation (1.41) and conservation of mass, momentum and heat transfer, the following boundary

layer equations are obtained

$$\frac{\partial u}{\partial x}+\frac{\partial v}{\partial y}=0, \tag{3.1}$$

$$\frac{\partial u}{\partial t}+u\frac{\partial u}{\partial x}+v\frac{\partial u}{\partial y}=\nu(1+\frac{1}{\beta})\frac{\partial^2 u}{\partial y^2}-\frac{\sigma B^2(t)}{\rho}u, \tag{3.2}$$

$$\frac{\partial T}{\partial t}+u\frac{\partial T}{\partial x}+v\frac{\partial T}{\partial y}=\frac{k}{\rho C_p}\frac{\partial^2 T}{\partial y^2}+\frac{\upsilon}{C_p}(1+\frac{1}{\beta})\left(\frac{\partial u}{\partial y}\right)^2, \tag{3.3}$$

where $B(t)=\frac{B_0}{\sqrt{1-ct}}$ is unsteady magnetic field.

Introducing the non-dimensional transformations

$$u(t,x,y) = \frac{ax}{1-ct}\frac{\partial g(x,\lambda)}{\partial \lambda}, v(t,x,y)=-\sqrt{\frac{a\upsilon}{1-ct}}g(x,\lambda), \tag{3.4}$$

$$T(t,x,y) = T_\infty+(T_f-T_\infty)\theta(x,\lambda), \text{ and } \lambda=\sqrt{\frac{a}{\upsilon(1-ct)}}y, \tag{3.5}$$

where c is constant. After using transformations $(3.4)-(3.5)$ our system $(3.1)-(3.3)$ have the following form

$$(1+\frac{1}{\beta})\frac{\partial^3 g}{\partial \lambda^3}+g\frac{\partial^3 g}{\partial \lambda^3}-(\frac{\partial g}{\partial \lambda})^2-A(\frac{\partial g}{\partial \lambda}+\frac{1}{2}\lambda\frac{\partial^2 g}{\partial \lambda^2})-M\frac{\partial g}{\partial \lambda}=0, \tag{3.6}$$

$$\frac{\partial^2 \theta}{\partial \lambda^2}-\Pr A(\theta+\frac{1}{2}\lambda\frac{\partial g}{\partial \lambda})-\Pr(\theta\frac{\partial g}{\partial \lambda}-g\frac{\partial \theta}{\partial \lambda})+(1+\frac{1}{\beta})\Pr Ec(\frac{\partial^2 g}{\partial \lambda^2})^2=0. \tag{3.7}$$

Here $A=\frac{c}{a}$ is unsteady parameter and $Ec=\frac{U_m^2}{C_p(T_f-T_\infty)}$ is Eckert number.

3.2 Lie group analysis

To find the symmetries for the system (3.6)-(3.7), we apply the Lie group technique. The infinitesimal generator can be written as

$$\vec{V}=\xi_1(x,\lambda,g,\theta)\partial_x+\xi_2(x,\lambda,g,\theta)\partial_\lambda+\phi_1(x,\lambda,g,\theta)\partial_g+\phi_2(x,\lambda,g,\theta)\partial_\theta. \tag{3.8}$$

By using the same method as discussed in chapter 2 for seeking the infinitesimals, we will have the following symmetries

$$\xi_1 = g_1(x), \xi_2 = c_1\lambda, \phi_1 = c_2 g, \phi_2 = c_3\theta, \tag{3.9}$$

where c_i $(i = 1, 2, 3)$ are arbitrary constants and $g_1(x)$ is arbitrary function of x.

There are three finite parameter Lie group symmetries represented by parameters c_i, and one infinite symmetry $g_1(x)$. Parameter c_1, c_2 and c_3 corresponds to the scaling in the variables λ, g and θ respectively.

As we discussed in chapter 2 the requirement for solvability is equivalent to the existence of a basis $\{V_1, V_2, ..., V_4\}$ of Lie algebra. The basis of the corresponding Lie algebra is as follows

$$V_1 = \partial_x, V_2 = \lambda\partial_\lambda, V_3 = g\partial_g, V_4 = \theta\partial_\theta. \tag{3.10}$$

Here we observe that, all entries of commutator table are zero. All the basis produce an Abelian Algebra. So we also can not say any thing about adjoint table.

Group invariant solutions

By following the same procedure as explained in chapter 2, the optimal system of our equations (3.6)-(3.7) is provided by

$I_1)$ $V_1 + V_2$	$I_2)$ $V_1 + V_3$	$I_3)$ $V_1 + V_4$
$I_4)$ $V_2 + V_4$	$I_5)$ $V_3 + V_4$	$I_6)$ $V_1 + V_2 + V_3$
$I_7)$ $V_1 + V_2 + V_4$	$I_8)$ $V_1 + V_2 + V_4$	$I_9)$ $V_1 + V_2 + V_4$
$I_{10})$ $V_i, i = 1, 2, 3, 4.$		

Further we will concentrate our attention on the classification of the group-invariant solutions. The system of invariants can be used to reduce the order of the original equations - constructing the reduced order system of equations. Doing this one can hope to find simple equations that can be integrated. Since differential equations can admit more than one symmetry, there are different ways to choose a set of similarity variables by starting from different symmetries.

Here we follow the procedure as explained in chapter 2 to reduce the governing partial differential equations into ordinary differential equations. For our system (3.6)-(3.7) we find

ten group invariants which lead to group invariant solutions which are as follows.

I_1) Invariants are $x = \eta, g = \lambda f(\eta), \theta = \theta(\eta)$. This set of invariant gives us trivial solutions.

I_2) Here invariants are $x = \eta, g = f(\eta), \theta = \lambda\theta(\eta)$. After using this set of invariants our system identically satisfied.

I_3) Invariants are $\eta = \frac{\lambda}{e^x}, g = f(\eta), \theta = \theta(\eta)$. After using this set of invariants our system appeared into following form which can be solved numerically

$$(1+\frac{1}{\beta})f''' + e^x ff'' - e^x(f')^2 - A(e^{2x}f' + \frac{1}{2}\eta f'') - Me^{2x}f' = 0, \tag{3.11}$$

$$\theta'' - \Pr A(e^{2x}\theta + \frac{1}{2}\eta\theta') - \Pr e^x(f'\theta - f\theta') + (1+\frac{1}{\beta})\Pr Ece^{-2x}(f'')^2 = 0. \tag{3.12}$$

I_4) Invariants are $\lambda = \eta, g = e^x f(\eta), \theta = \theta(\eta)$. After using this set of invariants our system takes the following form which can be solved numerically

$$(1+\frac{1}{\beta})f''' + e^x ff'' - e^x(f')^2 - A(f' + \frac{1}{2}\eta f'') - Mf' = 0, \tag{3.13}$$

$$\theta'' - \Pr A(\theta + \frac{1}{2}\eta\theta') - \Pr e^x(f'\theta - f\theta') + (1+\frac{1}{\beta})\Pr Ece^{2x}(f'')^2 = 0. \tag{3.14}$$

I_5) Invariants are $\lambda = \eta, g = f(\eta), \theta = e^x\theta(\eta)$. By using this set of invariants flow equation appeared same as in V_1 and heat transfer equation can be solved numerically i.e.

$$(1+\frac{1}{\beta})f''' + ff'' - (f')^2 - A(f' + \frac{1}{2}\eta f'') - Mf' = 0, \tag{3.15}$$

$$\theta'' - \Pr A(\theta + \frac{1}{2}\eta\theta') - \Pr(f'\theta - f\theta') + (1+\frac{1}{\beta})\Pr Ece^{-x}(f'')^2 = 0. \tag{3.16}$$

I_6) Invariants are $\eta = \frac{\lambda}{e^x}, g = \lambda f(\eta), \theta = \theta(\eta)$. After using this set of invariants our system takes the following form which can be solved numerically

$$(1+\frac{1}{\beta})[3f'' + \eta f'''] + \eta^2 ff'' - \eta^2(f')^2 - f^2 - A(f + \eta f' + \eta^2 f'') - M(f + \eta f') = 0, \tag{3.17}$$

$$\theta'' - \Pr Ae^{2x}(\theta + \frac{1}{2}\eta\theta') - \Pr e^x(2f'\theta + \eta f''\theta - \eta f\theta') + (1+\frac{1}{\beta})\Pr Ec(2f' + \eta f'')^2 = 0. \tag{3.18}$$

I_7) Invariants are $\eta = \frac{\lambda}{e^x}, g = f(\eta), \theta = \lambda\theta(\eta)$. By using this set of invariants flow equation

appeared same as in I_3 and the heat equation takes the following form which can be solved numerically

$$\eta\theta''+2\theta'-\Pr Ae^x(\lambda\theta+\frac{1}{2}\eta\theta+\frac{1}{2}\eta^2\theta')-\Pr e^x(\eta f'\theta-f\theta-\eta f\theta')+(1+\frac{1}{\beta})\Pr Ece^{-3x}(f'')^2=0. \quad (3.19)$$

I_8) Invariants are $x=\eta, g=\lambda f(\eta), \theta=\lambda\theta(\eta)$. This set of invariants gives us trivial solutions.
I_9) Invariants are $\eta=\lambda, g=e^x f(\eta), \theta=e^x\theta(\eta)$. This set of invariants reveals us same flow equation as in I_4 and similar heat equation as in I_5.

I_{10}) For this particular invariant V_1 we are interested to observe the behavior of physical parameters on flow and heat transfer phenomenon.

Unsteady stretching sheet

We consider the unsteady stretching sheet with convective boundary case. The sheet lies in the plane $y=0$ with the flow being confined to $y>0$. The coordinate x is being taken along the stretching surface and y is normal to the surface. Along the x-axis, two equal and opposite forces are applied, so that the surface is stretched, keeping the origin fixed. So our boundary conditions becomes

$$\begin{aligned} u(t,x,y) &= U_m(t,x), v(t,x,y)=0, \ \& \ -k\frac{\partial T(t,x,y)}{\partial y}=h[T_f-T], \text{at } y=0, \\ u(t,x,y) &\to 0, T(t,x,y)\to 0, \text{ at } y\to\infty, \end{aligned} \quad (3.20)$$

where

$$U_m(t,x)=\frac{ax}{1-ct} \text{ and } T_f(t,x)=T_\infty+\frac{a_1x}{1-ct}. \quad (3.21)$$

After using (3.4)-(3.5) the boundary conditions become

$$\begin{aligned} g(x,0) &= 0, \frac{\partial g(x,0)}{\partial\lambda}=1, \frac{\partial g(x,\infty)}{\partial\lambda}=0, \\ \frac{\partial\theta(x,0)}{\partial\lambda} &= -\gamma[1-\theta(x,0)], \theta(x,\infty)=0. \end{aligned} \quad (3.22)$$

where $\gamma=\frac{h}{k}\sqrt{\frac{\nu(1-ct)}{a}}$ is Biot number.

For this particular invariant, $\lambda = \eta, g = f(\eta), \theta = \theta(\eta)$ our system takes the following form

$$(1+\frac{1}{\beta})f''' + ff'' - (f')^2 - A(f' + \frac{1}{2}\eta f'') - Mf' = 0, \tag{3.23}$$

$$\theta'' - \Pr A(\theta + \frac{1}{2}\eta\theta') - \Pr(f'\theta - f\theta') + (1+\frac{1}{\beta})\Pr Ec(f'')^2 = 0, \tag{3.24}$$

with subject to the following boundary conditions

$$\begin{aligned} f(0) &= 0, f'(0) = 1, f'(\infty) = 0, \\ \theta'(0) &= -\gamma[1-\theta(0)], \theta(\infty) = 0. \end{aligned} \tag{3.25}$$

The skin friction coefficient and the local Nusselt number are defined as:

$$\begin{aligned} C_f &= \frac{\left(\mu_B + \frac{p_y}{\sqrt{2\pi_c}}\right)}{\rho(b\overline{x})^2}\left(\frac{\partial u}{\partial y}\right)_{y=0}, \\ Nu_x &= \frac{\bar{x}}{(T_w - T_\infty)}\left(\frac{\partial T}{\partial y}\right)_{y=0}. \end{aligned} \tag{3.26}$$

Using $(3.4)-(3.5)$ and (3.26), the dimensionless form of skin friction and local Nusselt number become

$$\begin{aligned} R_x^{1/2}C_f &= -\left(1+\frac{1}{\beta}\right)f''(0), \\ R_x^{-1/2}Nu_x &= -\theta'(0). \end{aligned} \tag{3.27}$$

In order to solve the non-linear Eqs. $(3.23)-(3.24)$ with boundary conditions (3.25), an analytical technique known as (HAM) is used. The detail of this method can be found in [103] and in chapter 1. According to the nature of this problem, following set of initial guesses and auxiliary linear operators for $f(\eta)$ and $\theta(\eta)$ are used

$$f_0(\eta) = 1 - \exp(-\eta), \quad \theta_0(\eta) = \exp(-\eta), \tag{3.28}$$

$$\mathcal{L}_f = \frac{d^3f}{d\eta^3} - \frac{df}{d\eta}, \quad \mathcal{L}_\theta = \frac{d^2\theta}{d\eta^2} + \frac{d\theta}{d\eta}. \tag{3.29}$$

The series solutions obtained by HAM for Eqs. $(3.23)-(3.24)$ subject to boundary conditions

(3.25) can be written as

$$f(\eta) = \sum_{m=0}^{\infty} f_m(\eta), \qquad \theta(\eta) = \sum_{m=0}^{\infty} \theta_m(\eta), \tag{3.30}$$

where

$$f_m(\eta) = \frac{1}{m!}\frac{\partial^m F(\eta;q)}{\partial q^m}\bigg|_{q=0}, \theta_m(\eta) = \frac{1}{m!}\frac{\partial^m \theta(\eta;q)}{\partial q^m}\bigg|_{q=0}. \tag{3.31}$$

Note that the two series (3.30) contain the auxiliary parameters $\hbar_f$ and $\hbar_\theta$ which influences the convergent rate and region of the two series. To get an idea of the admissible ranges of $\hbar_f$ and $\hbar_\theta$ in which the series solution converge, the so-called $\hbar-$curves are plotted at the 15th order of approximation. The range for the admissible values of $\hbar_f$ and $\hbar_\theta$ are $-0.7 < \hbar_f < 0$ and $-0.7 < \hbar_\theta < 0$ as shown in Figure 3.1. To proceed with the convergence of the series solutions (3.30), the homotopy- approximation is utilized, and the tabulated results for $-f''(0)$ and $-\theta'(0)$ at $\hbar_f = -0.3$ and $\hbar_\theta = -0.3$ are presented in Table 3.1. It is quite evident that the value of $-f''(0)$ converge up to 6 decimal places after 12th order of approximation and the values of $-\theta'(0)$ are convergent after 30th order of approximation.

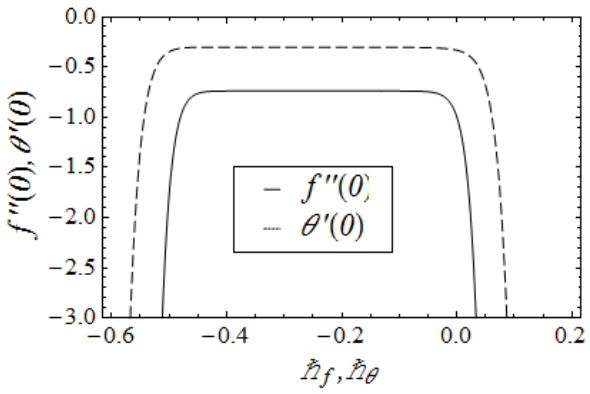

Figure 3.1: The $\hbar$-curves of at 15th-order of approximations when Ec=0.2, Pr=1, M=1, $\beta = 0.3$, A=0.5 and $\gamma = 0.5$

Order of Convergence	$-f''(0)$	$-\theta'(0)$
1	0.70625	0.310694
5	0.739195	0.304136
10	0.739337	0.302814
15	0.739336	0.302683
20	0.739336	0.302669
25	0.739336	0.302666
30	0.739336	0.302665

Table 3.1: Convergence table of $-f''(0)$ and $-\theta'(0)$ for various order of approximations when $Ec = 0.2, \Pr = 1, \beta = 0.3, M = 1, A = 0.5$ and $\gamma = 0.5$

3.3 Flow characteristics

The transformations for linear group are used to reduce the two independent variables into one and hence to reduce the governing equations into a system of non-linear ordinary differential equations (3.23)-(3.24) with boundary conditions (3.25) are solved numerically using the Runge-Kutta fourth-fifth order method with shooting technique. Then we hash out the influence of various parameters on velocity and temperature through graphs and tables. Figures 3.2-3.4 presents the effects of different parameters on velocity profile. In Figure 3.2, the effects of unsteady parameter on velocity profile are illustrated. It is observed that an increase in velocity occurs with increase in unsteady parameter A. Figure 3.3 shows the influence of magnetic field parameter on velocity profile $f'(\eta)$. It is quite clear that with an increase in the value of M the velocity decreases. The behavior is because of the application of magnetic field to an electrically conducting fluid give rise to a resistive force known as Lorentz force which causes the fluid to decelerate. Figure 3.4 depicts that the effects of Casson fluid parameter β on velocity profile. It is observed that a decrease in velocity occurs with increase in Casson fluid parameter β. The effects of various physical parameters on temperature profile $\theta(\eta)$ are presented in Figures 3.5-3.9. Figure 3.5 presents that with increase in thermal boundary layer thickness unsteady parameter A decreases. The influence of magnetic field parameter M on temperature profile $\theta(\eta)$ increasing as illustrated in Figure 3.6. In Figure 3.7 the effects of Casson fluid parameter β on thermal boundary layer thickness are presented. It is observed that when β increases $\theta(\eta)$ also increases. The influence of Eckert number Ec on temperature profile $\theta(\eta)$ are presented in

Figure 3.8. It is quite clear that with the increase of Ec the thermal boundary layer thickness $\theta(\eta)$ increases. Figure 3.9 shows that when we increase Biot Number γ the temperature profile $\theta(\eta)$ increases.

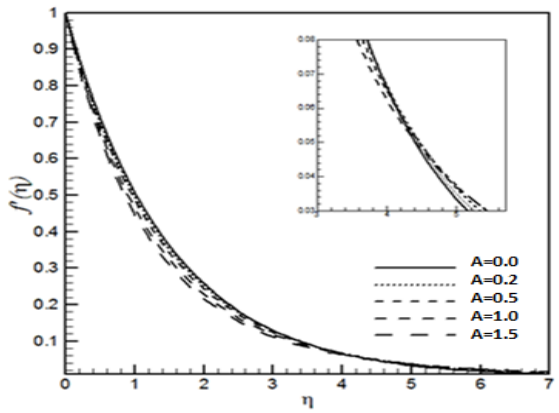

Figure 3.2: Effect of A on $f'(\eta)$

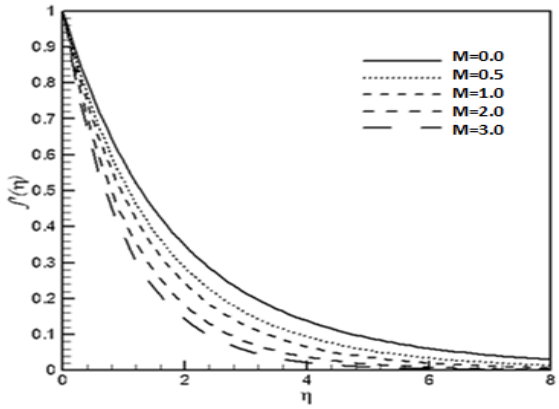

Figure 3.3: Effect of M on $f'(\eta)$

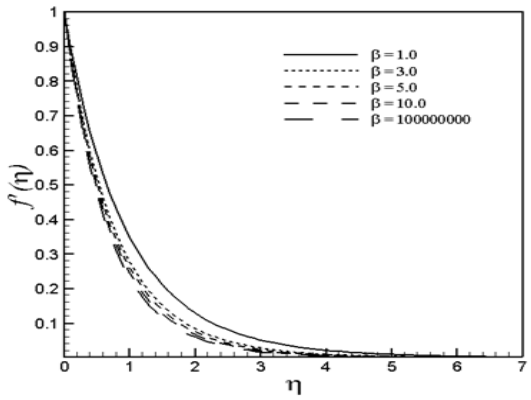

Figure 3.4: Effect of β on $f'(\eta)$

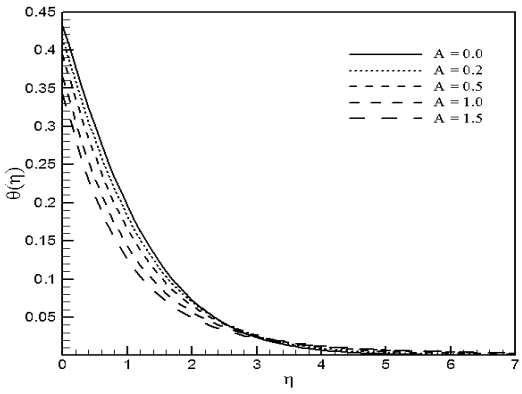

Figure 3.5: Effect of A on $\theta(\eta)$

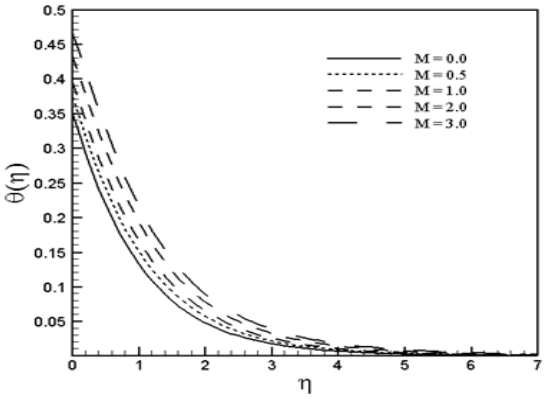

Figure 3.6: Effect of M on $\theta(\eta)$

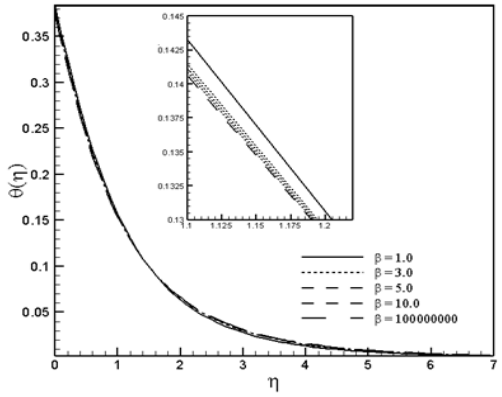

Figure 3.7: Effect of β on $\theta(\eta)$

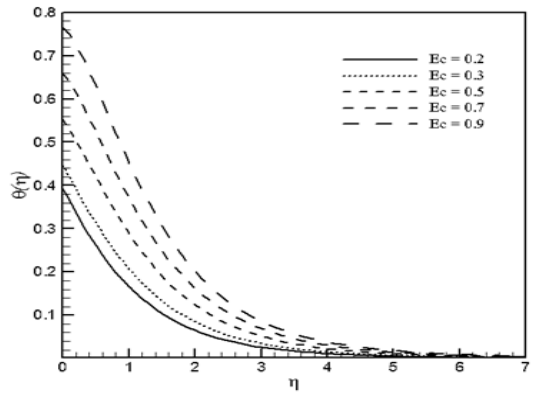

Figure 3.8: Effect of Ec on $\theta(\eta)$

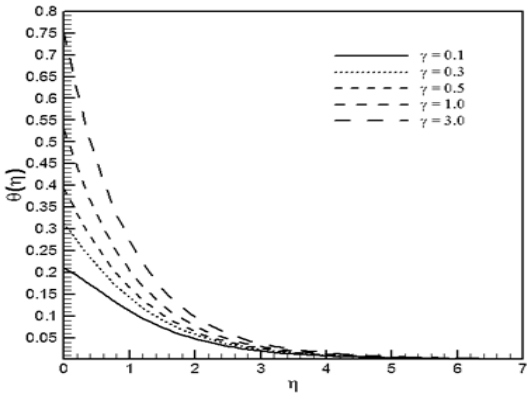

Figure 3.9: Effect of γ on $\theta(\eta)$

Table 3.2 presents the values of $-(1+\frac{1}{\beta})f''(0)$ for various values of unsteady parameter A, magnetic field parameter M and Casson fluid parameter β. The skin friction coefficient increases with M and A and decreases with β. Table 3.3 shows that the local Nusselt Number $-\theta'(0)$ increases with unsteady parameter A, Casson fluid parameter β and Biot Number γ and

decreases with magnetic field parameter M and Eckert Number Ec.

M	A	β	$-(1+\frac{1}{\beta})f''(0)$ HAM	$-(1+\frac{1}{\beta})f''(0)$ Numerical
0.0	0.5	0.3	2.42975	2.42975
0.5			2.84405	2.84405
1.0			3.20379	3.20379
2.0			3.82186	3.82186
3.0			4.35253	4.35253
1.0	0.0	0.3	2.94392	2.94392
	0.2		3.04953	3.04953
	0.5		3.20379	3.20379
	1.0		3.44959	3.44959
	1.5		3.68189	3.68189
1.0	0.5	1.0	2.17654	2.17654
		3.0	1.77714	1.77714
		5.0	1.68595	1.68595
		10.0	1.61417	1.61417
		∞	1.53905	1.53905

Table 3.2: Effects of various parameters on $-(1+\frac{1}{\beta})f''(0)$ when $\hbar_f = -0.3$

Ec	γ	M	A	β	$-\theta'(0)$ HAM	$-\theta'(0)$ Numerical
0.2	0.5	1.0	0.5	0.3	0.30267	0.30267
0.3					0.27597	0.27597
0.5					0.22257	0.22257
0.7					0.16917	0.16917
0.9					0.11577	0.11577
0.2	0.1	1.0	0.5	0.3	0.07865	0.07865
	0.3				0.20523	0.20523
	0.5				0.30267	0.30267
	1.0				0.47002	0.47002
	3.0				0.74446	0.74446
0.2	0.5	0.0	0.5	0.3	0.32483	0.32483
		0.5			0.31324	0.31324
		1.0			0.30267	0.30267
		2.0			0.28354	0.28354
		3.0			0.26631	0.26631
0.2	0.5	1.0	0.0	0.3	0.28328	0.28328
			0.2		0.29164	0.29164
			0.5		0.30267	0.30267
			1.0		0.31734	0.31734
			1.5		0.32847	0.32847
0.2	0.5	1.0	0.5	1.0	0.30708	0.30708
				3.0	0.30835	0.30835
				5.0	0.30856	0.30856
				10.0	0.30868	0.30868
				∞	0.30879	0.30879

Table 3.3: Effects of various parameters on $-\theta'(0)$ when $\Pr = 1$, $\hbar_\theta = -0.30$

3.4 Findings

For a particular invariant we have solved the governing system of ordinary differential equation by considering unsteady stretching sheet case. Homotopy Analysis Method and Numerical Method are used to solve these equations. Following observations are found from the unsteady stretching sheet case:

The velocity and temperature profiles decrease when the non-Newtonian Casson fluid parameter β increases. Magnetic field parameter M has opposite effects on velocity field $f'(\eta)$ and temperature profile $\theta(\eta)$. Unsteady parameter A for velocity and temperature profiles is

observed similar. The temperature profile increases with Eckert Number Ec and Biot Number γ. Skin friction increases with unsteady parameter A and magnetic field parameter M and decreases with Casson fluid parameter β. An unsteady parameter A, Casson fluid parameter β and Biot Number γ has increasing effects on Local Nusselt Number Nu_x and it decreases with magnetic field parameter M and Eckert Number Ec.

Chapter 4

Lie group study of Hall effects with thermal radiation and free convection phenomenon

This chapter devoted into two sections. In section 1 we consider the MHD stagnation point flow, heat and mass transfer with thermal radiation effects. After making the governing equations dimensionless we have applied the Lie group technique to find the symmetries of the governing equations. Further, we find the sub algebra and the group invariants solutions of the governing system. To observe the effects of different physical parameters on velocity, temperature and concentration profiles we consider the case of permeable plate with conduction on the walls. In the end, flow characteristics are discussed in detail with graphs.

In section 2, we apply the similarity technique on Hall effects with free convection, Casson fluid flow and heat transfer phenomenon. We use the dimensionless quantities on our governing system of partial differential equations. Further we investigate the system of differential equations in the light of scaling symmetry. After finding the similarity variables we convert the system into the ordinary differential equations. In the end, we solve the particular problem with boundary conditions and represent the results through graphs.

4.1 Lie group study of stagnation point flow with thermal radiation effects

4.1.1 Mathematical modeling

Consider a steady two-dimensional laminar flow of an incompressible Casson fluid, heat and mass transfer in the presence of thermal radiation effects. A uniform transverse magnetic field of strength B_0 is applied parallel to $\overline{y}$-axis. It is also assumed that the fluid is electrically conducting and the magnetic Reynolds number is small so that the induced magnetic field is neglected. No electric field is assumed to exist. Using Eq. (1.41) and conservation of mass, conservation of momentum, heat and mass transfer we have the following boundary layer equations

$$\frac{\partial \bar{u}}{\partial \bar{x}} + \frac{\partial \bar{v}}{\partial \bar{y}} = 0, \tag{4.1}$$

$$\bar{u}\frac{\partial \bar{u}}{\partial \bar{x}} + \bar{v}\frac{\partial \bar{u}}{\partial \bar{y}} = -\frac{1}{\rho}\frac{\partial p}{\partial \bar{x}} + \nu(1+\frac{1}{\beta})\frac{\partial^2 \bar{u}}{\partial \bar{y}^2} - \frac{\sigma B_0^2}{\rho}\bar{u}, \tag{4.2}$$

$$\bar{u}\frac{\partial T}{\partial \bar{x}} + \bar{v}\frac{\partial T}{\partial \bar{y}} = \frac{k}{\rho C_p}\frac{\partial^2 T}{\partial \bar{y}^2} - \frac{16\sigma_1 T_\infty^3}{3\rho C_p k_1}\frac{\partial^2 T}{\partial \bar{y}^2}, \tag{4.3}$$

$$\bar{u}\frac{\partial C}{\partial \bar{x}} + \bar{v}\frac{\partial C}{\partial \bar{y}} = D\frac{\partial^2 C}{\partial \bar{y}^2}. \tag{4.4}$$

For pressure gradient use $\bar{u} = \bar{u}_e(\bar{x})$ in the free stream, then by Eq. (4.2) become

$$-\frac{1}{\rho}\frac{\partial p}{\partial \bar{x}} = \bar{u}_e\frac{d\bar{u}_e}{d\bar{x}} + \frac{\sigma B_0^2}{\rho}\bar{u}_e. \tag{4.5}$$

We define the non-dimensionalized parameters as:

$$\begin{aligned} x &= \frac{\bar{x}}{L}, y = \frac{\bar{y}\sqrt{R}}{L}, u = \frac{\bar{u}}{u_\infty}, v = \frac{\bar{v}\sqrt{R}}{u_\infty}, \\ u_e &= \frac{\bar{u}_e}{u_\infty}, \theta = \frac{T-T_\infty}{T_f - T_\infty}, \phi = \frac{C-C_\infty}{C_w - C_\infty}, R = \frac{Lu_\infty}{\upsilon}. \end{aligned} \tag{4.6}$$

By using above transformations (4.6) and by considering the external velocity $u_e = x$, our system (4.1)-(4.4) becomes

$$\frac{\partial u}{\partial x} + \frac{\partial v}{\partial y} = 0, \tag{4.7}$$

$$u\frac{\partial u}{\partial x} + v\frac{\partial u}{\partial y} = (1 + \frac{1}{\beta})\frac{\partial^2 u}{\partial y^2} - M(u - x) + x, \tag{4.8}$$

$$u\frac{\partial \theta}{\partial x} + v\frac{\partial \theta}{\partial y} = \frac{1}{\mathrm{Pr}}\left(1 + \frac{4}{3Nr}\right)\frac{\partial^2 \theta}{\partial y^2}, \tag{4.9}$$

$$u\frac{\partial \phi}{\partial x} + v\frac{\partial \phi}{\partial y} = \frac{1}{Sc}\frac{\partial^2 \phi}{\partial y^2}. \tag{4.10}$$

Now introducing stream function as

$$u = \frac{\partial \psi}{\partial y}, v = -\frac{\partial \psi}{\partial x}. \tag{4.11}$$

Now our system (4.7)-(4.10) will be

$$\frac{\partial \psi}{\partial y}\frac{\partial^2 \psi}{\partial x \partial y} - \frac{\partial \psi}{\partial x}\frac{\partial^2 \psi}{\partial y^2} = (1 + \frac{1}{\beta})\frac{\partial^3 \psi}{\partial y^3} - M\left(\frac{\partial \psi}{\partial y} - x\right) + x, \tag{4.12}$$

$$\frac{\partial \psi}{\partial y}\frac{\partial \theta}{\partial x} - \frac{\partial \psi}{\partial x}\frac{\partial \theta}{\partial y} = \frac{1}{\mathrm{Pr}}\left(1 + \frac{4}{3Nr}\right)\frac{\partial^2 \theta}{\partial y^2}, \tag{4.13}$$

$$\frac{\partial \psi}{\partial y}\frac{\partial \phi}{\partial x} - \frac{\partial \psi}{\partial x}\frac{\partial \phi}{\partial y} = \frac{1}{Sc}\frac{\partial^2 \phi}{\partial y^2}. \tag{4.14}$$

4.1.2 Lie group analysis

Lie group theory is employed in search of symmetries of the equations. The infinitesimal generator for the problem is

$$\begin{aligned} \vec{V} &= \xi_1(x, y, \psi, \theta, \phi)\partial_x + \xi_2(x, y, \psi, \theta, \phi)\partial_y + \Gamma_1(x, y, \psi, \theta, \phi)\partial_\psi \\ &\quad \Gamma_2(x, y, \psi, \theta, \phi)\partial_\theta + \Gamma_3(x, y, \psi, \theta, \phi)\partial_\phi. \end{aligned} \tag{4.15}$$

A straightforward calculations as explained in chapter 2, yields

$$\xi_1 = c_2 x, \xi_2 = g(x), \Gamma_1 = c_1 + c_2\psi, \Gamma_2 = c_4 + c_5\theta, \Gamma_3 = c_6 + c_3\phi, \tag{4.16}$$

where c_i $(i = 1, 2, ..., 6)$ are arbitrary constants and $g(x)$ is arbitrary function of x.

There are six finite parameter Lie group symmetries represented by parameters c_i, and one infinite symmetry $g(x)$. Parameter c_1 corresponds to the translation in the variable ψ, c_2 corresponds to the scaling in ψ and x, c_3 corresponds to the scaling in ϕ, c_4 corresponds to the translation in θ, c_5 corresponds to scaling in θ and c_6 corresponds to translation in ϕ.

Here we have a $7-$dimensional vector space of infinitesimal generators closed under the operation of commutation, i.e., $7-$dimensional Lie algebra, the basis of the corresponding Lie algebra is as follows

$$V_1 = \partial_\psi, V_2 = x\partial_x + \psi\partial_\psi, V_3 = \phi\partial_\phi, V_4 = \partial_\theta, V_5 = \theta\partial_\theta, V_6 = \partial_\phi, V_7 = \partial_y. \tag{4.17}$$

As we discuss in chapter 2 the requirement for solvability is equivalent to the existence of a basis $\{V_1, V_2, ..., V_7\}$ of Lie algebra such that by Eq. (1.13) we can develop the following commutator table

[,]	V_1	V_2	V_3	V_4	V_5	V_6	V_7
V_1	0	0	V_1	0	0	0	0
V_2	0	0	-V_2	0	0	0	0
V_3	-V_1	V_2	0	0	0	0	0
V_4	0	0	0	0	0	0	V_7
V_5	0	0	0	0	0	-V_5	0
V_6	0	0	0	0	V_5	0	0
V_7	0	0	0	-V_7	0	0	0

Table 4.1: Commutator table

The commutator table 4.1 provides us the following Abelian Lie algebra

$$\begin{aligned}
[V_s, V_t] &= 0, \text{ as } s = t, [V_1, V_2] = 0, [V_1, V_4] = 0, [V_1, V_5] = 0, \\
[V_1, V_6] &= 0, [V_1, V_7] = 0, [V_2, V_4] = 0, [V_2, V_5] = 0, \\
[V_2, V_6] &= 0, [V_2, V_7] = 0, [V_3, V_4] = 0, [V_3, V_5] = 0, \\
[V_3, V_6] &= 0, [V_3, V_7] = 0, [V_4, V_5] = 0, [V_4, V_6] = 0, \\
[V_5, V_7] &= 0, [V_6, V_7] = 0.
\end{aligned}$$

By using the definition of adjoint representation from chapter 1, we can reconstruct the adjoint representation adG of the Lie group by summing the Lie series (1.14) obtaining the adjoint table.

Ad	V_1	V_2	V_3	V_4
V_1	V_1	V_2	$V_3 - \varepsilon V_1$	V_4
V_2	$V_1 e^{\varepsilon}$	V_2	$V_3 + \varepsilon V_2$	V_4
V_3	V_1	$V_2[\cosh\varepsilon - \sinh\varepsilon]$	V_3	V_4
V_4	V_1	V_2	V_3	V_4
V_5	V_1	V_2	V_3	V_4
V_6	V_1	V_2	V_3	V_4
V_7	V_1	V_2	V_3	$V_4 + \varepsilon V_7$

Ad	V_5	V_6	V_7
V_1	V_5	V_6	V_7
V_2	V_5	V_6	V_7
V_3	V_5	V_6	V_7
V_4	V_5	V_6	$V_7[\cosh\varepsilon - \sinh\varepsilon]$
V_5	V_5	$V_6 + \varepsilon V_5$	V_7
V_6	$V_5[\cosh\varepsilon - \sinh\varepsilon]$	V_6	V_7
V_7	V_5	V_6	V_7

Table 4.2: Adjoint table

The optimal system of our equations (4.12)-(4.14) is provided by those generated by

$I_1)\ V_2 + V_3$ $I_2)\ V_2 + V_4$ $I_3)\ V_2 + V_5$
$I_4)\ V_2 + V_6$ $I_5)\ V_2 + V_7$ $I_6)\ V_1 + V_7$
$I_7)\ V_3 + V_7$ $I_8)\ V_4 + V_7$ $I_9)\ V_5 + V_7$
$I_{10})\ V_6 + V_7$ $I_{11})\ V_1 + V_3 + V_7$ $I_{12})\ V_1 + V_4 + V_7$
$I_{13})\ V_1 + V_5 + V_7$ $I_{14})\ V_1 + V_6 + V_7$ $I_{15})\ V_2 + V_3 + V_4$
$I_{16})\ V_2 + V_3 + V_5$ $I_{17})\ V_2 + V_3 + V_7$ $I_{18})\ V_2 + V_4 + V_6$
$I_{19})\ V_2 + V_4 + V_7$ $I_{20})\ V_2 + V_5 + V_6$ $I_{21})\ V_2 + V_5 + V_7$
$I_{22})\ V_2 + V_6 + V_7$ $I_{23})\ V_3 + V_4 + V_7$ $I_{24})\ V_3 + V_5 + V_7$
$I_{25})\ V_4 + V_6 + V_7$ $I_{26})\ V_i (i = 1, 2, 3...7)$

Here we follow the procedure as mentioned in chapter 2 to reduce the governing partial differential equations into ordinary differential equations. For our system (4.12)-(4.14) we find the following twenty six group invariants which lead us to group invariant solutions which are as follows.

I_1) Invariants are $y = \eta, \psi = xf(\eta), \theta = \theta(\eta), \phi = x\phi(\eta)$. The system reduced into the

following form

$$(1+\frac{1}{\beta})f'''-f'^2+ff''-M(f'-1)+1=0, \tag{4.18}$$

$$\left(1+\frac{4}{3Nr}\right)\theta''+\Pr f\theta'=0, \tag{4.19}$$

$$\phi''+Scf\phi'-Scf'\phi=0. \tag{4.20}$$

The solution of the flow equation (4.18) and heat equation (4.19) will be solved later for V_2 and mass transfer equation (4.20) can be solved numerically.

I_2) The set of invariants are $y=\eta, \psi=xf(\eta), \theta=\ln x+\theta(\eta), \phi=\phi(\eta)$. Then the flow equation appeared same as I_1 and the other equations becomes

$$\left(1+\frac{4}{3Nr}\right)\theta''+\Pr f\theta'-\Pr f'=0, \tag{4.21}$$

$$\phi''+Scf\phi'=0. \tag{4.22}$$

The solution of (4.21) can be obtained numerically and mass transfer equation will be solved later for V_2.

I_3) The invariants are $y=\eta, \psi=xf(\eta), \theta=x\theta(\eta), \phi=\phi(\eta)$. The flow and mass transfer equations appeared same as in I_2 but the heat equation can be solved numerically which becomes

$$\left(1+\frac{4}{3Nr}\right)\theta''+\Pr f\theta'-\Pr f'\theta=0. \tag{4.23}$$

I_4) The invariants are $y=\eta, \psi=xf(\eta), \theta=\theta(\eta), \phi=\ln x+\phi(\eta)$. The flow and heat transfer equations appeared same as in I_1 but the mass transfer equation can be solved numerically which is

$$\phi''+Scf\phi'-Scf'=0. \tag{4.24}$$

I_5) Here the invariants are $\eta=\frac{e^y}{x}, \psi=xf(\eta), \theta=\theta(\eta), \phi=\phi(\eta)$. The system reduces to

following form that can be solved numerically

$$(1+\frac{1}{\beta})[\eta^3 f''' + 3\eta^2 f'' + \eta f'] + \eta^2 f f' + \eta f f' - \eta^2 f'^2 - M(\eta f' - 1) + 1 = 0, \tag{4.25}$$

$$\left(1+\frac{4}{3Nr}\right)[\eta\theta'' + \theta'] + \Pr f\theta' = 0, \tag{4.26}$$

$$\eta\phi'' + \phi' + Scf\phi' = 0. \tag{4.27}$$

I_6) The invariants are $x = \eta, \psi = y + f(\eta), \theta = \theta(\eta), \phi = \phi(\eta)$. These invariants give us no result.

I_7) The invariants are $x = \eta, \psi = f(\eta), \theta = \theta(\eta), \phi = e^y\phi(\eta)$. These invariants reveal us no result.

I_8) The invariants are $x = \eta, \psi = f(\eta), \theta = y + \theta(\eta), \phi = \phi(\eta)$. These invariants give us no result.

I_9) The invariants are $x = \eta, \psi = f(\eta), \theta = e^y\theta(\eta), \phi = \phi(\eta)$. These invariants give us no result.

I_{10}) The invariants are $x = \eta, \psi = y + f(\eta), \theta = \theta(\eta), \phi = y + \phi(\eta)$. These invariants give us no result.

I_{11}) Here the invariants are $x = \eta, \psi = y + f(\eta), \theta = \theta(\eta), \phi = e^y\phi(\eta)$. These invariants give us no result.

I_{12}) Here the invariants are $x = \eta, \psi = y + f(\eta), \theta = y + \theta(\eta), \phi = \phi(\eta)$. These invariants give us no result.

I_{13}) The invariants are $x = \eta, \psi = y + f(\eta), \theta = e^y\theta(\eta), \phi = \phi(\eta)$. These invariants give us no result.

I_{14}) The invariants are $x = \eta, \psi = y + f(\eta), \theta = \theta(\eta), \phi = y + \phi(\eta)$. These invariants give us no result.

I_{15}) The invariants are $y = \eta, \psi = xf(\eta), \theta = \ln x + \theta(\eta), \phi = x\phi(\eta)$. These invariants reduces the flow and mass transfer equations as I_1 but heat transfer equation as I_2.

I_{16}) Here the set of invariants are $y = \eta, \psi = xf(\eta), \theta = x\theta(\eta), \phi = x\phi(\eta)$. By using these invariants the flow and mass transfer equations reduces as I_1 but heat transfer equation appeared as I_3.

I_{17}) Here the set of invariants are $\eta = \frac{e^y}{x}, \psi = xf(\eta), \theta = \theta(\eta), \phi = x\phi(\eta)$. The flow and heat transfer equations are appeared the same as in I_5. But the mass transfer equation can be solved numerically which becomes

$$\eta^2\phi'' + (3\eta + Sc\eta f)\phi' + (1 + Scf - Sc\eta f')\phi = 0. \tag{4.28}$$

I_{18}) Here the set of invariants are $y = \eta, \psi = xf(\eta), \theta = \ln x + \theta(\eta), \phi = \ln x + \phi(\eta)$. The flow, heat transfer and mass transfer equations are appeared the same as in I_1, I_2 and I_4 respectively.

I_{19}) Here the invariants are $\eta = \frac{e^y}{x}, \psi = xf(\eta), \theta = \ln x + \theta(\eta), \phi = \phi(\eta)$. The flow and mass transfer equations are appeared same as in I_5. The heat transfer equation can be solved numerically which becomes

$$\left(1 + \frac{4}{3Nr}\right)[\eta\theta'' + \theta'] + \Pr f\theta' - \Pr f' = 0. \tag{4.29}$$

I_{20}) The set of invariants are $y = \eta, \psi = xf(\eta), \theta = x\theta(\eta), \phi = \ln x + \phi(\eta)$. Here the flow, heat transfer and mass transfer equations reduced similar as I_5, I_3 and I_5 respectively.

I_{21}) Here the invariants are $\eta = \frac{e^y}{x}, \psi = xf(\eta), \theta = x\theta(\eta), \phi = \phi(\eta)$. The flow and mass transfer equations are appeared same as in I_5. But the heat transfer equation can be solved numerically which becomes

$$\left(1 + \frac{4}{3Nr}\right)[\eta^2\theta'' + 3\eta\theta' + \theta] + \Pr \eta f\theta' + \Pr(f - \eta f')\theta = 0. \tag{4.30}$$

I_{22}) Here the invariants are $\eta = \frac{e^y}{x}, \psi = xf(\eta), \theta = \theta(\eta), \phi = \ln x + \phi(\eta)$. The flow and heat transfer equations are appeared same as in I_5. But the mass transfer equation can be solved numerically which becomes

$$\eta\phi'' + (1 + Scf)\phi' - Scf' = 0. \tag{4.31}$$

I_{23}) The invariants are $x = \eta, \psi = f(\eta), \theta = y + \theta(\eta), \phi = e^y\phi(\eta)$. These invariants give us no result.

I_{24}) The invariants are $x = \eta, \psi = f(\eta), \theta = e^y\theta(\eta), \phi = e^y\phi(\eta)$. These invariants give us no

result.

I_{25}) The invariants are $x = \eta, \psi = f(\eta), \theta = y + \theta(\eta), \phi = y + \phi(\eta)$. These invariants give us no result.

I_{26}) The invariant are $y = \eta, \psi = xf(\eta), \theta = \theta(\eta), \phi = \phi(\eta)$. For this particular invariant we are considering the following permeable plate case.

Permeable plate case

We are interested in solving the system of differential equations in the light of physical fluid parameters. We consider the porous plate case with heat conduction on the boundary. The plate lies in the plane $\overline{y} = 0$ with the flow being confined to $\overline{y} > 0$. The coordinate $\overline{x}$ is being taken along the surface of the plate, $\overline{y}$ is normal to the surface and keeping the origin fixed. Then our boundary conditions as follows

$$\begin{aligned} \bar{u} &= 0, \bar{v} = -v_w, -k\frac{\partial T}{\partial \bar{y}} = h_f[T_f - T], C = C_w \text{ at } \bar{y} = 0, \\ \bar{u} &\to \bar{u}_e(\bar{x}), T \to T_\infty, C \to C_\infty \text{ as } \bar{y} \to \infty. \end{aligned} \tag{4.32}$$

Here v_w is mass transfer velocity, $\bar{u}_e$ is free stream velocity, h_f is heat transfer coefficient, T_f is wall temperature.

Further using the non-dimensional parameters (4.6) our boundary conditions become

$$\begin{aligned} u(x,y) &= 0, v(x,y) = -S, \frac{\partial \theta(x,y)}{\partial y} = -Bi[1 - \theta(x,y)], \\ \phi(x,y) &= 1 \text{ at } y = 0, \end{aligned} \tag{4.33}$$

$$u(x,y) = u_e, \theta(x,y) = 0 \text{ and } \phi(x,y) = 0 \text{ as } y \to \infty, \tag{4.34}$$

where $S = \frac{v_w\sqrt{R}}{u_\infty}$, a positive value of S represents suction and negative value of S represents injection and $Bi = \frac{h_f L}{k\sqrt{R}}$ is Biot number.

Finally, after employing stream function boundary conditions take the following form

$$\frac{\partial \psi(x,0)}{\partial y} = 0, \frac{\partial \psi(x,0)}{\partial x} = S, \frac{\partial \theta(x,0)}{\partial y} = -Bi[1 - \theta(x,0)], \phi(x,0) = 1, \tag{4.35}$$

$$\frac{\partial \psi(x,\infty)}{\partial y} = u_e, \theta(x,\infty) = 0 \text{ and } \phi(x,\infty) = 0. \tag{4.36}$$

For particular invariant V_2 now our system takes the following form

$$(1+\frac{1}{\beta})f'''(\eta) + f(\eta)f''(\eta) - f'(\eta)^2 - M(f'(\eta)-1) + 1 = 0, \tag{4.37}$$

$$\left(1+\frac{4}{3Nr}\right)\theta''(\eta) + \Pr f(\eta)\theta'(\eta) = 0, \tag{4.38}$$

$$\phi''(\eta) + Scf(\eta)\phi'(\eta) = 0, \tag{4.39}$$

$$f(0) = S, f'(0) = 0, f'(\infty) = 1, \tag{4.40}$$

$$\theta'(0) = -Bi[1-\theta(0)], \theta(\infty) = 0, \phi(0) = 1, \phi(\infty) = 0. \tag{4.41}$$

The skin friction coefficient, the Nusselt number and the Sherwood number are defined as

$$\begin{aligned} C_f &= \frac{(\mu_B + \frac{p_y}{\sqrt{2\pi_c}})}{\bar{u}_e^2}\left(\frac{\partial \bar{u}}{\partial \bar{y}}\right)_{\bar{y}=0}, \\ Nu &= \frac{\bar{x}}{(T_f - T_\infty)}\left(\frac{\partial T}{\partial \bar{y}}\right)_{\bar{y}=0}, \\ Sh &= \frac{\bar{x}}{(C_w - C_\infty)}\left(\frac{\partial C}{\partial \bar{y}}\right)_{\bar{y}=0}. \end{aligned} \tag{4.42}$$

By substituting Eq. (4.6) and (4.11) into Eq. (4.42) the form of skin friction coefficient, the Nusselt number and the Sherwood number as follows

$$\begin{aligned} \sqrt{R}C_f &= (1+\frac{1}{\beta})f''(0), \\ R^{\frac{-1}{2}}Nu &= -\theta'(0), \\ R^{\frac{-1}{2}}Sh &= -\phi'(0). \end{aligned} \tag{4.43}$$

4.1.3 Flow characteristics

The system of non-linear ordinary differential equations (4.37)-(4.39) with boundary conditions (4.40)-(4.41) has been solved numerically using MATLAB boundary value problem solver for ode's. In order to validate our study, we have made a comparison of values of $-f''(0)$ with

those reported earlier [63, 104, 105] and presented in Table 4.3. By keeping $S = M = 0$, $\beta = \infty$ we have found that the values obtained in this study are in good agreement with those reported earlier [63, 104, 105].

[63]	[104]	[105]	Present
1.232588	1.2326	1.232588	1.232592

Table 4.3: Comparison of skin friction coefficient $f''(0)$ when $M = S = 0$, and $\beta = \infty$

The effects of various parameters for example, the magnetic field parameter M, Casson fluid parameter β, suction parameter S, Prandtl number Pr, thermal radiation parameter Nr, Biot number Bi and Schmidt number Sc on velocity $f'(\eta)$, temperature $\theta(\eta)$ and concentration $\phi(\eta)$ profiles are shown in Figures 4.1-4.13. In Figure 4.1 velocity profile $f'(\eta)$ is plotted for different values of M. It is observed that with an increase in the value of M the velocity profile decreases. This is because the magnetic force acts as a resistance to the flow. Figure 4.2 presents the influence of Casson fluid parameter β on velocity profile. It reveals that a decrease in velocity occurs with increase in Casson fluid parameter. Figure 4.3 illustrates the effects of suction parameter on velocity profile. An increase in suction parameter S causes the velocity profile to decrease.

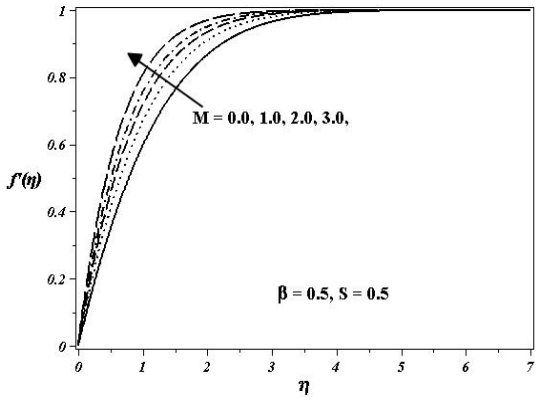

Figure 4.1: Effects of M on $f'(\eta)$

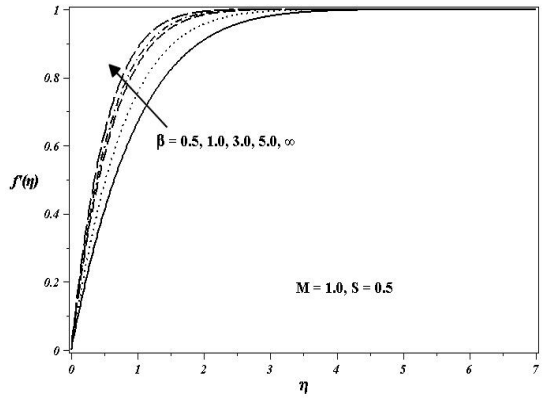

Figure 4.2: Effects of β on $f'(\eta)$

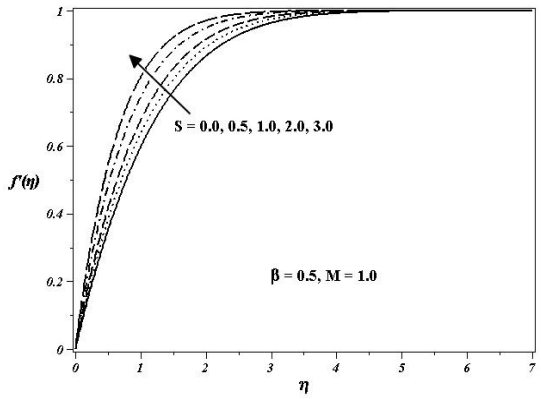

Figure 4.3: Effects of S on $f'(\eta)$

The influence of different physical parameters on temperature are presented in Figures 4.4-4.9. In Figure 4.4 the effects of magnetic field parameter M on temperature profile $\theta(\eta)$ are shown. It is observed that the influence of magnetic field parameter on $\theta(\eta)$ are increasing. Figure 4.5 depicts that the boundary layer thickness increases with the increase of Casson fluid parameter β. With an increase in suction parameter S, the boundary layer thickness increases as revealed in Figure 4.6. From Figure 4.7, it is observed that the thickness of thermal boundary layer decreases with increase the Prandtl number Pr . Figure 4.8 demonstrates that the thermal radiation parameter Nr enhances fluid temperature. On the other hand, Figure 4.9 depicts that when increase in the Biot number Bi the temperature profile increases.

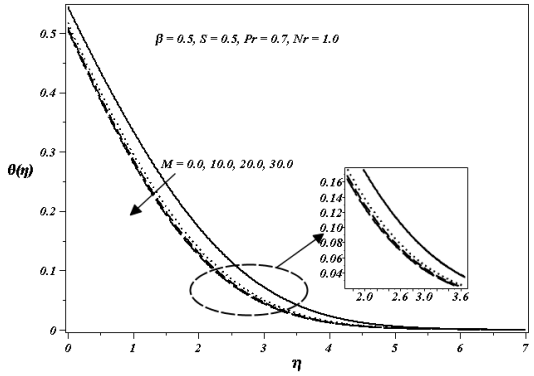

Figure 4.4: Effects of M on $\theta(\eta)$

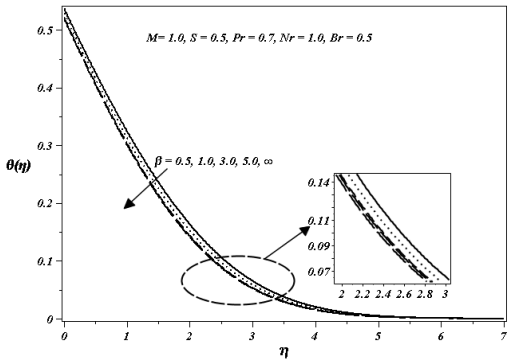

Figure 4.5: Effects of β on $\theta(\eta)$

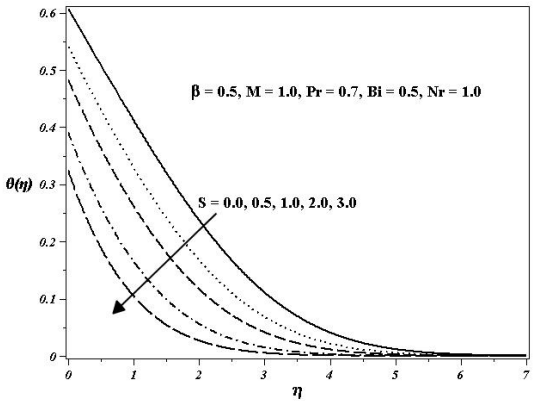

Figure 4.6: Effects of S on $\theta(\eta)$

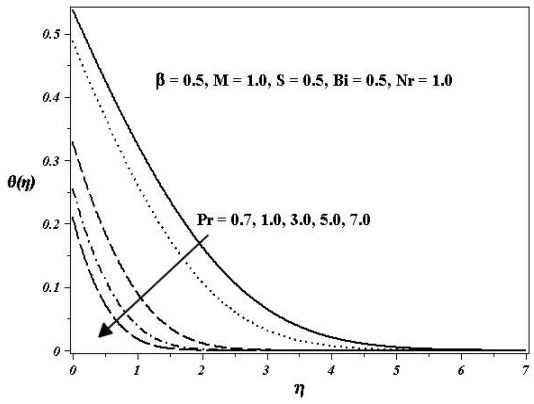

Figure 4.7: Effects of Pr on $\theta(\eta)$

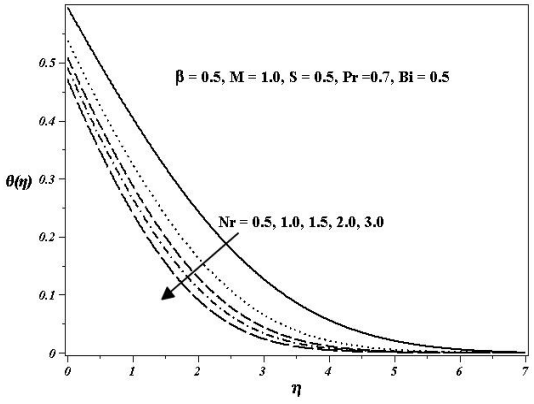

Figure 4.8: Effects of Nr on $\theta(\eta)$

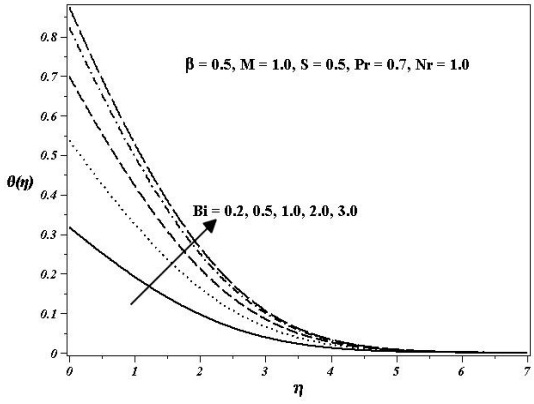

Figure 4.9: Effects of Bi on $\theta(\eta)$

In Figure 4.10 the effects of magnetic field parameter M on concentration field $\phi(\eta)$ are presented. It is revealed that the concentration boundary layer increases with magnetic field parameter M. From Figure 4.11, it is observed that concentration profile increases with increase in Casson fluid parameter β. In Figure 4.12, the effects of suction parameter S on $\phi(\eta)$ are shown. It is quite clear that with an increase in S the concentration field decreases. On the other hand when the concentration field increases as the value of Schmidt number Sc decreases which is presented in Figure 4.13.

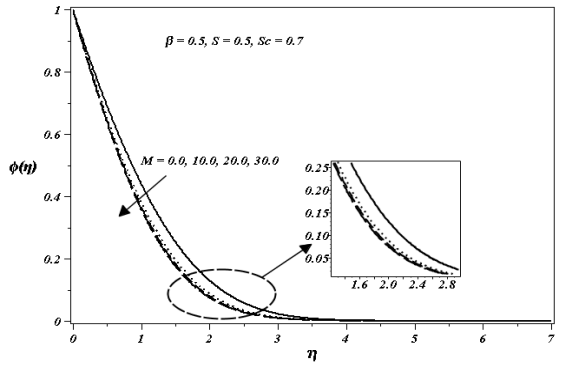

Figure 4.10: Effects of M on $\phi(\eta)$

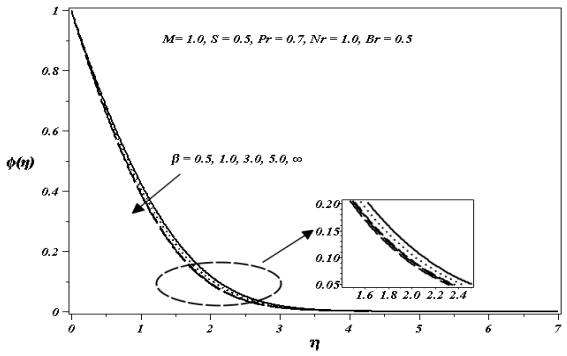

Figure 4.11: Effects of β on $\phi(\eta)$

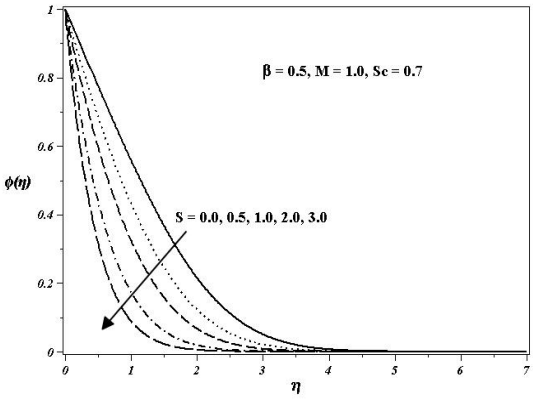

Figure 4.12: Effects of S on $\phi(\eta)$

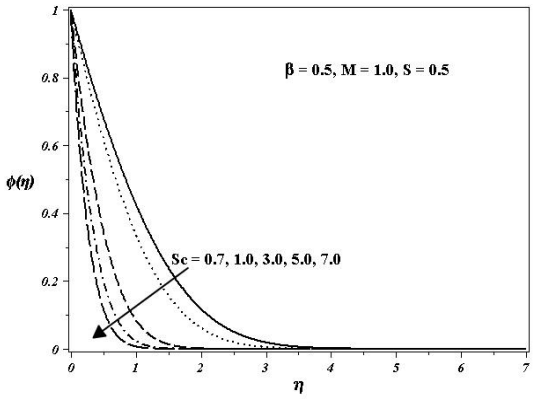

Figure 4.13: Effects of Sc on $\phi(\eta)$

4.1.4 Findings

Group theoretical method is used to find the group invariant solutions of stagnation point Casson fluid, heat and mass transfer phenomenon. By using the group theoretic method we evaluate the six finite and one infinite symmetries of the non-dimensional partial differential equations. Further, these symmetries are used to list the Lie algebra, commutator table, adjoint table, abelian Lie algebra and the optimal system for the governing system. Furthermore, the optimal system helps us to find the twenty six group invariant solutions. For a particular invariant we solve the ordinary differential equations by setting the permeable flat plate case.

The governing equations are further solved by numerical technique and the results are also expressed in the form of graphs. The following results are observed:

The magnetic field M, Casson fluid β and suction parameters S has increasing behavior for velocity profile and decreasing for temperature and concentration profiles. Prandtl number Pr and Radiation parameter Nr for temperature profile are observed similar. The temperature profile increases when Biot number Bi increases. The concentration profile increases when Schmidt number decreases.

4.2 Similarity analysis of Hall effects on free convection Casson fluid flow

4.2.1 Mathematical modeling

Here we consider the steady, incompressible, three dimensional free convection, electrically conducting Casson fluid flow. In the presence of a strong, non-uniform magnetic field normal to the boundary, the temperature at the boundary is T_w and the temperature of the free stream is T_∞. For weakly ionized gases, ion slip, viscous and electrical dissipation and the thermoelectric pressure are considered negligible. By considering the rectangular Cartesian coordinates (x, y, z), taking x and y coordinates parallel and normal to the boundary respectively. The leading edge of the boundary is taken along $z-$axis. The effects of Hall current give rise to a force in the z-direction which induces a cross flow in that direction, hence the flow becomes three-dimensional. For the simplicity of the problem, we assume that there is no variation of flow and heat transfer quantities in the z-direction. The equation of conservation of electric charge $\operatorname{div} \vec{j} = 0$ gives j_y =constant, which is zero since $j_y = 0$ at the boundary which is electrically non-conducting. Thus $j_y = 0$ everywhere in the flow. By following the above assumptions, we obtain from Eqs. (1.27)–(1.30) the following boundary layer equations

$$\frac{\partial u}{\partial x} + \frac{\partial v}{\partial y} = 0, \tag{4.44}$$

$$u\frac{\partial u}{\partial x} + v\frac{\partial u}{\partial y} = \nu(1 + \frac{1}{\beta})\frac{\partial^2 u}{\partial y^2} + g\beta_1(T - T_\infty) - \frac{B_y}{\rho}j_z, \tag{4.45}$$

$$u\frac{\partial w}{\partial x}+v\frac{\partial w}{\partial y}=\nu(1+\frac{1}{\beta})\frac{\partial^2 w}{\partial y^2}+\frac{B_y}{\rho}j_x, \tag{4.46}$$

$$u\frac{\partial T}{\partial x}+v\frac{\partial T}{\partial y}=\frac{k}{\rho C_p}\frac{\partial^2 T}{\partial y^2}-\frac{1}{\rho c_p}\frac{\partial q_r}{\partial y}, \tag{4.47}$$

where

$$\begin{aligned} B_y &= \frac{B_0}{x}, j_x=\frac{\sigma}{1+m^2}[E_x-wB_y+m(E_z+uB_y), \\ j_z &= \frac{\sigma}{1+m^2}[E_z+uB_y-m(E_x-wB_y)], q_r=-\frac{4\sigma_1}{3k_1}\frac{\partial T^4}{\partial y}. \end{aligned} \tag{4.48}$$

For further derivation of Eqs. (4.45)-(4.46) we assumed that the induced magnetic field can be neglected in comparison with an applied magnetic field, so that $\vec{B}=(0,B_y,0)$ where $B_y=\frac{B_0}{x}$. The magnetic field is uniform in the free stream and Eq. (1.32) shows that there is no electric current there. Thus

$$j_x=0 \text{ and } j_z=0 \text{ when } y\to\infty. \tag{4.49}$$

From Eq. (1.33) gives

$$E_x=\text{Constant, and } E_z=\text{Constant}. \tag{4.50}$$

For the semi-infinite plate, and for Eq. (4.49) we obtain

$$E_x=E_y=0, \tag{4.51}$$

everywhere in the fluid.

The dimensionless quantities are introduced here

$$\bar{x}=\frac{xu_\infty}{\nu}, \bar{y}=\frac{yu_\infty}{\nu}, \bar{u}=\frac{u}{u_\infty}, \bar{v}=\frac{v}{u_\infty}, \bar{w}=\frac{w}{u_\infty}, \theta=\frac{T-T_\infty}{T_w-T_\infty}. \tag{4.52}$$

After using above dimensionless variables Eqs. (4.44)-(4.47) becomes

$$\frac{\partial \bar{u}}{\partial \bar{x}}+\frac{\partial \bar{v}}{\partial \bar{y}}=0, \tag{4.53}$$

$$\bar{u}\frac{\partial \bar{u}}{\partial \bar{x}}+\bar{v}\frac{\partial \bar{u}}{\partial \bar{y}}=(1+\frac{1}{\beta})\frac{\partial^2 \bar{u}}{\partial \bar{y}^2}+Gr\theta-\frac{M}{x^2(1+m^2)}(\bar{u}+m\bar{w}), \tag{4.54}$$

$$\bar{u}\frac{\partial \bar{w}}{\partial \bar{x}}+\bar{v}\frac{\partial \bar{w}}{\partial \bar{y}}=(1+\frac{1}{\beta})\frac{\partial^2 \bar{w}}{\partial \bar{y}^2}+\frac{M}{x^2(1+m^2)}(m\bar{u}-\bar{w}), \tag{4.55}$$

$$\bar{u}\frac{\partial \theta}{\partial \bar{x}}+\bar{v}\frac{\partial \theta}{\partial \bar{y}}=\frac{1}{\mathrm{Pr}}(1+\frac{4}{3Nr})\frac{\partial^2 \theta}{\partial \bar{y}^2}, \tag{4.56}$$

where $Gr=\frac{g\beta_1\nu(T_w-T_\infty)}{u_\infty^3}$ is Grashof number, m is Hall parameter.

Scaling group of transformations

We scale all independent and dependent variables(up dash is old variable and down are new variables) as

$$\begin{aligned}\underline{\mathrm{x}} &= \lambda^{c_1}\bar{x}, \underline{\mathrm{y}}=\lambda^{c_2}\bar{y}, \underline{\mathrm{u}}=\lambda^{c_3}\bar{u},\\ \underline{\mathrm{v}} &= \lambda^{c_4}\bar{v}, \underline{\mathrm{w}}=\lambda^{c_5}\bar{w}, \underline{\theta}=\lambda^{c_6}\theta.\end{aligned} \tag{4.57}$$

By employing (4.57) onto Eqs. (4.53)-(4.56) our system becomes

$$\lambda^{c_1-c_3}\frac{\partial \underline{\mathrm{u}}}{\partial \bar{x}}+\lambda^{c_2-c_4}\frac{\partial \underline{\mathrm{v}}}{\partial \underline{\mathrm{y}}}=0, \tag{4.58}$$

$$\begin{aligned}\lambda^{c_1-2c_3}\underline{\mathrm{u}}\frac{\partial \underline{\mathrm{u}}}{\partial \bar{x}}+\lambda^{c_2-c_3-c_4}\underline{\mathrm{v}}\frac{\partial \underline{\mathrm{u}}}{\partial \underline{\mathrm{y}}}-(1+\frac{1}{\beta})\lambda^{2c_2-c_3}\frac{\partial^2 \underline{\mathrm{u}}}{\partial \underline{\mathrm{y}}^2}-\lambda^{-c_6}Gr\underline{\theta}\\ +\frac{M}{\underline{\mathrm{x}}^2(1+m^2)}(\lambda^{2c_1-c_3}\underline{\mathrm{u}}+\lambda^{2c_1-c_5}m\underline{\mathrm{w}})=0,\end{aligned} \tag{4.59}$$

$$\lambda^{c_1-c_3-c_5}\underline{\mathrm{u}}\frac{\partial \underline{\mathrm{w}}}{\partial \bar{x}}+\lambda^{c_2-c_5-c_4}\underline{\mathrm{v}}\frac{\partial \underline{\mathrm{w}}}{\partial \underline{\mathrm{y}}}-(1+\frac{1}{\beta})\lambda^{2c_2-c_5}\frac{\partial^2 \underline{\mathrm{w}}}{\partial \underline{\mathrm{y}}^2}-\frac{M}{\underline{\mathrm{x}}^2(1+m^2)}(\lambda^{2c_1-c_3}m\underline{\mathrm{u}}-\lambda^{2c_1-c_5}\underline{\mathrm{w}})=0, \tag{4.60}$$

$$\lambda^{c_1-c_3-c_6}\underline{\mathrm{u}}\frac{\partial \underline{\theta}}{\partial \bar{x}}+\lambda^{c_2-c_6-c_4}\underline{\mathrm{v}}\frac{\partial \underline{\theta}}{\partial \underline{\mathrm{y}}}-\frac{1}{\mathrm{Pr}}(1+\frac{4}{3Nr})\lambda^{2c_2-c_6}\frac{\partial^2 \underline{\theta}}{\partial \underline{\mathrm{y}}^2}=0. \tag{4.61}$$

Now comparing the Eqs.(4.58)-(4.61) with Eqs. (4.53)-(4.56) we found the following set of equations

$$\begin{aligned} c_2 - c_1 + c_3 - c_4 &= 0, && (4.62)\\ 2c_2 - c_1 + c_3 &= 0, && (4.63)\\ 2c_3 - c_1 - c_6 &= 0, && (4.64)\\ c_1 + c_3 &= 0, && (4.65)\\ 3c_1 + 2c_3 - c_5 &= 0, && (4.66)\\ c_1 + c_5 &= 0. && (4.67) \end{aligned}$$

After some simple calculations, we have the following invariance conditions in terms of c_1

$$c_2 = c_1, c_3 = -c_1, c_4 = -c_1, c_5 = -c_1, c_6 = -3c_1. \tag{4.68}$$

Here we write the characteristic equation after using above Eq. (4.68) then corresponding similarity variables are

$$\frac{dx}{x} = \frac{dy}{y} = \frac{du}{-u} = \frac{dv}{-v} = \frac{dw}{-w} = \frac{d\theta}{-3\theta}, \tag{4.69}$$

$$\eta = \frac{y}{x}, u = \frac{f(\eta)}{x}, v = \frac{g(\eta)}{x}, w = \frac{h(\eta)}{x}, u = \frac{\theta(\eta)}{x^3}. \tag{4.70}$$

Here we are using scaling symmetries so our all finite parameters are in form of single parameter. In this situation we can not produce commutator table, Abelian Lie algebra and adjoint table.

After using above new invariants our system becomes into the following form

$$g' - \eta f' - f = 0, \tag{4.71}$$

$$-f(\eta f)' + gf' = (1 + \frac{1}{\beta})f'' + Gr\theta - \frac{M}{1+m^2}(f + mh), \tag{4.72}$$

$$-f(\eta h)' + gh' = (1 + \frac{1}{\beta})h'' + \frac{M}{1+m^2}(mf - h), \tag{4.73}$$

$$-f(\eta\theta' + 3\theta) + g\theta' = \frac{1}{\mathrm{Pr}}(1 + \frac{4}{3Nr})\theta''. \tag{4.74}$$

Equation (4.71) becomes as $g = \eta f$ after integration. Now our system will be converted into the following ordinary differential equations

$$(1+\frac{1}{\beta})f'' + f^2 + Gr\theta - \frac{M}{1+m^2}(f+mh) = 0, \tag{4.75}$$

$$(1+\frac{1}{\beta})h'' + fh + \frac{M}{1+m^2}(mf-h) = 0, \tag{4.76}$$

$$(1+\frac{4}{3Nr})\theta'' + 3\,\mathrm{Pr}\, f\theta = 0. \tag{4.77}$$

Flat plate case

To solve the system (4.75)-(4.77) in the light of fluid parameters, we consider that the fluid passing over a flat plate, so we set up the boundary conditions as

$$\begin{aligned} u(x,0) &= 0, v(x,0), w(x,0) = 0, \\ u(x,\infty) &= 0, w(x,\infty) = 0, \\ T(x,0) &= T_w, T(x,\infty) = 0. \end{aligned} \tag{4.78}$$

After using the dimensionless quantities to Eq. (4.78) the boundary condition becomes

$$\begin{aligned} \bar{u}(\bar{x},0) &= 0, \bar{v}(\bar{x},0) = 0, \bar{w}(\bar{x},0) = 0, \\ \bar{u}(\bar{x},\infty) &= 0, \bar{w}(\bar{x},\infty) = 0, \\ \theta(\bar{x},0) &= 1, \theta(\bar{x},\infty) = 0. \end{aligned} \tag{4.79}$$

These conditions become as follows when we use the similarity variables

$$\begin{aligned} f(0) &= 0, h(0) = 0, \theta(0) = 1, \\ f(\infty) &= 0, h(\infty) = 0, \theta(\infty) = 0. \end{aligned} \tag{4.80}$$

4.2.2 Flow characteristics

By using the numerical approach i.e, fourth order Runge–Kutta-Fehlberg scheme with the shooting method the ordinary differential Eqs. (4.75)-(4.77) with boundary conditions (4.80) are solved. A step size of $\eta = 0.01$ was selected with $\eta_\infty = 15$ to be satisfactory for a convergence criterion of 10^{-6} in all cases. The numerical computations have been carried out by fixing various values of the parameters involved $\beta = 0.5, M = 1.0, m = 0.5, Gr = 0.5, \mathrm{Pr} = 0.71, Nr = 0.5$ and the results are represented through graphs. The effects of Casson fluid parameter β on axial velocity profile $f(\eta)$ and transverse velocity profile $h(\eta)$ are presented in Figure 4.14. It is noticed that with the enhancement of β the axial velocity profile $f(\eta)$ and the transverse velocity profile $h(\eta)$ decreases. Figure 4.15 depicts the influence of magnetic field parameter M on velocities profile. It is observed that with the increase in the magnetic field parameter both velocities are decreasing. This is mainly due to the fact that the application of the magnetic field to an electrically conducting fluid gives rise to Lorentz force which causes the fluid to decelerate. The behavior of Hall parameter m with velocity profiles is presented in Figure 4.16. With the increase of Hall parameter m, both the axial velocity profile $f(\eta)$ and the transverse velocity profile $h(\eta)$ decrease. Figure 4.17 represents the effect of Grashof Number Gr on velocity profiles. The axial velocity $f(\eta)$ decrease where as transverse velocity $h(\eta)$ increase as the value of Gr is enhanced. It is observed that the influence of radiation parameter Nr on temperature profile $\theta(\eta)$ is increasing which is shown in Figure 4.18.

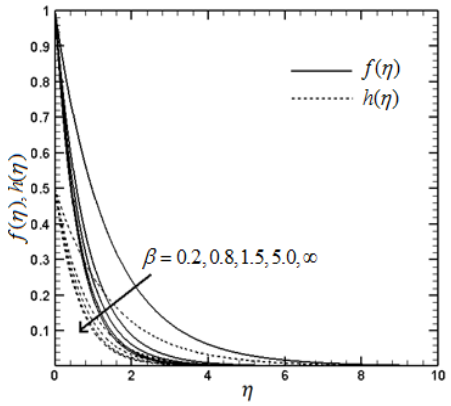

Figure 4.14: Effect of β on $f(\eta)$ and $h(\eta)$

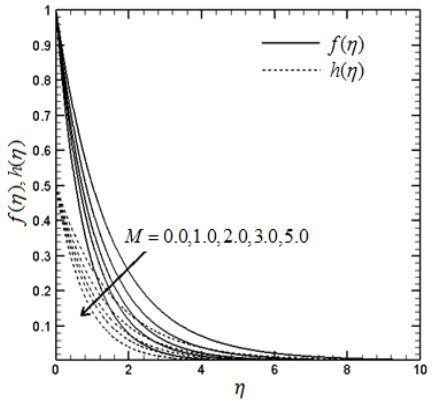

Figure 4.15: Effect of M on $f(\eta)$ and $h(\eta)$

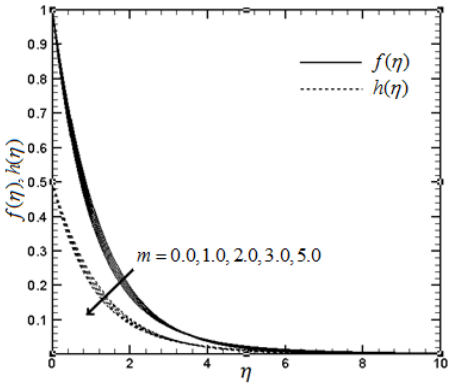

Figure 4.16: Effect of m on $f(\eta)$ and $h(\eta)$

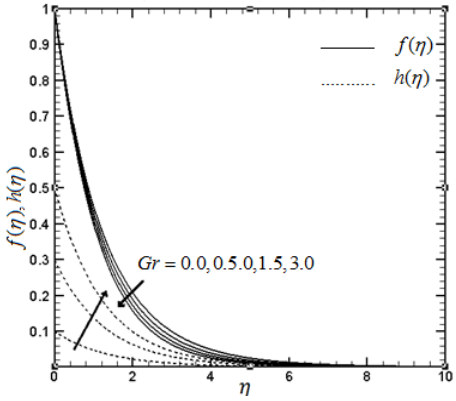

Figure 4.17: Effect of Gr on $f(\eta)$ and $h(\eta)$

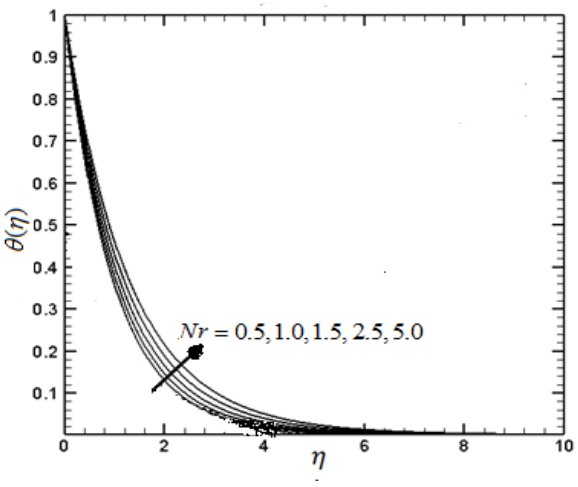

Figure 4.18: Effect of Nr on $\theta(\eta)$

4.2.3 Findings

After solving the system of ordinary differential equations by using the numerical approach we have observed the following flow characteristics results:

With enhancement of Casson fluid parameter the axial and transverse velocities decrease. It is observed that the influence of magnetic field parameter on axial velocity profile and transverse velocity profile is decreasing. Further the axial velocity profile and transverse velocity profile are decreasing as the Hall effect parameter increases. The effects of Grashof number on both velocity profiles are observed opposite. The radiation parameter increases with the temperature profile.

Chapter 5

Lie group study of MHD Casson fluid flow in channel with stretching walls in the presence of source/sink effects

The focus of this chapter is on the symmetry analysis of MHD Casson fluid flow with heat and mass transfer analysis in channel with stretching walls. After finding the similarity variables of the governing system of differential equations, we have listed the group invariants. Furthermore, we presented the group invariant solutions for the system of governing differential equations. For a particular invariant we describe the flow characteristics in detail with graphs and tabular forms.

5.1 Mathematical modeling

We investigate the steady two-dimensional incompressible laminar Casson fluid flow in a parallel plate channel bounded by the planes $\bar{y} = \pm a$ where $2a$ is the channel width. We also consider the flow to be symmetric about the center line $\bar{y} = 0$ of the channel. The flow is driven by stretching of the channel walls in the presence of uniform magnetic field of strength B_0 imposed

along the normal to the channel walls parallel to $\bar{y}$-axis. Here, we take the fluid to be electrically conducting. Further we also consider the heat and mass transfer processes in the presence of source/sink effects. Using Eq. (1.41) conservation of mass, momentum, heat and mass transfer, the following boundary layer equations are obtained

$$\frac{\partial \bar{u}}{\partial \bar{x}} + \frac{\partial \bar{v}}{\partial \bar{y}} = 0, \tag{5.1}$$

$$\bar{u}\frac{\partial \bar{u}}{\partial \bar{x}} + \bar{v}\frac{\partial \bar{u}}{\partial \bar{y}} = -\frac{1}{\rho}\frac{\partial \bar{p}}{\partial \bar{x}} + (1+\frac{1}{\beta})\nu\frac{\partial^2 \bar{u}}{\partial \bar{y}^2} - \frac{\sigma B_0^2}{\rho}\bar{u}, \tag{5.2}$$

$$\bar{u}\frac{\partial \bar{v}}{\partial \bar{x}} + \bar{v}\frac{\partial \bar{v}}{\partial \bar{y}} = -\frac{1}{\rho}\frac{\partial \bar{p}}{\partial \bar{y}} + (1+\frac{1}{\beta})\nu\frac{\partial^2 \bar{v}}{\partial \bar{y}^2}, \tag{5.3}$$

$$\bar{u}\frac{\partial T}{\partial \bar{x}} + \bar{v}\frac{\partial T}{\partial \bar{y}} = \frac{k}{\rho C_p}\frac{\partial^2 T}{\partial \bar{y}^2} + \frac{Q_0}{\rho c_p}(T - T_0), \tag{5.4}$$

$$\bar{u}\frac{\partial C}{\partial \bar{x}} + \bar{v}\frac{\partial C}{\partial \bar{y}} = D\frac{\partial^2 C}{\partial \bar{y}^2}, \tag{5.5}$$

subject to the boundary conditions

$$\begin{aligned} \bar{u}(\bar{x}, \pm a) &= u_w = b\bar{x}, \bar{v}(\bar{x}, a) = 0, \bar{v}(\bar{x}, -a) = 0, \\ T(\bar{x}, a) &= T_w, T(\bar{x}, -a) = 0 \text{ and } C(\bar{x}, a) = C_w, C(\bar{x}, -a) = 0. \end{aligned} \tag{5.6}$$

Using the following transformations to make the system dimensionless

$$x = \frac{\bar{x}}{a}, y = \frac{\bar{y}}{a}, u = \frac{\bar{u}}{ab}, v = \frac{\bar{v}}{ab}, \bar{p} = \mu b p,\ \theta = \frac{T - T_0}{T_w - T_0} \text{ and } \phi = \frac{C - C_0}{C_w - C_0}. \tag{5.7}$$

In view of the similarity variables defined in Eq. (5.7), the equations (5.1)-(5.5) with boundary conditions (5.6) have the following forms

$$\frac{\partial u}{\partial x} + \frac{\partial v}{\partial y} = 0, \tag{5.8}$$

$$u\frac{\partial u}{\partial x} + v\frac{\partial u}{\partial y} = -\frac{1}{R}\frac{\partial p}{\partial x} + \frac{1}{R}(1+\frac{1}{\beta})\frac{\partial^2 u}{\partial y^2} - \frac{M}{R}u, \tag{5.9}$$

$$u\frac{\partial v}{\partial x} + v\frac{\partial v}{\partial y} = -\frac{1}{R}\frac{\partial p}{\partial y} + \frac{1}{R}(1+\frac{1}{\beta})\frac{\partial^2 v}{\partial y^2}, \tag{5.10}$$

$$u\frac{\partial\theta}{\partial x}+v\frac{\partial\theta}{\partial y}=\frac{1}{R\,\mathrm{Pr}}\frac{\partial^2\theta}{\partial y^2}+\frac{Q}{R}\theta, \tag{5.11}$$

$$u\frac{\partial\phi}{\partial x}+v\frac{\partial\phi}{\partial y}=\frac{1}{RSc}\frac{\partial^2\phi}{\partial y^2}, \tag{5.12}$$

$$\begin{aligned} u(x,\pm1) &= x, v(x,1)=0, v(x,-1)=0, \\ \theta(x,1) &= 1, \theta(x,-1)=0 \text{ and } \phi(x,1)=1, \phi(x,-1)=0, \end{aligned} \tag{5.13}$$

where $R=\frac{a^2b}{\upsilon}$ is stretching Reynolds number, $Q=\frac{a^2Q_0}{\mu C_p}$ is source/sink parameter and $Sc=\frac{a^2b}{D}$ is Schmidt number.

After differentiating Eq. (5.9) w.r.t. y and Eq. (5.10) w.r.t. x and elimination of pressure from the resulting equations using $p_{xy}=p_{yx}$ yield

$$\begin{aligned} &\frac{\partial u}{\partial y}\frac{\partial u}{\partial x}+\frac{\partial v}{\partial y}\frac{\partial u}{\partial y}+u\frac{\partial^2 u}{\partial y\partial x}+v\frac{\partial^2 u}{\partial y^2}-\frac{1}{R}\left(1+\frac{1}{\beta}\right)\frac{\partial^3 u}{\partial y^3}+\frac{M}{R}\frac{\partial u}{\partial y} \\ = \;& \frac{\partial u}{\partial x}\frac{\partial v}{\partial x}+u\frac{\partial^2 v}{\partial x^2}+\frac{\partial v}{\partial x}\frac{\partial v}{\partial y}+v\frac{\partial^2 v}{\partial x\partial y}-\frac{1}{R}\left(1+\frac{1}{\beta}\right)\frac{\partial^3 v}{\partial y^3}. \end{aligned} \tag{5.14}$$

Introducing the stream function relations as

$$u=\frac{\partial\psi}{\partial y}, v=-\frac{\partial\psi}{\partial x}. \tag{5.15}$$

By using Eq. (5.15) our system becomes

$$\frac{\partial \psi}{\partial y}\frac{\partial}{\partial x}\left[\frac{\partial^2 \psi}{\partial x^2}+\frac{\partial^2 \psi}{\partial y^2}\right]-\frac{\partial \psi}{\partial x}\frac{\partial}{\partial y}\left[\frac{\partial^2 \psi}{\partial x^2}+\frac{\partial^2 \psi}{\partial y^2}\right]$$

$$-\frac{1}{R}(1+\frac{1}{\beta})\frac{\partial^2}{\partial y^2}\left[\frac{\partial^2 \psi}{\partial x^2}+\frac{\partial^2 \psi}{\partial y^2}\right]+\frac{M}{R}\frac{\partial^2 \psi}{\partial y^2}=0, \tag{5.16}$$

$$\frac{\partial \psi}{\partial y}\frac{\partial \theta}{\partial x}-\frac{\partial \psi}{\partial x}\frac{\partial \theta}{\partial y}=\frac{1}{R\,\mathrm{Pr}}\frac{\partial^2 \theta}{\partial y^2}+\frac{Q}{R}\theta, \tag{5.17}$$

$$\frac{\partial \psi}{\partial y}\frac{\partial \phi}{\partial x}-\frac{\partial \psi}{\partial x}\frac{\partial \phi}{\partial y}=\frac{1}{RSc}\frac{\partial^2 \phi}{\partial y^2}, \tag{5.18}$$

$$\begin{aligned}\frac{\partial \psi(x,\pm 1)}{\partial y} &= x, \frac{\partial \psi(x,1)}{\partial x}=0, \frac{\partial \psi(x,-1)}{\partial x}=0,\\ \theta(x,1) &= 1, \theta(x,-1)=0 \text{ and } \phi(x,1)=1, \phi(x,-1)=0.\end{aligned} \tag{5.19}$$

5.2 Lie group analysis

In this section, we determine the symmetries of the problem. The infinitesimal generator for the current problem can be expressed as

$$\vec{V}=\xi_1(x,y,\psi,\theta,\phi)\partial_x+\xi_2(x,y,\psi,\theta,\phi)\partial_y+\Phi_1(x,y,\psi,\theta,\phi)\partial_\psi$$

$$+\Phi_2(x,y,\psi,\theta,\phi)\partial_\theta+\Phi_3(x,y,\psi,\theta,\phi)\partial_\phi. \tag{5.20}$$

To calculate the symmetries of the governing system (5.16)-(5.18), the infinitesimal Lie group point transformations are defined as:

$$\begin{aligned}x^* &= x+\epsilon\xi_1(x,y,\psi,\theta,\phi)+O(\epsilon^2),\\ y^* &= y+\epsilon\xi_2(x,y,\psi,\theta,\phi)+O(\epsilon^2),\\ \Psi^* &= \Psi+\epsilon\Phi_1(x,y,\psi,\theta,\phi)+O(\epsilon^2),\\ \theta^* &= \theta+\epsilon\Phi_2(x,y,\psi,\theta,\phi)+O(\epsilon^2),\\ \phi^* &= \phi+\epsilon\Phi_3(x,y,\psi,\theta,\phi)+O(\epsilon^2).\end{aligned} \tag{5.21}$$

For the equations (5.16)-(5.18) the infinitesimals are calculated with the help of software package [25] as:

$$\begin{aligned}\xi_1(x,y,\psi,\theta,\phi) &= c_5 + c_6 x, \xi_2(x,y,\psi,\theta,\phi) = g(x), \Phi_1(x,y,\psi,\theta,\phi) = c_4 + c_6\psi, \\ \Phi_2(x,y,\psi,\theta,\phi) &= c_1\theta, \Phi_3(x,y,\psi,\theta,\phi) = c_3 + c_2\phi, \end{aligned} \tag{5.22}$$

where $c_i (i = 1, 2, ..., 6)$, are arbitrary constants and $g(x)$ is arbitrary function of x.

There are six finite parameter Lie group symmetries represented by parameters c_i, and one infinite symmetry $g(x)$. Parameter c_1 corresponds to the scaling in the variable θ, c_2 corresponds to the scaling in ϕ, c_3 corresponds to the translation in ϕ, c_4 corresponds to the translation in ψ, c_5 corresponds to translation in x and c_6 corresponds to the scaling in x and ψ.

Now we have a $7-$dimensional vector space of infinitesimal generators closed under the operation of commutation, i.e., $7-$dimensional Lie algebra, the basis of the corresponding Lie algebra is as follows

$$V_1 = \theta\partial_\theta, V_2 = \phi\partial_\phi, V_3 = \partial_\phi, V_4 = \partial_\psi, V_5 = \partial_x, V_6 = x\partial_x + \psi\partial_\psi, V_7 = \partial_y. \tag{5.23}$$

The commutator table follows

[,]	V_1	V_2	V_3	V_4	V_5	V_6	V_7
V_1	0	0	0	0	0	0	V_1
V_2	0	0	0	0	0	0	0
V_3	0	0	0	V_4	0	0	0
V_4	0	0	-V_4	0	0	0	0
V_5	0	0	0	0	0	0	-V_5
V_6	0	0	0	0	0	0	-V_6
V_7	-V_1	0	0	0	V_5	V_6	0

Table 5.1: Commutator table

The commutator Table 5.1 provides us the following Abelian Lie algebra

$$
\begin{aligned}
[V_s, V_t] &= 0, \text{ as } s = t, [V_1, V_2] = 0, [V_1, V_3] = 0, [V_1, V_4] = 0, \\
[V_1, V_5] &= 0, [V_1, V_6] = 0, [V_2, V_3] = 0, [V_2, V_4] = 0, \\
[V_2, V_5] &= 0, [V_2, V_6] = 0, [V_2, V_7] = 0, [V_3, V_5] = 0, \\
[V_3, V_6] &= 0, [V_3, V_7] = 0, [V_4, V_5] = 0, [V_4, V_6] = 0, \\
[V_4, V_7] &= 0, [V_5, V_6] = 0, [V_5, V_6] = 0.
\end{aligned}
$$

The adjoint representation adG of the Lie group by summing the Lie series (1.14) is given as follows.

Ad	V_1	V_2	V_3	V_4
V_1	V_1	V_2	V_3	V_4
V_2	V_1	V_2	V_3	V_4
V_3	V_1	V_2	V_3	$V_4[\cosh\varepsilon - \sinh\varepsilon]$
V_4	V_1	V_2	$V_3 + \varepsilon V_4$	V_4
V_5	V_1	V_2	V_3	V_4
V_6	V_1	V_2	V_3	V_4
V_7	$V_1 e^{\varepsilon}$	V_2	V_3	V_4

Ad	V_5	V_6	V_7
V_1	V_5	V_6	$V_7 - \varepsilon V_1$
V_2	V_5	V_6	V_7
V_3	V_5	V_6	V_7
V_4	V_5	V_6	V_7
V_5	V_5	V_6	$V_7 + \varepsilon V_5$
V_6	V_5	V_6	$V_7 + \varepsilon V_6$
V_7	$V_5[\cosh\varepsilon - \sinh\varepsilon]$	$V_6[\cosh\varepsilon - \sinh\varepsilon]$	V_7

Table 5.2: Adjoint table

Similar to chapter 2, we have the following optimal system for our equations (5.16)-(5.18)

$I_1)\ V_5 + V_1$	$I_2)\ V_5 + V_2$	$I_3)\ V_5 + V_3$
$I_4)\ V_5 + V_4$	$I_5)\ V_7 + V_1$	$I_6)\ V_7 + V_2$
$I_7)\ V_7 + V_3$	$I_8)\ V_7 + V_4$	$I_9)\ V_7 + V_6$
$I_{10})\ V_1 + V_6$	$I_{11})\ V_2 + V_6$	$I_{12})\ V_3 + V_6$
$I_{13})\ V_5 + V_7 + V_1$	$I_{14})\ V_5 + V_7 + V_2$	$I_{15})\ V_5 + V_7 + V_3$
$I_{16})\ V_5 + V_7 + V_4$	$I_{17})\ V_5 + V_1 + V_2$	$I_{18})\ V_5 + V_1 + V_3$
$I_{19})\ V_5 + V_1 + V_4$	$I_{20})\ V_5 + V_2 + V_4$	$I_{21})\ V_5 + V_3 + V_4$
$I_{22})\ V_7 + V_1 + V_2$	$I_{23})\ V_7 + V_1 + V_3$	$I_{24})\ V_7 + V_1 + V_4$
$I_{25})\ V_7 + V_1 + V_6$	$I_{26})\ V_7 + V_2 + V_4$	$I_{27})\ V_7 + V_2 + V_6$
$I_{28})\ V_7 + V_3 + V_4$	$I_{29})\ V_7 + V_3 + V_6$	$I_{30})\ V_i (i = 1, 2, 3...7)$.

Here we follow the procedure mentioned in chapter 2 to reduce the governing partial differential equations into ordinary differential equations. For the system (5.16)-(5.18) we find the following thirty group invariants which lead us to group invariant solutions.

I_1) Invariants are $y = \eta, \psi = f(\eta), \theta = e^x\theta(\eta), \phi = \phi(\eta)$. The system reduced into the following form

$$(1 + \frac{1}{\beta})f'''' - Mf'' = 0, \tag{5.24}$$

$$\theta'' + \Pr[Q - Rf']\theta = 0, \tag{5.25}$$

$$\phi'' = 0, \text{ implies } \phi = a_5 + a_6\eta. \tag{5.26}$$

The solution of the flow equation (5.24) is

$$f(\eta) = a_1 + a_2\eta + a_3e^{\sqrt{\frac{M}{a}}\eta} + a_4e^{-\sqrt{\frac{M}{a}}\eta},$$

where a_i are integration constants and $a = 1 + \frac{1}{\beta}$. Then the heat transfer equation will take the following form which can be solved numerically

$$\theta'' + \Pr[Q - R\sqrt{\frac{M}{a}}(a_2 + a_3e^{\sqrt{\frac{M}{a}}\eta} - a_4e^{-\sqrt{\frac{M}{a}}\eta})]\theta = 0.$$

I_2) Invariants are $y = \eta, \psi = f(\eta), \theta = \theta(\eta), \phi = e^x\phi(\eta)$. The flow equation is reduced similar

as I_1 and the other two equations reduced into the following form

$$\theta'' + \Pr Q\theta = 0, \text{implies } \theta(\eta) = a_1 \cos\sqrt{\Pr Q}\eta + a_2 \sin\sqrt{\Pr Q}\eta, \tag{5.27}$$

$$\phi'' - ScRf'\phi = 0. \tag{5.28}$$

The mass equation will take the following form which can be solved numerically

$$\phi'' - ScR\sqrt{\frac{M}{a}}(a_2 + a_3 e^{\sqrt{\frac{M}{a}}\eta} - a_4 e^{-\sqrt{\frac{M}{a}}\eta})\phi = 0.$$

I_3) Invariants are $y = \eta, \psi = f(\eta), \theta = \theta(\eta), \phi = x + \phi(\eta)$. The flow and heat transfer equations are reduced similar to as I_2 and the other equation is reduced into the following form

$$\phi'' - ScR\sqrt{\frac{M}{a}}(a_2 + a_3 e^{\sqrt{\frac{M}{a}}\eta} - a_4 e^{-\sqrt{\frac{M}{a}}\eta}) = 0, \tag{5.29}$$

$$\phi(\eta) = ScR\sqrt{\frac{a}{M}}(a_2 + a_3 e^{\sqrt{\frac{M}{a}}\eta} - a_4 e^{-\sqrt{\frac{M}{a}}\eta}) + a_5\eta + a_6.$$

I_4) Here the invariants are $y = \eta, \psi = x + f(\eta), \theta = \theta(\eta), \phi = \phi(\eta)$. The flow and heat transfer equations are reduced similar I_2 and the other equation is reduced into the following form

$$(1 + \frac{1}{\beta})f'''' + Rf''' - Mf' = 0, \tag{5.30}$$

$$\theta'' + R\Pr\theta' + \Pr Q\theta = 0, \tag{5.31}$$

$$\phi'' + ScR\phi' = 0. \tag{5.32}$$

The solutions of the above equations will be

$$f(\eta) = a_1 + a_2\eta + a_3 e^{n_1\eta} + a_4 e^{n_2\eta},$$

$$\theta(\eta) = b_1 e^{m_1\eta} + b_2 e^{m_2\eta},$$

$$\phi(\eta) = d_1 e^{-RSc\eta} + d_2,$$

where $n_1 = \frac{-R+\sqrt{R^2+4aM}}{2a}$, $n_2 = \frac{-R-\sqrt{R^2+4aM}}{2a}$, $m_1 = \frac{R\Pr+\sqrt{R^2\Pr^2-4\Pr Q}}{2}$, $m_2 = \frac{R\Pr-\sqrt{R^2\Pr^2-4\Pr Q}}{2}$.

I_5) Invariants are $x = \eta, \psi = f(\eta), \theta = e^y\theta(\eta), \phi = \phi(\eta)$. These invariants give us no results about the system.

I_6) Invariants are $x = \eta, \psi = f(\eta), \theta = \theta(\eta), \phi = e^y\phi(\eta)$. These invariants give us no results about the system.

I_7) Invariants are $x = \eta, \psi = f(\eta), \theta = \theta(\eta), \phi = y+\phi(\eta)$. These invariants give us no results about the system.

I_8) Invariants are $x = \eta, \psi = y + f(\eta), \theta = \theta(\eta), \phi = \phi(\eta)$. These invariants give us results about the system as

$$f''' = 0, \text{ implies } f(\eta) = \frac{a_1}{2}\eta^2 + a_2\eta + a_3,$$

$$\theta' - \frac{Q}{R}\theta = 0, \text{ implies } \theta(\eta) = b_1 e^{\frac{Q}{R}\eta},$$

$$\phi' = 0, \text{ implies } \phi(\eta) = d_1.$$

I_9) Here the invariants are $\eta = \frac{e^y}{x}, \psi = xf(\eta), \theta = \theta(\eta), \phi = \phi(\eta)$. These invariants give us very complicated equations that can not be solved analytically.

I_{10}) Here the invariants are $y = \eta, \psi = xf(\eta), \theta = \theta(\eta), \phi = \ln x + \phi(\eta)$. These invariants reveal the following equations

$$(1 + \frac{1}{\beta})f'''' + Rff''' - Rf'f'' - Mf'' = 0, \tag{5.33}$$

$$\theta'' + \Pr Rf\theta' + \Pr Q\theta = 0, \tag{5.34}$$

$$\phi'' + RSc(f\phi' - f') = 0. \tag{5.35}$$

The flow and heat transfer equations will be solved later for V_6, and mass transfer equation can be solved numerically.

I_{11}) Here the invariants are $y = \eta, \psi = xf(\eta), \theta = x\theta(\eta), \phi = \phi(\eta)$. These invariants reveal the same flow equation as in I_{10} while the other are as following

$$\theta'' + \Pr R(f\theta' - f'\theta + \frac{Q}{R}\theta) = 0, \tag{5.36}$$

$$\phi'' + RScf\phi' = 0. \tag{5.37}$$

The solution of heat transfer equation can be obtained numerically and the solution of mass transfer equation will be solved later for V_6.

I_{12}) Here the invariants are $y = \eta, \psi = xf(\eta), \theta = \theta(\eta), \phi = x\phi(\eta)$. These invariants give us the same equations for flow and heat transfer as in I_{10}, and the mass transfer equation is as following which can be solved numerically.

$$\phi'' + RSc(f\phi' - f'\phi) = 0. \tag{5.38}$$

The solution of flow and heat transfer equations will be presented later for V_6, and mass transfer equation can be solved numerically.

I_{13}) Here the invariants are $y - x = \eta, \psi = f(\eta), \theta = e^x\theta(\eta), \phi = \phi(\eta)$. These invariants give us the following system of equations

$$2(1 + \frac{1}{\beta})f'''' - Mf'' = 0, \tag{5.39}$$

$$\theta'' + \Pr[Q - Rf']\theta = 0, \tag{5.40}$$

$$\phi'' = 0, \text{ implies } \phi = a_5 + a_6\eta. \tag{5.41}$$

The solution of the flow equation (5.39) is

$$f(\eta) = a_1 + a_2\eta + a_3e^{\sqrt{\frac{M}{2a}}\eta} + a_4e^{-\sqrt{\frac{M}{2a}}\eta},$$

where a_i are integration constants and $a = 1 + \frac{1}{\beta}$. Then the heat transfer equation will take the following form which can be solved numerically

$$\theta'' + \Pr[Q - R(a_2 + a_3\sqrt{\frac{M}{2a}}e^{\sqrt{\frac{M}{2a}}\eta} - a_4\sqrt{\frac{M}{2a}}e^{-\sqrt{\frac{M}{2a}}\eta})]\theta = 0.$$

I_{14}) Invariants are $y - x = \eta, \psi = f(\eta), \theta = \theta(\eta), \phi = e^x\phi(\eta)$. The flow and heat equations are reduced similar to as I_{13} and I_2 respectively and the mass transfer equation is reduced

into the following form

$$\phi'' - ScRf'\phi = 0. \tag{5.42}$$

The mass equation will take the following form which can be solved numerically

$$\phi'' - ScR(a_2 + a_3\sqrt{\frac{M}{2a}}e^{\sqrt{\frac{M}{2a}}\eta} - a_4\sqrt{\frac{M}{2a}}e^{-\sqrt{\frac{M}{2a}}\eta})\phi = 0.$$

I_{15}) Invariants are $y - x = \eta, \psi = f(\eta), \theta = \theta(\eta), \phi = x + \phi(\eta)$. The flow and heat equations are reduced similar as I_{13} and I_2 respectively and the mass transfer equation is reduced to following form

$$\phi'' - ScRf' = 0. \tag{5.43}$$

Then the solution of above equation is represented as

$$\phi(\eta) = ScR[\frac{a_2}{2}\eta^2 + \sqrt{\frac{2a}{M}}(a_3e^{\sqrt{\frac{M}{2a}}\eta} - a_4e^{-\sqrt{\frac{M}{2a}}\eta})] + a_5\eta + a_6.$$

I_{16}) Invariants are $y - x = \eta, \psi = x + f(\eta), \theta = \theta(\eta), \phi = \phi(\eta)$. The heat and mass transfer equations are reduced similar to as I_4 and the flow equation reduced to the following form

$$2(1 + \frac{1}{\beta})f'''' - (M + 2R)f'' = 0, \tag{5.44}$$

which has the solution as

$$f(\eta) = a_1 + a_2\eta + a_3e^{\sqrt{\frac{2R+M}{2a}}\eta} + a_4e^{-\sqrt{\frac{2R+M}{2a}}\eta}.$$

I_{17}) Invariants are $y = \eta, \psi = f(\eta), \theta = e^x\theta(\eta), \phi = e^y\phi(\eta)$. The flow, heat and mass transfer equations are reduced to the similar ones as I_1 and I_2 respectively.

I_{18}) Invariants are $y = \eta, \psi = f(\eta), \theta = e^x\theta(\eta), \phi = x + \phi(\eta)$. The flow, heat and mass transfer equations are reduced to the similar ones as I_1 and I_3 respectively.

I_{19}) Invariants are $y = \eta, \psi = x + f(\eta), \theta = e^x\theta(\eta), \phi = \phi(\eta)$. The flow and mass transfer equations are reduced to the similar ones as I_4, and heat transfer equation reduced to the

following form which can be solved numerically

$$\theta'' - R\,\mathrm{Pr}\,\theta' + \mathrm{Pr}(Q - Rf')\theta = 0.$$

I_{20}) Invariants are $y = \eta, \psi = x + f(\eta), \theta = \theta(\eta), \phi = e^x\phi(\eta)$. The flow and heat transfer equations are reduced to the similar one as I_4, and mass transfer equation reduced to the following form which can be solved numerically

$$\phi'' - RSc\phi' - ScRf'\phi = 0.$$

I_{21}) Invariants are $y = \eta, \psi = x + f(\eta), \theta = \theta(\eta), \phi = x + \phi(\eta)$. The flow and heat transfer equations are reduced to the similar ones as I_4, and mass equation is reduced to the following form

$$\phi'' + RSc\phi' - ScRf' = 0. \tag{5.45}$$

Above equation implies the solution

$$\phi(\eta) = d_1e^{-RSc\eta} + d_2 + a_2(RSc\eta - 1) + \frac{a_3}{n_1 + RSc}e^{n_1\eta} + \frac{a_4}{n_2 + RSc}e^{n_2\eta},$$

where $n_1 = \frac{-R+\sqrt{R^2+4aM}}{2a}$, $n_2 = \frac{-R-\sqrt{R^2+4aM}}{2a}$.

I_{22}) Invariants are $x = \eta, \psi = f(\eta), \theta = e^y\theta(\eta), \phi = e^y\phi(\eta)$. The flow equation identically satisfies, heat and mass transfer equations are reduced to similar one as I_5 and I_6 respectively.

I_{23}) Invariants are $x = \eta, \psi = f(\eta), \theta = e^y\theta(\eta), \phi = y + \phi(\eta)$. The flow equation identically satisfies, heat and mass transfer equations are reduced to similar one as I_5 and I_7 respectively.

I_{24}) Invariants are $x = \eta, \psi = y + f(\eta), \theta = e^y\theta(\eta), \phi = \phi(\eta)$. The flow equation appeared the same as I_8, but the heat and mass transfer equations are reduced to the following forms

$$\theta' - (f' + \frac{1}{R\,\mathrm{Pr}} + \frac{Q}{R})\theta = 0, \text{ implies} \tag{5.46}$$

$$\theta(\eta) = b_1Exp[a_2\eta + \frac{a_1}{2}\eta^2 + \frac{1}{R\,\mathrm{Pr}} + \frac{Q}{R}],$$

$$\phi' = 0, \text{ implies } \phi(\eta) = d_1. \tag{5.47}$$

I_{25}) Invariants are $\eta = \frac{e^y}{x}, \psi = xf(\eta), \theta = x\theta(\eta), \phi = \phi(\eta)$. The flow and mass transfer equations are reduced to similar one as I_9, and heat equation is reduced to the following form which can be solved numerically

$$\eta^2\theta'' + \eta\theta' + \Pr R(\eta f\theta' - \eta f'\theta + \frac{Q}{R}\theta) = 0. \tag{5.48}$$

I_{26}) Invariants are $x = \eta, \psi = y + f(\eta), \theta = \theta(\eta), \phi = e^y\phi(\eta)$. The flow, heat and mass transfer equations are reduced to similar one as I_8, I_8 and I_6 respectively.
I_{27}) Invariants are $\eta = \frac{e^y}{x}, \psi = xf(\eta), \theta = \theta(\eta), \phi = e^y\phi(\eta)$. The flow and heat transfer equations are reduced to similar one as I_9, and mass transfer equation is reduced into the following form which can be solved numerically

$$\eta\phi'' + (1 + \Pr Rf)\phi' = 0. \tag{5.49}$$

I_{28}) Invariants are $x = \eta, \psi = y + f(\eta), \theta = \theta(\eta), \phi = y + \phi(\eta)$. The flow and heat transfer equations are reduced to similar one as I_8, and mass transfer equation is reduced to the following form

$$\phi' - f' = 0, \text{implies} \tag{5.50}$$

$$\phi(\eta) = a_2\eta + \frac{a_1}{2}\eta^2 + d_3.$$

I_{29}) Invariants are $\eta = \frac{e^y}{x}, \psi = xf(\eta), \theta = \theta(\eta), \phi = y + \phi(\eta)$. The flow and heat transfer equations are reduced to similar ones as I_9, and mass transfer equation is reduced into the following form which can be solved numerically

$$\eta^2\phi'' + \eta\phi' + RSc(f + \eta f\phi' - \eta f') = 0. \tag{5.51}$$

I_{30}) Here the invariants are $y = \eta, \psi = xf(\eta), \theta = \theta(\eta), \phi = \phi(\eta)$. We will solve these reduced equations by considering stretching walls case to observe the impact of physical parameters on flow, heat and mass transfer phenomenon.

Stretching walls case

For the interest of physical parameters in fluid we consider the stretching walls case. After using the invariants our system becomes

$$(1+\frac{1}{\beta})f''''+Rff'''-Rf'f''-Mf''=0, \tag{5.52}$$

$$\theta''+\Pr Rf\theta'+\Pr Q\theta=0, \tag{5.53}$$

$$\phi''+RScf\phi'=0, \tag{5.54}$$

$$\begin{aligned} F'(\pm 1) &= 1, F(1)=0, F'(-1)=0, F(-1)=0, \\ \theta(1) &= 1, \theta(-1)=0, \phi(1)=1, \phi(-1)=0. \end{aligned} \tag{5.55}$$

5.3 Flow characteristics

In order to solve the governing system of ordinary differential equations (5.52)-(5.54) subject to boundary conditions (5.55), a numerical technique is used. We present our findings in graphical and tabular forms collectively with the discussion and their interpretations. The effects of Casson fluid parameter β, magnetic field parameter M and Reynolds number R on velocity profile are presented in Figures 5.1-5.3 respectively. From Figure 5.1 it is observed that with the increase of Casson fluid parameter β the velocity $f'(\eta)$ decreases. Figure 5.2 depicts the influence of magnetic field parameter M on velocity profile $f'(\eta)$. It is entirely clear that a decrease in velocity with an increase in the magnetic field parameter M. The velocity profiles are stretched towards the boundaries and the velocity decreases in the central region of the channel due to the damping effects of the magnetic field parameter M. The effects of Reynolds number R on velocity profile are shown in Figure 5.3. The velocity profile decreases in the central region of the channel and the profile is stretched towards the boundaries as increase in the value of Reynolds number R.

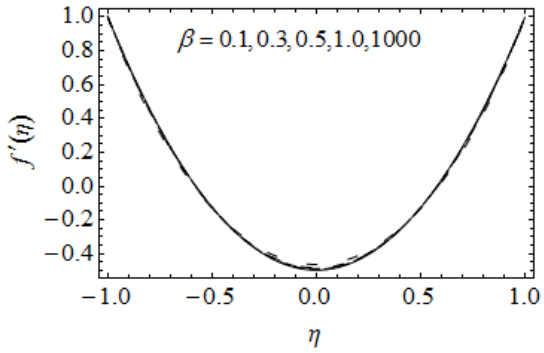

Figure 5.1: Effects of β on $f'(\eta)$

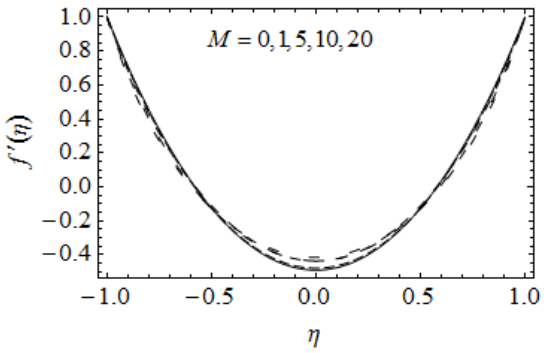

Figure 5.2: Effects of M on $f'(\eta)$

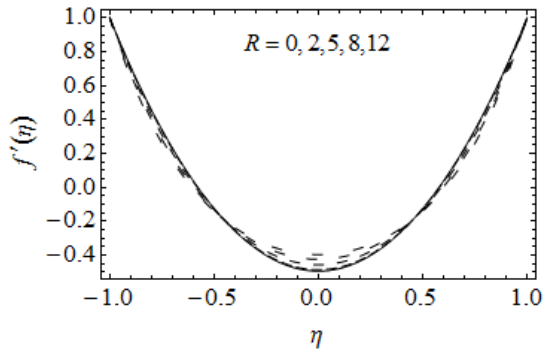

Figure 5.3: Effects of R on $f'(\eta)$

The influence of various physical parameters on temperature profile $\theta(\eta)$ are given in Figures 5.4-5.8. Figure 5.4 shows the effect of Casson fluid parameter β on temperature profile $\theta(\eta)$. It is revealed that as the Casson fluid parameter β increases, the temperature profile $\theta(\eta)$ is also increasing. Influence of magnetic parameter M are plotted in Figure 5.5. With an increase in magnetic field parameter M the resistive forces become strong which increase the temperature. The variation of Reynolds number R on temperature profile $\theta(\eta)$ is sketched in Figure 5.6. With a rise in the value of Reynolds number R, the temperature profile falls. Figures 5.7 and 5.8 are

illustrating the influence of source($Q > 0$) and sink($Q < 0$) effects on the temperature profile $\theta(\eta)$. It is noticed that in case of source the temperature increases with increase in the value of heat generation parameter Q. However it is noticed that temperature decreases in case of sink.

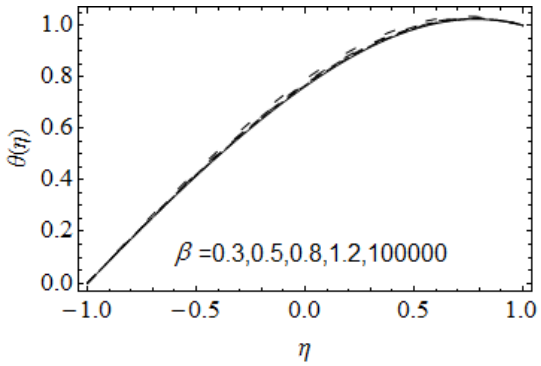

Figure 5.4: Effects of β on $\theta(\eta)$

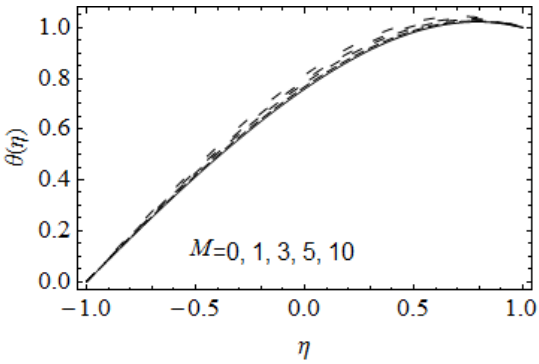

Figure 5.5: Effects of M on $\theta(\eta)$

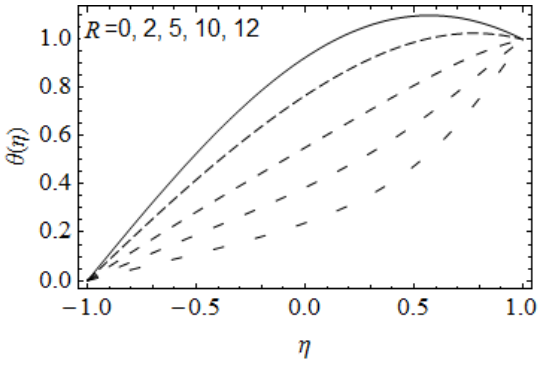

Figure 5.6: Effects of R on $\theta(\eta)$

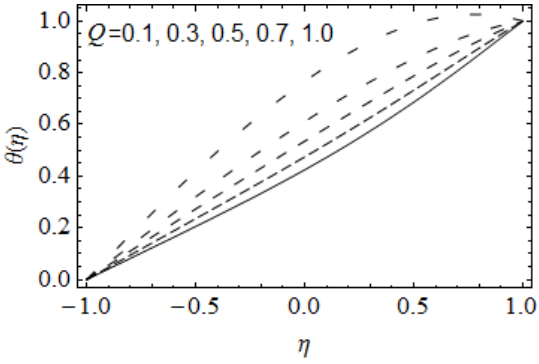

Figure 5.7: Effects of $Q > 0$ on $\theta(\eta)$

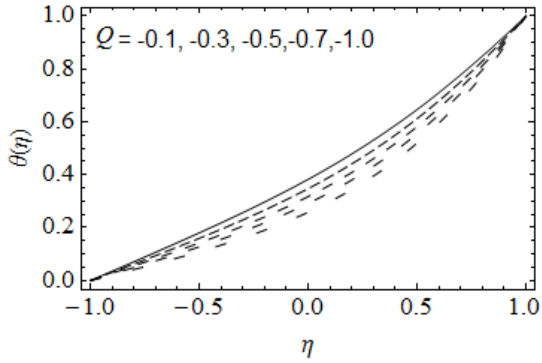

Figure 5.8: Effects of $Q < 0$ on $\theta(\eta)$

Figures 5.9-5.12 are sketched to examine the effect of different physical parameters on concentration profile $\phi(\eta)$. Figure 5.9 shows that with the increase of Casson fluid parameter β, the concentration profile $\phi(\eta)$ decreases. An increase in the concentration profile $\phi(\eta)$ is observed in Figure 5.10 with increase in magnetic field parameter M. Figure 5.11 illustrated that when the Reynolds number R rises the concentration profile falls. It is noticed that with the increase in Schmidt number Sc the concentration profile $\phi(\eta)$ decreases which is plotted in Figure 5.12.

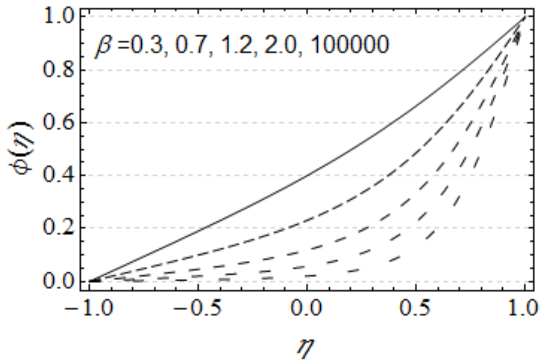

Figure 5.9: Effects of β on $\phi(\eta)$

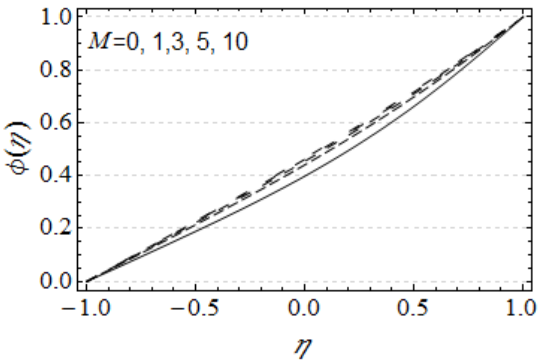

Figure 5.10: Effects of M on $\phi(\eta)$

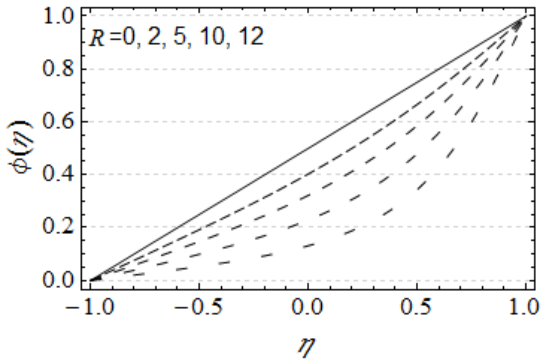

Figure 5.11: Effects of R on $\phi(\eta)$

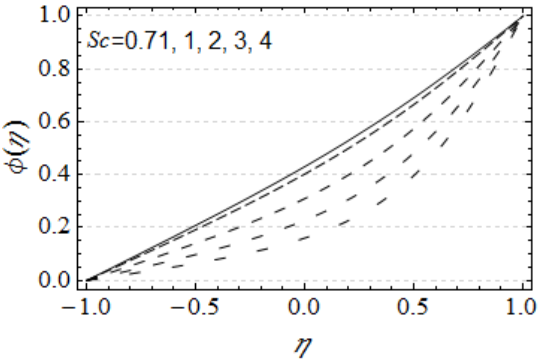

Figure 5.12: Effects of Sc on $\phi(\eta)$

Here the tabular study of the physical quantities like shear stress $(1+\frac{1}{\beta})f''(-1)$, heat transfer rate $\theta'(-1)$ and mass transfer rate $\phi'(-1)$ is presented for different values of physical parameters. Table 5.3 presents the influence of magnetic field parameter M on shear stress, heat transfer rate and mass transfer rate. It is noticed that with the rise of magnetic field M, the shear stress and the mass transfer rate increase while heat transfer rate decreases at the channel walls. Due to the magnetic field that exerts the friction force which tends to drag the fluid and mass transfer towards the channel walls. Further, the frictional force tends to increase the fluid temperature while the difference of the walls and fluid temperature cause a decrease in heat transfer rate. Table 5.4 predicts the effects of Reynolds number R(stretching rate) on the shear stress, heat transfer rate and the mass transfer rate. With rise of stretching rate, the channel walls force the fluid to move rapidly towards the channel walls and as a result the shear stress increases. From the flow region the fluid is carrying away the heat, hence with the increase in the temperature difference the heat transfer rate also increases. By applying the stretching rate the mass transfer also increases. In Table 5.5, the influence of Casson fluid parameter β on the shear stress, heat transfer rate and mass transfer rate is shown. It is observed that with increase of Casson fluid parameter β, the shear stress rate and mass transfer rate are decreasing but reversal for heat transfer rate. Table 5.6 presents the source/sink effects on the heat transfer rate. The quantity $-\theta'(-1)$ is decreasing for source($Q>0$) but opposite for sink($Q<0$). The effects of Prandtle number Pr on the heat transfer rate $-\theta'(-1)$ are observed decreasing as we increase the value of Pr which is tabulated in Table 5.7. In Table 5.8, the influence of Schmidt

number Sc is shown for the mass transfer rate. It is observed that when we increase the value of Schmidt number Sc the mass transfer rate decreases.

M	$-(1+\frac{1}{\beta})\ f''(-1)$	$-\theta'(-1)$	$-\phi'(-1)$
0	9.17172	-1.49699	-0.54828
1	9.36976	-1.51054	-0.54782
3	9.75488	-1.53298	-0.54694
5	10.12640	-1.55078	-0.54610
10	11.00250	-1.58235	-0.54421

Table 5.3: Effects of Magnetic field parameter M on shear stress $-(1+\frac{1}{\beta})\ f''(-1)$, heat transfer rate $-\theta'(-1)$ and mass transfer rate $-\phi'(-1)$ when $\beta = 0.5, R = 2, \mathrm{Pr} = Sc = 0.71, Q = 1$

R	$-(1+\frac{1}{\beta})\ f''(-1)$	$-\theta'(-1)$	$-\phi'(-1)$
0	9.19812	0.84816	0.5
2	9.36976	0.96495	0.54782
5	9.62803	1.17209	0.62266
8	9.88705	1.43111	0.70056
12	10.23320	1.90441	0.80779

Table 5.4: Effects of Reynolds number R on shear stress $-(1+\frac{1}{\beta})\ f''(-1)$, heat transfer rate $-\theta'(-1)$ and mass transfer rate $-\phi'(-1)$ when $\beta = 0.5, M = 1, \mathrm{Pr} = Sc = 0.71, Q = 1$

β	$-(1+\frac{1}{\beta})\ f''(-1)$	$-\theta'(-1)$	$-\phi'(-1)$
0.2	18.3706	-0.96598	0.54820
0.5	9.36976	-0.96495	0.54782
1.0	6.36889	-0.96393	0.54744
1.5	4.50941	-0.96332	0.54721
∞	3.36612	-0.96096	0.54634

Table 5.5: Effects of Casson fluid parameter β on shear stress $-(1+\frac{1}{\beta})\ f''(-1)$, heat transfer rate $-\theta'(-1)$ and mass transfer rate $-\phi'(-1)$ when $R = 2, M = 1, \mathrm{Pr} = Sc = 0.71, Q = 1$

Q	$-\theta'(-1)$
0.1	-0.57620
0.3	-0.63964
0.5	-0.71370
0.7	-0.80101
1.0	-0.96495
-0.1	-0.52138
-0.3	-0.47366
-0.5	-0.43184
-0.7	-0.39498
-1.0	-0.34736

Table 5.6: Effects of source($Q > 0$)/sink($Q < 0$) on heat transfer rate $-\theta'(-1)$ when $R = 2, M = 1, \mathrm{Pr} = 0.71, \beta = 0.5$

Pr	$-\theta'(-1)$
0.10	-0.54229
0.50	-0.77625
0.71	-0.96495
1.0	-1.37233
1.5	-3.39266

Table 5.7: Effects of Prandtl number Pr on heat transfer rate $-\theta'(-1)$ when $R = 2, M = 1, Q = 1, \beta = 0.5$

Sc	$-\phi'(-1)$
0.1	-0.50659
0.71	-0.54782
1.0	-0.56803
1.5	-0.60377
2.0	-0.64057

Table 5.8: Effects of Schmidt number Sc on mass transfer rate $-\phi'(-1)$ when $R = 2, M = 1, \beta = 0.5$

5.4 Findings

In this chapter Lie group approach is used for MHD Casson fluid flow with heat and mass transfer phenomenon in the presence of source/sink effects. We found the six finite and one infinite symmetries for the non-dimenssional system of partial differential equations. The de-

termined symmetries are further used to find the Lie algebra, commutator table, adjoint table, Abelian Lie algebra and optimal system for the governing system. Furthermore, the optimal system guide us to find the thirty group invariant solutions for the system. We consider the stretching walls phenomenon for one particular invariant to observe the influence of physical parameters on flow, heat and mass transfer. A numerical technique is being used to solve the ordinary differential equations. The solutions are presented in the form of graphs and tables. The following observations have been collected for the flow characteristics:

It is noticed that with the rise in Casson fluid parameter β decreases the velocity profile $f'(\eta)$, the concentration profile $\phi(\eta)$, shear stress rate $-(1+\frac{1}{\beta})f''(-1)$ and the mass transfer rate $-\phi'(-1)$ but increases the temperature profile $\theta(\eta)$ and heat transfer rate $-\theta'(-1)$ at the channel walls. With the increase of magnetic field parameter M, the velocity profile, the concentration profile and the heat transfer rate decreases while increase the temperature profile, shear stress and mass transfer rate. The velocity, temperature, and the concentration profiles decrease when we enhanced the Reynolds number R, but the shear stress, heat and mass transfer rates are observed increasing. The impact of heat generation parameter Q on temperature profile and heat transfer rate is observed opposite. The Prandtl number Pr shows the reverse behavior on temperature profile and heat transfer rate. The effects of Schmidt number Sc on concentration profile and mass transfer rate are observed similar.

Chapter 6

Lie group study of non-Newtonian flow with heat transfer over a stretching rotating disk

In this chapter, the cylindrical coordinates will be considered. We analyze the MHD three dimensional Casson fluid flow with heat transfer by using the Lie group approach. The governing partial differential equations are converted into ordinary differential equations by symmetry analysis. Lie algebra of the governing system is further expressed in the form of Abelian Lie algebra, commutator and adjoint tables and optimal system of group invariants. Furthermore, the group invariants are listed, and for a particular invariant we solve the ordinary differential equations over a stretching rotating disk. To observe the physical parameter's behavior of the fluid we present the graphs and tables in the end of this chapter.

6.1 Mathematical modeling

Consider a steady three dimensional incompressible laminar Casson fluid flow with heat transfer phenomenon. The cylindrical coordinates $(\bar{r}, \phi, \bar{z})$ are used for the axisymmetric flow and variation with respect to ϕ is ignored. A uniform magnetic field of strength B_0 is applied in the radial direction. The effects of induced magnetic field are negligible as magnetic Reynolds number is assumed to be small. Using (1.41), conservation of mass, momentum and heat

transfer, the following equations are obtained

$$\frac{1}{\bar{r}}\frac{\partial(\bar{r}\bar{u})}{\partial\bar{r}}+\frac{\partial\bar{w}}{\partial\bar{z}}=0, \tag{6.1}$$

$$\bar{u}\frac{\partial\bar{u}}{\partial\bar{r}}+\bar{w}\frac{\partial\bar{u}}{\partial\bar{z}}-\frac{\bar{v}^2}{\bar{r}}=-\frac{1}{\rho}\frac{\partial\bar{p}}{\partial\bar{r}}+\nu(1+\frac{1}{\beta})\left\{\frac{\partial^2\bar{u}}{\partial\bar{r}^2}+\frac{1}{\bar{r}}\frac{\partial\bar{u}}{\partial\bar{r}}+\frac{\partial^2\bar{u}}{\partial\bar{z}^2}-\frac{\bar{u}}{\bar{r}^2}\right\}-\frac{\sigma B_0^2}{\rho}\bar{u}, \tag{6.2}$$

$$\bar{u}\frac{\partial\bar{v}}{\partial\bar{r}}+\bar{w}\frac{\partial\bar{v}}{\partial\bar{z}}+\frac{\bar{u}\bar{v}}{\bar{r}}=\nu(1+\frac{1}{\beta})\left\{\frac{\partial^2\bar{v}}{\partial\bar{r}^2}+\frac{1}{\bar{r}}\frac{\partial\bar{v}}{\partial\bar{r}}+\frac{\partial^2\bar{v}}{\partial\bar{z}^2}-\frac{\bar{v}}{\bar{r}^2}\right\}-\frac{\sigma B_0^2}{\rho}\bar{v}, \tag{6.3}$$

$$\bar{u}\frac{\partial\bar{w}}{\partial\bar{r}}+\bar{w}\frac{\partial\bar{w}}{\partial\bar{z}}=-\frac{1}{\rho}\frac{\partial\bar{p}}{\partial\bar{z}}+\nu(1+\frac{1}{\beta})\left\{\frac{\partial^2\bar{w}}{\partial\bar{r}^2}+\frac{1}{\bar{r}}\frac{\partial\bar{w}}{\partial\bar{r}}+\frac{\partial^2\bar{w}}{\partial\bar{z}^2}\right\}, \tag{6.4}$$

$$\bar{u}\frac{\partial\bar{T}}{\partial\bar{r}}+\bar{w}\frac{\partial\bar{T}}{\partial\bar{z}}=\frac{k}{\rho C_p}\left\{\frac{\partial^2\bar{T}}{\partial\bar{r}^2}+\frac{1}{\bar{r}}\frac{\partial\bar{T}}{\partial\bar{r}}+\frac{\partial^2\bar{T}}{\partial\bar{z}^2}\right\}+\frac{Q_0}{\rho C_p}(\bar{T}-T_\infty). \tag{6.5}$$

In above system of equations $\overline{u},\overline{v}$ and $\bar{w}$ are the velocity components in $\overline{r}$, ϕ and $\overline{z}$ directions respectively and $\bar{p}$ is the pressure.

To make the boundary layer equations we set up the dimensionless transformations which are defined as

$$\begin{aligned} r &= \frac{\bar{r}}{R_1}, z=\frac{\bar{z}}{R_1}\sqrt{R}, u=\frac{\bar{u}}{\Omega R_1}, v=\frac{\bar{v}}{\Omega R_1}, w=\frac{\bar{w}\sqrt{R}}{\Omega R_1}, \\ p &= \frac{\bar{p}}{\rho(\Omega R_1)^2}, T=\frac{\bar{T}-T_\infty}{T_0}, \mathrm{Re}=\frac{\Omega R_1^2}{\nu}, \end{aligned} \tag{6.6}$$

where R is Reynolds number, R_1 is the reference length and T_0 is reference temperature. It must be mentioned that the corresponding scales of the axial direction are smaller by a factor $R^{\frac{-1}{2}}$. After using the above dimensionless transformations (6.6) we will have the system of equations (6.1)-(6.5) as

$$\frac{1}{r}\frac{\partial(ru)}{\partial r}+\frac{\partial w}{\partial z}=0, \tag{6.7}$$

$$u\frac{\partial u}{\partial r}+w\frac{\partial u}{\partial z}-\frac{v^2}{r}=-\frac{\partial p}{\partial r}+(1+\frac{1}{\beta})\frac{1}{R}\left\{\frac{\partial^2 u}{\partial r^2}+\frac{1}{r}\frac{\partial u}{\partial r}+R\frac{\partial^2 u}{\partial z^2}-\frac{u}{r^2}\right\}-Mu, \tag{6.8}$$

$$u\frac{\partial v}{\partial r}+w\frac{\partial v}{\partial z}+\frac{uv}{r}=(1+\frac{1}{\beta})\frac{1}{R}\left\{\frac{\partial^2 v}{\partial r^2}+\frac{1}{r}\frac{\partial v}{\partial r}+R\frac{\partial^2 v}{\partial z^2}-\frac{v}{r^2}\right\}-Mv, \tag{6.9}$$

$$\frac{1}{R}(u\frac{\partial w}{\partial r}+w\frac{\partial w}{\partial z})=-\frac{\partial p}{\partial z}+(1+\frac{1}{\beta})\frac{1}{R^2}\left\{\frac{\partial^2 w}{\partial r^2}+\frac{1}{r}\frac{\partial w}{\partial r}+R\frac{\partial^2 w}{\partial z^2}\right\}, \tag{6.10}$$

$$u\frac{\partial T}{\partial r}+w\frac{\partial T}{\partial z}=\frac{1}{\Pr}\frac{1}{R}\left\{\frac{\partial^2 T}{\partial r^2}+\frac{1}{r}\frac{\partial T}{\partial r}+R\frac{\partial^2 T}{\partial z^2}\right\}+QT. \tag{6.11}$$

For high Reynolds number $R\to\infty$ our boundary layer equations (6.7)-(6.11) are

$$\frac{1}{r}\frac{\partial(ru)}{\partial r}+\frac{\partial w}{\partial z}=0, \tag{6.12}$$

$$u\frac{\partial u}{\partial r}+w\frac{\partial u}{\partial z}-\frac{v^2}{r}=-\frac{\partial p}{\partial r}+(1+\frac{1}{\beta})\frac{\partial^2 u}{\partial z^2}-Mu, \tag{6.13}$$

$$u\frac{\partial v}{\partial r}+w\frac{\partial v}{\partial z}+\frac{uv}{r}=(1+\frac{1}{\beta})\frac{\partial^2 v}{\partial z^2}-Mv, \tag{6.14}$$

$$-\frac{\partial p}{\partial z}=0, \tag{6.15}$$

$$u\frac{\partial T}{\partial r}+w\frac{\partial T}{\partial z}=\frac{1}{\Pr}\frac{\partial^2 T}{\partial z^2}+QT. \tag{6.16}$$

The pressure is dependent only on z which is studied by [88] that comes from property of similarity transformation. Therefore in Eq. (6.13) it directly implies that $\frac{\partial p}{\partial r}=0$. And by Eq. (6.15) it is obvious that pressure will remain constant in the axial direction and in the boundary layer region. For pressure term it is concluded that in the boundary layer region it will remain constant.

6.2 Lie group analysis

In this section we have applied the group theoretical technique to calculate the symmetries for the system of partial differential Eqs. (6.12)-(6.16). The infinitesimal generator for the system of partial differential equations is represented as

$$\begin{aligned}\vec{V} &= \xi_1(r,z,u,v,w,T)\partial_r+\xi_2(r,z,u,v,w,T)\partial_z+\Phi_1(r,z,u,v,w,T)\partial_u\\ &\quad+\Phi_2(r,z,u,v,w,T)\partial_v+\Phi_3(r,z,u,v,w,T)\partial w+\Phi_4(r,z,u,v,w,T)\partial_T.\end{aligned} \tag{6.17}$$

The infinitesimal Lie group point transformations for the invariance of the Eqs. (6.12)-(6.16) are expressed as

$$\begin{aligned} r^* &= r + \epsilon\xi_1(r,z,u,w,v,T) + O(\epsilon^2), \\ z^* &= z + \epsilon\xi_2(r,z,u,w,v,T) + O(\epsilon^2), \\ u^* &= u + \epsilon\Phi_1(r,z,u,w,v,T) + O(\epsilon^2), \\ v^* &= v + \epsilon\Phi_2(r,z,u,w,v,T) + O(\epsilon^2), \\ w^* &= w + \epsilon\Phi_3(r,z,u,w,v,T) + O(\epsilon^2), \\ T^* &= T + \epsilon\Phi_4(r,z,u,w,v,T) + O(\epsilon^2). \end{aligned} \tag{6.18}$$

For Eqs.(6.12)-(6.16) we have used the software package [25] to find the infinitesimals as

$$\begin{aligned} \xi_1(r,z,u,w,v,T) &= c_2 r, \xi_2(r,z,u,w,v,T) = f_1(r), \Phi_1(r,z,u,w,v,T) = c_2 u, \\ \Phi_2(r,z,u,w,v,T) &= c_2 v, \Phi_3(r,z,u,w,v,T) = u f_1\prime(r), \Phi_4(r,z,u,w,v,T) = c_1 T. \end{aligned} \tag{6.19}$$

Here (6.19) ensures us two finite parameter Lie group transformations and two infinite parameter Lie group transformations i.e, $f_1(r)$ and $f_1'(r)$. Where parameter c_1 represents the scaling in T, and c_2 represents the scaling in r, u and v.

Now we have a 4−dimensional vector space of infinitesimal generators closed under the operation of commutation, i.e., 4−dimensional Lie algebra, the basis of the corresponding Lie algebra are as follows

$$V_1 = \partial_T, V_2 = r\partial_r + u\partial_u + v\partial_v, V_3 = \partial_z, V_4 = u\partial_w. \tag{6.20}$$

As we mentioned in chapter 2 that the requirement for solvability is equivalent to the existence of a basis $\{V_1, V_2, ..., V_4\}$ of Lie algebra such that by Eq. (1.13) we can develop the following commutator table

[,]	V_1	V_2	V_3	V_4
V_1	0	0	V_1	0
V_2	0	0	0	0
V_3	-V_1	0	0	-2V_4
V_4	0	0	2V_4	0

Table 6.1: Commutator table

The following Abelian Lie algebra obtained from commutator Table 6.1

$$\begin{aligned}[V_s, V_t] &= 0, \text{ as } s = t, [V_1, V_2] = 0, [V_1, V_4] = 0,\\ [V_2, V_3] &= 0, [V_2, V_4] = 0.\end{aligned}$$

By using the definition of adjoint representation from chapter 1, we can reconstruct the adjoint representation adG of the Lie group by summing the Lie series (1.14) obtaining the adjoint table.

Ad	V_1	V_2	V_3	V_4
V_1	V_1	V_2	$V_3 - \varepsilon V_1$	V_4
V_2	V_1	V_2	V_3	V_4
V_3	$V_1 e^{\varepsilon}$	V_2	V_3	$V_4 e^{2\varepsilon}$
V_4	V_1	V_2	$V_3 - 2\varepsilon V_4$	V_4

Table 6.2: Adjoint table

The optimal system of our equations (6.12)-(6.16) is as follows

$I_1)$ $V_1 + V_2$ $\quad$ $I_2)$ $V_2 + V_3$ $\quad$ $I_3)$ $V_2 + V_4$
$I_4)$ $V_1 + V_3$ $\quad$ $I_5)$ $V_3 + V_4$ $\quad$ $I_6)$ $V_1 + V_2 + V_3$
$I_7)$ $V_2 + V_3 + V_4$ $\quad$ $I_8)$ $V_1 + V_3 + V_4$ $\quad$ $I_9)$ $V_i (i = 1, 2, 3, 4)$.

By using optimal system we can reduce the governing partial differential equations into ordinary differential equations. We find the following nine group invariants which lead us to group invariant solutions as follow

$I_1)$ Invariants are $z = \eta, u = rf(\eta), v = rg(\eta), w = h(\eta), T = \ln r + \theta(\eta)$. The system reduced into the following form, which can be solved numerically

$$2f + h' = 0, \tag{6.21}$$

$$(1 + \frac{1}{\beta})f'' - f^2 - hf' + g^2 - Mf = 0, \tag{6.22}$$

$$(1 + \frac{1}{\beta})g'' - fg - hg' - gf - Mg = 0, \tag{6.23}$$

$$\theta'' - \Pr(h\theta' + f) + \Pr Q(\ln r + \theta) = 0. \tag{6.24}$$

I_2) Invariants are $\eta = \frac{e^z}{r}, u = rf(\eta), v = rg(\eta), w = h(\eta), T = \theta(\eta)$. The system is reduced into the following form, which can be solved numerically

$$\eta h' - \eta f' + 2f = 0, \tag{6.25}$$

$$(1 + \frac{1}{\beta})[\eta^2 f'' + \eta f'] - f^2 - h(f - h)f' + g^2 - Mf = 0, \tag{6.26}$$

$$(1 + \frac{1}{\beta})[\eta^2 g'' + \eta g'] - h(f - h)f' - 2gf - Mg = 0, \tag{6.27}$$

$$\eta^2\theta'' + \eta\theta' + \Pr \eta(f - h)\theta' + \Pr Q\theta = 0. \tag{6.28}$$

I_3) Here the invariants are $\eta = z, u = rf(\eta), v = rg(\eta), w = h(\eta), T = \theta(\eta)$. The continuity and flow equations are reduced into the same as in I_1, but the heat transfer equation takes the following form, which will be solved later in detail for V_2

$$\theta'' + \Pr(Q\theta - h\theta') = 0. \tag{6.29}$$

I_4) Invariants are $\eta = r, u = f(\eta), v = g(\eta), w = h(\eta), T = z + \theta(\eta)$. The system becomes

$$\eta f' + f = 0, \tag{6.30}$$

$$ff' - \frac{g^2}{\eta} + Mf = 0, \tag{6.31}$$

$$fg' + \frac{gf}{\eta} + Mg = 0, \tag{6.32}$$

$$f\theta' + h - Q(z + \theta) = 0. \tag{6.33}$$

The above system of differential equations provides us the following informations about f and g but no information about h and θ.

$$\begin{aligned} f(\eta) &= \frac{a_1}{\eta}, \\ g(\eta) &= \frac{a_2}{\eta} Exp[-\frac{M}{a_1}\eta]. \end{aligned}$$

I_5) Invariants are $\eta = r, u = f(\eta), v = g(\eta), w = h(\eta), T = \theta(\eta)$. The system becomes similar as

I_4 except heat equation which is

$$f\theta' - Q\theta = 0.\text{implies} \tag{6.34}$$

$$\theta(\eta) = b_1 Exp[-\frac{Q}{2a_1}\eta^2].$$

I_6) Here Invariants are $\eta = \frac{e^z}{r}, u = rf(\eta), v = rg(\eta), w = h(\eta), T = \ln r + \theta(\eta)$. The system reduced similar as I_2 except the heat equation which can be solved numerically

$$\eta^2\theta'' + \eta\theta' + \Pr\eta(f-h)\theta' + \Pr Q\theta - f = 0. \tag{6.35}$$

Invariants I_7 and I_8 are appeared the same as I_2 and I_4 respectively.

I_9) Here the invariants for V_2 are $\eta = z, u = rf'(\eta), v = rg(\eta), w = h(\eta), T = \theta(\eta)$.

Here we are interested to solve the governing system of differential equations, for that the stream function $\psi(r,z)$ as follows

$$u = \frac{1}{r}\frac{\partial\psi}{\partial z}, w = -\frac{1}{r}\frac{\partial\psi}{\partial r}. \tag{6.36}$$

After using the combined form of Eq. (6.36) and I_9 which gives

$$\psi = r^2 f(\eta). \tag{6.37}$$

By Eq.(6.36) and Eq. (6.37) the form of w is

$$w = -2f(\eta). \tag{6.38}$$

Continuity Equation (6.12) is identically satisfied by similarity transformations Eq. (6.36) and Eq. (6.38). Now our boundary layer Eqs. (6.13)-(6.16) are conveniently transformed into self similar form

$$(1+\frac{1}{\beta})f''' + ff'' - (f')^2 + g^2 - Mf' = 0, \tag{6.39}$$

$$(1+\frac{1}{\beta})g'' + 2fg' - 2f'g - Mg = 0, \tag{6.40}$$

$$\theta'' + 2\,\mathrm{Pr}\, f\theta' + \mathrm{Pr}\, Q\theta = 0. \tag{6.41}$$

Stretching rotating disk

To solve the system (6.39)-(6.41) for the physical interest of fluid flow with heat transfer analysis, we consider the stretching rotating disk phenomenon. The disk is rotating about its axis $\bar{r} = 0$ with constant angular velocity Ω, but stretching in radial direction with velocity $u_w(\bar{r})$. Then the boundary conditions are

$$\begin{aligned} \bar{u}(\bar{r},0) &= \alpha\Omega\bar{r}u_w(\frac{\bar{r}}{R_1}), \bar{v}(\bar{r},0) = \Omega\bar{r}v_w(\frac{\bar{r}}{R_1}), \bar{w}(\bar{r},0) = 0, \\ \bar{u}(\bar{r},\infty) &= 0, \bar{v}(\bar{r},\infty) = 0, \bar{T}(\bar{r},0) = T_w, \bar{T}(\bar{r},\infty) = T_\infty. \end{aligned} \tag{6.42}$$

Where R_1 is the reference length and α is disk stretching parameter.

By using (6.6) we have the dimensionless boundary conditions as

$$\begin{aligned} u(r,0) &= \alpha r u_w(r), v(r,0) = r v_w(r), w(r,0) = 0, \\ u(r,\infty) &= 0, v(r,\infty) = 0, T(r,0) = T_w, T(r,\infty) = 0. \end{aligned} \tag{6.43}$$

By using I_9 our system of ordinary differential equations with corresponding boundary conditions will be as follows

$$(1+\frac{1}{\beta})f''' + ff'' - (f')^2 + g^2 - Mf' = 0, \tag{6.44}$$

$$(1+\frac{1}{\beta})g'' + 2fg' - 2f'g - Mg = 0, \tag{6.45}$$

$$\theta'' + 2\,\mathrm{Pr}\, f\theta' + \mathrm{Pr}\, Q\theta = 0, \tag{6.46}$$

$$\begin{aligned} f'(0) &= \alpha, f'(\infty) = 0, f(0) = 0, g(0) = 1, \\ g(\infty) &= 0, \theta(0) = 1, \theta(\infty) = 0. \end{aligned} \tag{6.47}$$

The dimensionless forms of radial Skin friction coefficient and the Local Nusselt number will

take the following forms

$$R_r^{1/2} C_f = -(1 + \frac{1}{\beta}) f''(0), \tag{6.48}$$

$$R_r^{-1/2} N u_r = -\theta'(0). \tag{6.49}$$

6.3 Flow characteristics

The system of non-linear ordinary differential equations (6.44)-(6.46) with boundary conditions (6.47) has been solved numerically using MATLAB boundary value problem solver for ode's. The effects of various physical parameters for example $M, \beta, \alpha, \Pr$ and Q on vertical velocity $f(\eta)$, azimuthal velocity $g(\eta)$, radial velocity $f'(\eta)$ and temperature profile $\theta(\eta)$ are presented here through graphs keeping the parameters fixed as $\beta = 5, M = 1, \alpha = 0.5, \Pr = 1$ and $Q = 0.2$. Figures 6.1-6.4 show the effect of Casson fluid parameter β on vertical velocity, azimuthal velocity, radial velocity and temperature profiles. Figure 6.1 depicts the influence of Casson fluid parameter β on vertical velocity $f(\eta)$. It is evident that with increase of β, the vertical velocity decreases. The variation of Casson fluid β with radial velocity $f'(\eta)$ is presented in Figure 6.2. It is observed that as the value of β increases, the radial velocity decreases. The azimuthal velocity $g(\eta)$ decreases and the temperature profile increases with increase of Casson fluid parameter respectively as figure out in Figure 6.3 and Figure 6.4 respectively. Figures 6.5-6.8 are plotted to observe the behavior of magnetic field parameter M with vertical velocity $f(\eta)$, azimuthal velocity $g(\eta)$, radial velocity $f'(\eta)$ and temperature profile $\theta(\eta)$. It is observed that when we raised the value of magnetic field parameter M, the vertical velocity $f(\eta)$, radial velocity $f'(\eta)$ and azimuthal velocity $g(\eta)$ decrease which is presented in Figure 6.5, Figure 6.6 and Figure 6.7 respectively. This is mainly due to the fact that application of magnetic field to an electrically conducting fluid gives rise to Lorentz force, which causes the fluid to decelerate. It is noticed that in Figure 6.8 when we increase the value of magnetic field parameter M, the temperature profile $\theta(\eta)$ increases. The influence of stretching parameter α on the vertical velocity $f(\eta)$, azimuthal velocity $g(\eta)$, radial velocity $f'(\eta)$ and temperature profile $\theta(\eta)$ are illustrated in Figure 6.9-6.12. It is observed that the vertical velocity $f(\eta)$ and the radial velocity $f'(\eta)$ are enhanced with the increase of stretching parameter α which is presented in Figure 6.9 and Figure 6.10 respectively. The effect of stretching parameter α on azimuthal

velocity $g(\eta)$ and temperature profile $\theta(\eta)$ are observed decreasing as shown in Figure 6.11 and Figure 6.12 respectively. Figure 6.13 depicts the influence of heat generation parameter Q on temperature profile $\theta(\eta)$. The temperature profile $\theta(\eta)$ is enhanced with the rise in the value of heat generation parameter Q. The temperature profile $\theta(\eta)$ is observed decreasing with increase the value of Prandtl number Pr as illustrated in Figure 6.14.

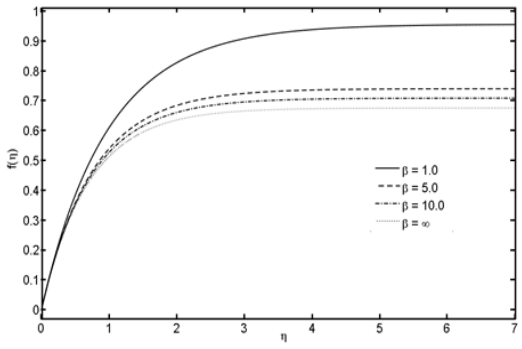

Figure 6.1: Effect of β on $f(\eta)$

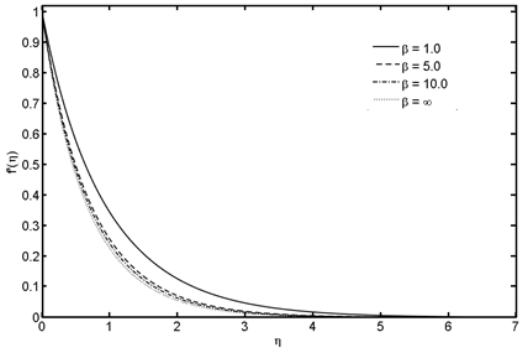

Figure 6.2: Effect of β on $f'(\eta)$

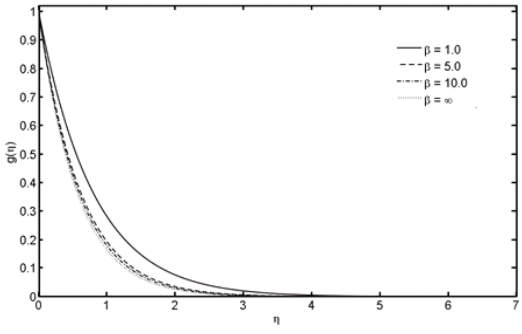

Figure 6.3: Effect of β on $g(\eta)$

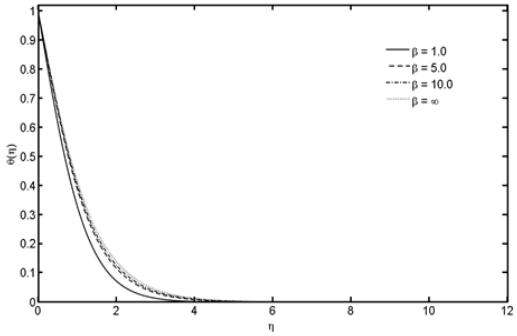

Figure 6.4: Effect of β on $\theta(\eta)$

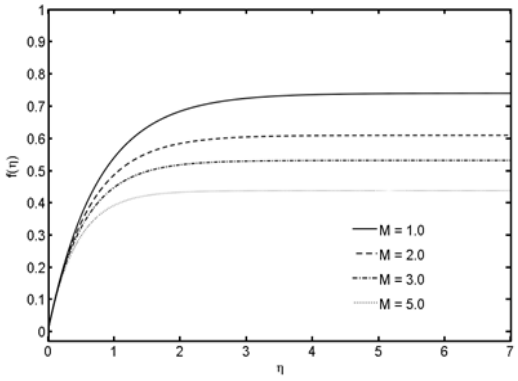

Figure 6.5: Effect of M on $f(\eta)$

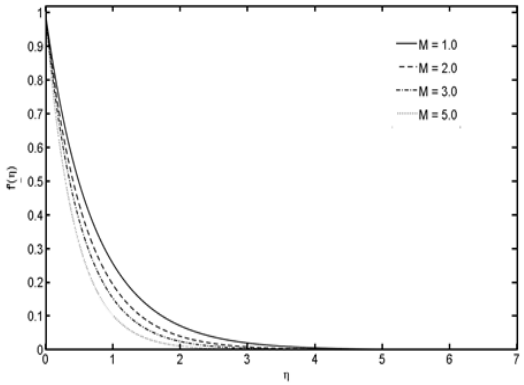

Figure 6.6: Effect of M on $f'(\eta)$

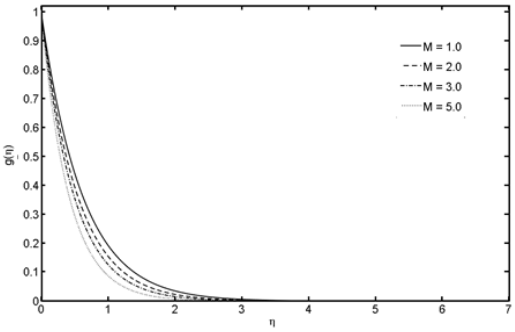

Figure 6.7: Effect of M on $g(\eta)$

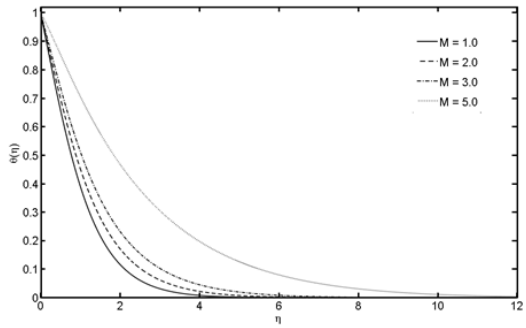

Figure 6.8: Effect of M on $\theta(\eta)$

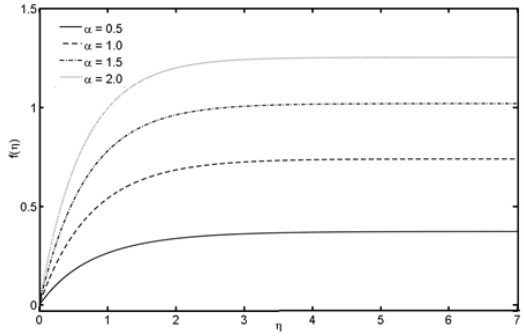

Figure 6.9: Effect of α on $f(\eta)$

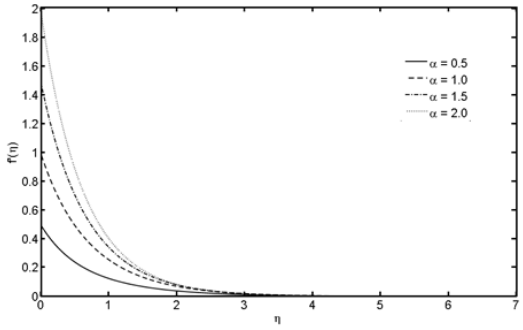

Figure 6.10: Effect of α on $f'(\eta)$

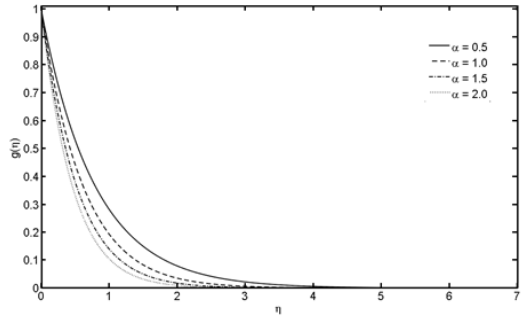

Figure 6.11: Effect of α on $g(\eta)$

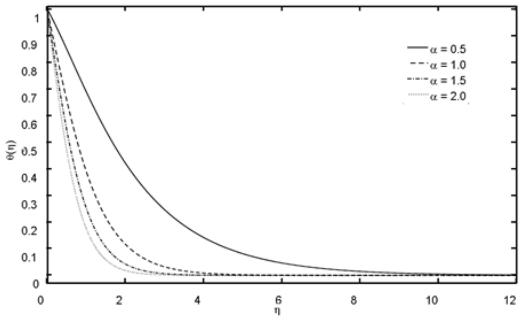

Figure 6.12: Effect of α on $\theta(\eta)$

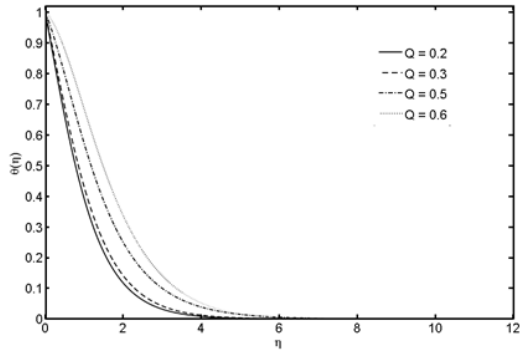

Figure 6.13: Effect of Q on $\theta(\eta)$

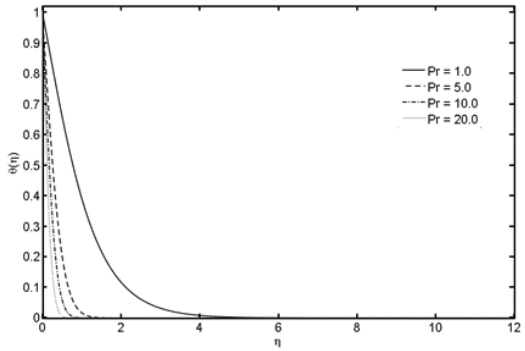

Figure 6.14: Effect of Pr on $\theta(\eta)$

Table 6.3 presents the values of $-(1+\frac{1}{\beta})f''(0)$ and $-(1+\frac{1}{\beta})g'(0)$ for various values of Casson fluid parameter β, magnetic field parameter M, stretching parameter α. It is observed that the radial coefficient of Skin friction decreases with β and increases with M and α. The Nusselt number $-\theta'(0)$ is observed decreasing with increase of β, M and Q, but increases with increase of α and Pr which is shown in Table 6.4.

β	M	α	$-(1+\frac{1}{\beta})f''(0)$	$-(1+\frac{1}{\beta})g'(0)$
1.0	1.0	1.0	2.277542	2.489494
5.0			1.764178	1.928352
10.0			1.689071	1.846256
∞			1.610458	1.760328
5.0	1.0	1.0	1.764178	1.928352
	2.0		2.083880	2.207942
	3.0		2.357394	2.460628
	5.0		2.823436	2.904377
5.0	1.0	0.5	0.941246	1.529623
		1.0	1.764178	1.928352
		1.5	2.781624	2.258467
		2.0	3.957420	2.546689

Table 6.3: Effects of various parameters on $-(1+\frac{1}{\beta})f''(0)$ and $-(1+\frac{1}{\beta})g'(0)$

β	M	α	Q	Pr	$-\theta'(0)$
1.0	1.0	1.0	0.2	1.0	0.769584
5.0					0.681830
10.0					0.663905
∞					0.643032
5.0	1.0	1.0	0.2	1.0	0.681830
	2.0				0.595398
	3.0				0.513667
	5.0				0.264789
5.0	1.0	0.5	0.2	1.0	0.131568
		1.0			0.681830
		1.5			0.951916
		2.0			1.158453
5.0	1.0	1.0	0.2	1.0	0.681830
			0.3		0.592362
			0.5		0.317842
			0.6		0.117566
5.0	1.0	1.0	0.2	1.0	0.681830
				5.0	1.990968
				10.0	2.963776
				20.0	4.337936

Table 6.4: Effects of various parameters on $-\theta'(0)$

6.4 Findings

In this chapter we analyze the MHD three dimensional Casson fluid flow with heat transfer in cylindrical coordinates by employing Lie group method. By making the governing system dimensionless we find the symmetries of the system. Two finite and two infinite symmetries are found. Further, these symmetries are used to find the Lie algebra, commutator table, adjoint table, Abelian Lie algebra and optimal system for the system of partial differential equations. Optimal system helps us to figure out the nine group invariant solutions. Furthermore, we consider the case of stretching rotating disk for a particular invariant to observe the influence of physical parameters on flow and heat transfer phenomenon. The solution of the ordinary differential equation is presented through graphs and tables. After the flow and heat transfer analysis in the light of physical parameters of fluid, the following results have been obtained:

The increase in Casson fluid parameter β decreases the vertical velocity $f(\eta)$, the azimuthal

velocity $g(\eta)$, radial velocity $f'(\eta)$, radial coefficient of Skin friction $-(1+\frac{1}{\beta})f''(0)$ and the Nusselt number $-\theta'(0)$ while increases the temperature profile $\theta(\eta)$. With the increase of magnetic field parameter M, the vertical velocity $f(\eta)$, the azimuthal velocity $g(\eta)$, radial velocity $f'(\eta)$ and the Nusselt number $-\theta'(0)$ decrease while increases the temperature profile $\theta(\eta)$ and radial coefficient of Skin friction $-(1+\frac{1}{\beta})f''(0)$. The vertical and radial velocities decrease when we enhanced the stretching parameter α, but the azimuthal velocity, temperature profile, radial coefficient of Skin friction and the Nusselt number are observed increasing. The impact of heat generation parameter Q on temperature profile and Nusselt number is observed opposite. The Prandtl number Pr shows the reverse behavior on temperature profile and the Nusselt number.

Chapter 7

Summary and future directions

In this chapter we summarize our study and suggest some future directions.

7.1 Summary

The focus of this study was to find the Lie group invariant (similarity) solutions to some multidimensional (two and three dimensional) non-Newtonian fluid flow problems describing Casson fluid with heat transfer phenomenon. For Lie group analysis three well known laws i.e. conservation laws of mass, momentum and energy were considered. Initially all the three laws were investigated through boundary layer approximation. To make these boundary layer equations dimensionless, we used appropriate variables. The governing dimensionless system was further studied through Lie group approach. By employing this technique, the translation and scaling symmetries were found. These symmetries played a vital role to investigate further properties of the governing partial differential equations. We also calculated the commutator table, Abelian Lie algebra, adjoint representation table and optimal system of the Lie algebra of group operators. Following the optimal system, we calculated the group invariant solutions of the governing partial differential equations. Further for a particular invariant, we considered the boundary value conditions by taking different geometries to examine the flow characteristics. The main purpose was to observe the influence of different physical parameters on velocity and temperature profiles, skin friction and local Nusselt number. For this purpose we have plotted the graphs and the numerical values were displayed in tables of pertinent parameters involving

in the physical problems .While investigating the flow and heat characteristics we observed that there is a decrease in velocity profile and local Nusselt number as the values of the Casson fluid parameter and magnetic field parameter increase. We also noticed that with the increase of Casson fluid parameter, magnetic field parameter and Prandtl number, the temperature profile also rises. Furthermore, the effects of Casson fluid parameter and magnetic field parameter on skin friction were observed.

The results of the symmetry group analysis of some multidimensional fluid flow with heat transfer phenomenon can be summarized by the following remarks:

The local Lie symmetries of the equations were presented. We also presented the commutator table, adjoint representation and abelian Lie algebra. The optimal system of transformations was calculated. By following the optimal system, we listed the group invariants. We presented all the analytical solutions of the reduced system of equations. The equation that had to be solved numerically was written in the reduced form using the invariants of the transformations. For one particular invariant we considered the boundary conditions to solve the system of ordinary differential equations. We demonstrated the application of Lie symmetry method on some particular equations proving that the invariants can help us to simplify very much the task of finding the solutions of some given differential equations. The Lie group approach in its general form is particularly effective since it furnishes both general Lie symmetries and all their invariants in a constructive way. We found that the application of this method gave us a straightforward way to construct solutions of nonlinear equations.

7.2 Some future directions

We have applied the Lie group approach on fluid problems and found their analytical and numerical solutions. These analytical solutions can be very useful for the investigation of different physical systems where the flow and heat processes are important. It appears that the exact analytical solutions of differential equations are based on exploiting some symmetry of these equations with respect to certain transformations. In this study we suggest following future work to the readers:

- This work can be studied by applying Non-Classical and Potential symmetries.
- We still have freedom to apply the Lie group technique for other Non-Newtonian fluid models i.e. Eyring Powell fluid, Nanofluid, Micropolar fluid, Oldroyd B, Maxwell fluid, Jeffrey fluid, Burger's fluid, and many others.
- Lie group method has been applied on Newtonian fluid but still there are many problems which can be solved by applying Lie group method.
- This work can be extended by considering different geometries.

7.3 Research progress during Ph.D. studies

Publications

1. Irreversibility analysis of MHD flow over an exponentially stretching sheet, Heat Transfer Asian-Research Journal, 44 (3), 211-226, (2013)
2. Heat Source/Sink Effects on Non-Newtonian MHD fluid flow and heat transfer over a Permeable Stretching Surface; Lie Group Analysis, Indian Journal of Physics, 88 (1), 75-82, (2014)
3. Conserved integrals for inviscid compressible fluid flow in Riemannian manifolds, Proceeding of Royal Society A, 471, (2015)
4. Group Theoretical Analysis of Non-Newtonian Fluid Flow, Heat & Mass Transfer over a Stretching Surface in the Presence of Thermal Radiations, Journal of Applied Fluid Mechanics, 9 (3), 1515-1524, (2016)
5. Three dimensional flow of magnetohydrodynamics Casson fluid over an unsteady stretching sheet embedded in a porous medium, Journal of Applied Mechanics and Technical Physics, 57 (2), (2016)
6. Computational modeling of MHD flow of Non-Newtonian fluid over an unsteady stretching sheet with viscous dissipation effects, Journal of Applied Mechanics and Technical Physics, 57 (5) (2016)

Accepted Papers

1. Group Invariants for Relativistic Fluid with Electromagnetic Field, Journal of Vectorial Relativity, (2011)

Bibliography

[1] A. Cohen, An Introduction to the Lie Theory of One-Parameter Groups with Application to the Solution of Differential Equations: New York, G.E. Stechert, (1911), (1931 reprint).

[2] A. R. Forsyth, Theory of Differential Equations: Dover, New York, Volumes V and VI. (1959).

[3] L. V. Ovsiannikov, Group Analysis of Differential Equations: Moscow, Nauka. English translation. Academic Press, 1982. See also (in Russian) Group Properties of Differential Equations: Novosibirsk, Izd. Sibirsk. Otd. Akad. Nauk SSSR, (1962).

[4] G. Birkhoff, Hydrodynamics: Princeton University Press, (1960).

[5] U. G. I. Barenblat and Y. B. Zel'dovich, Self-similar solutions as intermediate asymptotics: Ann. Rev. Fluid Mech., 4, 285-312, (1972).

[6] N. H. Ibragimov, Classification of the invariant solutions to the equations for the two-dimensional transient-state flow of a gas: J. Appl. Mech. Tech. Phys., 7(4), 19-22, (1966).

[7] G. Bluman and J. D. Cole, Similarity Methods for Differential Equations: Appl. Math. Sci., 13, Springer-Verlag, (1974).

[8] R. Anderson, S. Kumei and C. Wulfman, Generalization of the concept of invariance of differential equations: results of applications to some Schrodinger equations: Phys. Rev. Lett., 28, 988, (1972).

[9] W. Chester, Continuous transformations and differential equations: J. Inst. Math. Appl., 19, 343-376, (1977).

[10] B. K. Harrison and F. B. Estabrook, Geometric approach to invariance groups and solutions of partial differential equations: J. Math. Phys., 12(4), 653-666, (1971).

[11] A. G. Hansen, Similarity Analysis of Boundary Value Problems in Engineering, Prentice Hall, (1964).

[12] W. F. Ames, Nonlinear Partial Differential Equations in Engineering, Academic Press, (1972).

[13] P. J. Olver, Applications of Lie Groups to Differential Equations: Graduate Texts in Mathematics 107, Springer-Verlag, (1986).

[14] G. W. Bluman and S. Kumei, Symmetries and Differential Equations: Applied Mathematical Sciences 81, Springer-Verlag, (1989).

[15] C. Rogers and W. F. Ames, Nonlinear Boundary Value Problems in Science and Engineering: Mathematics in Science and Engineering 183, Academic Press, (1989).

[16] H. Stephani, Differential Equations: Their Solution Using Symmetries: Cambridge University Press, (1989).

[17] N. H. Ibragimov, Elementary Lie Group Analysis and Ordinary Differential Equations: John Wiley & Sons, (1998).

[18] V. K. Andreev, O. K. Kaptsov, V. V. Pukhnachov and A. A. Rodionov, Application of Group-Theoretical Methods in Hydrodynamics: Kluwer Academic Publishers, (1998).

[19] P. Hydon, Symmetry Methods for Differential Equations: a beginner's guide: Cambridge Texts in Applied Mathematics, Cambridge Press, (2000).

[20] G. Baumann, Symmetry Analysis of Differential Equations with Mathematica: Springer-Telos Electronic Library of Science, (1998).

[21] G. Bluman and S. Anco, Symmetry and Integration Methods for Differential Equations: volume 154 of Applied Mathematical Sciences, Springer, New York, first edition, (2002).

[22] N. H. Ibragimov, CRC Handbook of Lie Group Analysis of Differential Equations: Volume 1, CRC Press, (1994-1996).

[23] F. Schwarz, Symmetries of differential equations from Sophus Lie to computer algebra: SIAM Rev., 30, 450, (1988).

[24] F. Schwarz, Computer algebra software for scientific applications: In Proceedings of the 1993 C1SM Advanced School on Computerized Symbolic Manipulation in Mechanics, Udine, Italy, E. Kreuzer, Editor, Springer-Verlag, (1994).

[25] L. Margheriti and F. Oliveri, A Mathematica package for obtaining the optimal system of subalgebras of a Lie algebra: Preprint, 1–21, (2008).

[26] W. Hereman, Review of symbolic software for the computation of Lie symmetries of differential equations: Euromath. Bull., 2, 45-82, (1994).

[27] B. C. Sakiadis, Boundary-layer behavior on continuous solid surfaces: I. Boundary-layer equations for two-dimensional and axisymmetric flow: AIChE J., 7**,** 26–28**,** (1961).

[28] L. J. Crane, Flow past a stretching sheet: Zeitschrift für angewandte Mathematik und Physik, 21**,** 645**-**647, (1970).

[29] P. S. Gupta and A. S. Gupta, Heat and Mass Transfer on a stretching sheet with suction or blowing: Can. J. of Chem. Eng., 55**,** 744−746**,** (1977).

[30] L. J. Grubka and K. M. Bobba, Heat Transfer Characteristics of a continuous, stretching surface with variable temperature: J. Heat Tras., 107(1), 248-250, (1985).

[31] I. Chung Liu, Flow and heat transfer of an electrically conducting fluid of second grade in a porous medium over a stretching sheet subject to a transverse magnetic field: Int. J. Non-Lin. Mech. 40**,** 465 − 474**,** (2005).

[32] S. P. Anjali and B. Ganga, Effects of Viscous and Joules Dissipation on MHD Flow, Heat and Mass Transfer past a Stretching Porous Surface Embedded in a Porous Medium: Nonlin. Anal., Model. and Control, 14, 3, 303–314 (2009).

[33] R. Bhargava, H. S. Takhar, S. Rawat, T. A. Beg and O. A. Beg, Finite Element Solutions For Non-Newtonian Pulsatile Flow in a Non-Darcian Porous Medium Conduit: Non. Lin. Analysis, 12(3)**,** 317-327, (2007).

[34] O. A. Bég, A.Y. Bakier and V. R. Prasad, Numerical study of free convection magnetohydrodynamic heat and mass transfer from a stretching surface to a saturated porous medium with Soret and Dufour effects: Computational Materials Science, 46, 57−65, (2009).

[35] M. Yurusoy and M. Pakdemirli, Exact solutions of boundary layer equations of a special non-Newtonian fluid over a stretching sheet: Mech. Res. Commun. 26,171−175,(1999).

[36] A. Mehmood and A. Ali, Symmetry Reduction of Unsteady MHD aligned second grade Flow Equations: Math. Comp. Appl.10 (3),395−402 (2005).

[37] A. Ahmed Afify, Some new exact solutions for MHD aligned creeping flow and heat transfer in second grade fluids by using Lie group analysis: Nonlinear Analysis 70,3298−3306 (2009).

[38] I. P. Kandasamy, P. Loganathan, R. Muhaimin and P. P. Arasu, Lie group analysis for thermal-diffusion and diffusion-thermo effects on free convective flow over a porous stretching surface with variable stream conditions in the presence of thermophoresis particle deposition: Nonlinear Anal., Hybrid Syst., 5, 20−31, (2011).

[39] M. N. Tufail, A. S. Butt and A. Ali, Heat source/sink effects on Non-Newtonian MHD fluid flow and heat transfer over a permeable stretching surface: Lie group analysis: Indian J. Phy. 88(1) 75-82 (2013).

[40] A. J. Chamkha, Coupled heat and mass transfer by natural convection about a truncated cone in the presence of magnetic field and radiation effects: Numer. Heat Transfer A. Appl. 39, 511–530, (2001).

[41] M. A. A. Mahmoud, Thermal radiation effect on unsteady MHD free convection flow past a vertical plate with temperature-dependent viscosity: Can. J. Chem. Eng. 87, 47–52, (2009).

[42] R. Cortell, Effects of viscous dissipation and radiation on thermal boundary layer over a nonlinearly stretching sheet: Phys. Lett. A 372, 631–636, (2008).

[43] R. C. Bataller, Radiation effects on Blasius flow: Appl. Math. Comput. 198, 333–338, (2008).

[44] K. L. Hsiao, Mixed convection with radiation effect over a nonlinearly stretching sheet: World Acad. Sci. Eng. Technol. 62, 242–338, (2010).

[45] M. N. Tufail, A. S. Butt and A. Ali, Group theoretical analysis of Non-Newtonian fluid flow, heat and mass transfer over a stretching surface in the presence of thermal radiation: J. App. Fluid Mech., 9(3), 1515-1524, (2016).

[46] N. T. M. Eldabe, A. A. Hassanet and M. A. A. Mohamed, Effects of couple stresses on the MHD of a non-Newtonian unsteady flow between two parallel porous plates: Z. Naturforsch 58, 204-210, (2003).

[47] A. Ali and A. Mehmood, Homotopy analysis of unsteady boundary layer flow adjacent to permeable stretching surface in a porous medium: Comm. in Nonlin. Sci. and Num. Sim. 13(2), 340-349, (2008).

[48] M. S. Abel, N. Mahesha and J. Tawade, Heat transfer in a liquid film over an unsteady stretching surface with viscous dissipation in presence of external magnetic field: Appl. Math. Modeling, 33(8), 3430-3441, (2009).

[49] J. Zueco and O. A. Beg, Network numerical simulation applied to pulsatile non-Newtonian flow through a channel with couple stress and wall mass flux effects: Int. J. Appl. Math. Mech. 5, 1-16, (2009).

[50] M. A. A. Mahmoud and A. M. Megahed, MHD flow and heat transfer in a non-Newtonian liquid film over an unsteady sheet with variable fluid properties: Canad. J. Phys. 87(10), 1065-1071, (2009).

[51] S. Mukhopadhyay, P. Ranjan De and G. C. Layek, Heat transfer characteristics for the Maxwell fluid flow past an unsteady stretching permeable surface embedded in a porous medium with thermal radiation: JAMT, 54(3), 385-396, (2013).

[52] M. M. Khader and A. M. Megahed, Numerical studies for flow and heat transfer of the Powell-Eyring fluid thin film over an unsteady stretching sheet with internal heat generation using the ehebyshev finite difference method: JAMT, 54(3), 440-450, (2013).

[53] T. C. Chiam, Stagnation point flow towards a stretching plate: J. Phys. Soc. Jpn., 63, 2443-2444, (1994).

[54] T. R. Mahapatra and A. S. Gupta, Heat transfer in stagnation point flow towards a stretching sheet: Heat Mass Transfer, 38**,** 517-521, (2002).

[55] R. Nazar, N. Amin, D. Filip and I. Pop, Stagnation point flow of a micropolar fluid towards a stretching sheet: Int. J. Nonlinear Mech. 39**,** 1227-1235, (2004).

[56] T. R. Mahapatra, S. Dholey and A. S. Gupta, Oblique stagnation point flow of an incompressible viscoelastic fluid towards a stretching surface: Int. J. Non-Linear Mech.*,* 42, 484-499, (2007).

[57] Y. Y. Lok, N. Amin and I. Pop, Unsteady mixed convection flow of a micropolar fluid near the stagnation point on a vertical surface: Int. J. Therm. Sci.*,* 45**,** 1149-1157, (2006).

[58] K. Sadeghy, H. Hajibeygi and S. M. Taghavi, Stagnation-point flow of upper-convected Maxwell fluid: Int. J. Nonlinear Mech.*,* 41, 1242-1247, (2006).

[59] A. Ishak, R. Nazar, N. Amin, D. Filip and I. Pop, Mixed convection of the stagnation-point flow towards a stretching vertical permeable sheet: Malaysian J. Math. Sci., 2, 217-226, (2007).

[60] F. Labropulu and D. Li, Stagnation-point flow of a second grade fluid with slip: Int. J. Non-Linear Mech. 43**,** 941-947, (2008).

[61] D. Pal, Heat and mass transfer in stagnation-point flow towards a stretching surface in the presence of buoyancy force and thermal radiation: Meccanica, 44, 145-158, (2009).

[62] M. Sajid, Z. Abbas, T. Javed and N. Ali, Boundary layer flow of an Oldroyd-B fluid in the region of stagnation point over a stretching sheet: Can. J. Phys.*,* 88**,** 635-640, (2010).

[63] M. A. A. Hamad, M. J. Uddin and A. I. M. Ismail, Radiation effects on heat and mass transfer in MHD stagnation-point flow over a permeable flat plate with thermal convective surface boundary condition, temperature dependent viscosity and thermal conductivity: Nuclear Eng. Design, 242, 194-200, (2012).

[64] M. Katagiri, The effect of Hall currents on the magnetohydrodynamic boundary layer flow past a semi-infinite flat plate: J. Phys. Soc. Japan 27, 1051–1059, (1969).

[65] I. Pop, The effect of Hall currents on hydromagnetic flow near an accelerated plate: J. Math. Phys. Sci. 5, 375–385, (1971).

[66] M. A. Hossain, Effect of Hall current on unsteady hydromagnetic free convection flow near an infinite vertical porous plate: J. Phys. Soc. Japan 55 (7), 2183–2190, (1986).

[67] M. A. Hossain and R. I. M. A. Rashid, Hall effects on hydromagnetic free convection & flow along a porous flat plate with mass transfer: J. Phys. Soc. Japan 56, 97–104, (1987).

[68] M. A. Hossain and K. Mohammad, Effect of Hall current on hydromagnetic free convection flow near an accelerated porous plate: Jpn. J. Appl. Phys. 27 (8), 1531–1535, (1988).

[69] P. C. Ram, Hall effects on free convective flow and mass transfer through a porous medium: Waerme-Stoffubertrag. 22, 223–225, (1988).

[70] P. C. Ram, Hall effects on the hydromagnetic free convective flow and mass transfer through a porous medium bounded by an infinite vertical porous plate with constant heat flux: Int. J. Energy Res. 12, 227–231, (1988).

[71] I. Pop and T. Watanabe, Hall effects on magnetohydrodynamic free convection about a semi-infinite vertical flat plate: Int. J. Eng. Sci. 32, 1903–1911, (1994).

[72] I. Pop and T. Watanabe, Hall effects on magnetohydrodynamic boundary layer flow over a continuous moving flat plate: Acta Mech. 108, 35–47, (1995).

[73] L. Dresner, Similarity solutions of nonlinear partial differential equations: Research Notes in Mathematics, No. 88, Pitman, Boston, (1983).

[74] R. Seshadri and T. Y. Na, Group Invariance in Engineering: Boundary Value Problems, Springer, New York, (1985).

[75] M. Pakdemirli, Similarity analysis of boundary layer equations of a class of non-Newtonian fluids: Int. J. Non-Linear Mech. 29, 187-196, (1994).

[76] A. A. Megahedam, S. R. Komy and A. A. Affify, Similarity analysis in magnetohydrodynamics: Hall effects on free convection flow and mass transfer past a semi-infinite vertical flat plate: Int. J. Non-Lin. Mech. 38, 513–520, (2003).

[77] A. S. Berman, Laminar flow in channel with porous walls: Journal of Applied Physics, 24, 1232–1235, (1953).

[78] R. M. Terrill, Laminar flow in a uniformly porous channel with large injection: Aeronautics Quarterly, 15, 299–310, (1965).

[79] S. M. Cox, Two dimensional flow of a viscous fluid in a channel with porous walls: Journal of Fluid Mechanics, 227, 1–33, (1991).

[80] G. M. Shrestha and R. M. Terril, Laminar flow through parallel and uniformly porous walls of different permeability: ZAMP, 16, 470–482, (1965).

[81] G. M. Shrestha and R. M. Terril, Laminar flow with large injection through parallel and uniformly porous walls of different permeability: Quarterly Journal of Mechanics and Applied Mathematics, 21, 413–432, (1968).

[82] J. F. Brady, Flow development in a porous channel and tube: Physics of Fluids, 27, 1061–1067, (1984).

[83] E. B. Waston, W. H. H. Banks, M. B. Zaturska and P. G. Drazen, On transition to chaos in two dimensional channel flow symmetrically driven by accelerating walls: Journal of Fluid Mechanics, 12, 451–485, (1990).

[84] W. A. Robinson, The existence of multiple solutions for the laminar flow in a uniformly porous channel with suction at both walls: Journal of Fluid Mechanics, 12, 451–485, (1990).

[85] C. L. Taylor, W. H. H. Banks, M. B. Zaturska and P. G. Drazin, Three dimensional flow in porous channel: Quarterly Journal of Applied Mechanics, 44, 105–133, (1991).

[86] R. S. Sutton and A. G. Barto, Exact Navier-Stokes solution for pulsatory viscous channel flow with arbitrary pressure gradient: Journal of Propulsion and Power, 24, 1412–1423, (2008).

[87] T. Fang, J. Zhang and S. Yao, Slip MHD viscous flow over a stretching sheet-an exact solution: Communications in Nonlinear Science and Numerical Simulation, 14, 3731–3737, (2009).

[88] T. V. Kármán, Über laminare und turbulente Reibung, Zeit. Angew: Math. Phys. 1 (4), 233–252, (1921).

[89] W. Cochran, The flow due to a rotating disc: Mathematical Proceedings of the Cambridge Philosophical Society, Cambridge Univ. Press, 365–375, (1934).

[90] K. Millsaps and K. Pohlhausen, Heat transfer by laminar flow from a rotating plate: J. Aerosp. Sci. 19 (2), 120–126, (1952).

[91] T. Von Kármán and C. Lin, On the existence of an exact solution of the equations of Navier Stokes: Commun. Pure Appl. Math., 14 (3), 645–655, (1961).

[92] T. Fang, Flow over a stretchable disk: Phys. Fluids 19, 128105, (2007).

[93] T. Fang and J. Zhang, Flow between two stretchable disks-an exact solution of the Navier–Stokes equations: Int. Commun. Heat Mass Transfer 35 (8), 892–895, (2008).

[94] M. Awad, Heat transfer from a rotating disk to fluids for a wide range of Prandtl numbers using the asymptotic model: J. Heat Transfer 130 (1), (2008).

[95] M. Turkyilmazoglu, Exact solutions corresponding to the viscous incompressible and conducting fluid flow due to a porous rotating disk: J. Heat Transfer 131 (9), (2009).

[96] I. V. Shevchuk, Convective Heat and Mass Transfer in Rotating Disk Systems: Springer, Berlin, (2009).

[97] M. Turkyilmazoglu, MHD fluid flow and heat transfer due to a stretching rotating disk: Int. J. Therm. Sci., 51, 195–201, (2012).

[98] M. Turkyilmazoglu and P. Senel, Heat and mass transfer of the flow due to a rotating rough and porous disk: Int. J. Therm., Sci. 63, 146–158, (2013).

[99] S. Asghar, M. Jalil, M. Hussan and M. Turkyilmazoglu, Lie group analysis of flow and heat transfer over a stretching rotating disk: Int. J. Heat and Mass Tran. 69, 140–146, (2014).

[100] C. Alexa and D. Vrinceanu, Symmetry analysis of the 1+1 dimensional relativistic imperfect fluid dynamics: Physics/9710004 (2003).

[101] M. Nakamura and T. Sawada, Numerical study on the flow of a non-Newtonian fluid through an axisymmetric stenosis: ASME J. Biomech. Eng., 110 137, (1988).

[102] R. Cortell, A note on magnetohydrodynamic flow of a power-law fluid over a stretching sheet: Appl. Math. Comput., 168, 557-566, (2005).

[103] S. J. Liao, Beyond perturbation: Introduction to homotopy analysis method, Boca Raton: Chapman and Hall, CRC Press; (2003).

[104] K. A. Yih, Uniform suction/blowing effect on forced convection about a wedge: uniform heat flux: Acta Mech. 128, 173–181, (1988).

[105] N. A. Yacob, A. Ishak and I. Pop, Falkner-Skan problem for a static or moving wedge in nanofluids: Int. J. Therm. Sci., 50, 133–139, (2011).